Effect of Accelerated Weathering on the Physical and Mechanical Properties of Natural – Fiber Thermoplastic Composites

By

Thomas Lundin

A thesis submitted in partial fulfillment of the requirements for the degree of

Master of Science
(Civil Engineering)

at the

University of Wisconsin – Madison

2002

Abstract

The effects of accelerated weathering on the physical and mechanical properties of natural fiber thermoplastic composites (NFTC) were determined. The research consisted of four distinct phases: Phase I consisted of a screening study to determine favorable formulations of potential roofing products; in Phase II, the effects of length of exposure on chromaticity and flexural engineering properties were determined; in Phase III a degraded layer due to accelerated weathering was identified and a mechanistic prediction of mechanical properties was formulated; finally, in Phase IV full size manufactured roofing panels were evaluated under natural and accelerated weathering.

In Phase I, eighty-eight different NFTC formulations were compression molded into rectangular bars and exposed for 1500 hours in a WeatherOmeter according to American Standard Test Method (ASTM) G26. Two recycled polymers; High Density Polyethylene (HDPE) and Polypropylene (PP) were compounded with four different natural fibers; coir, jute, sisal, and wood, and additives including a compatibilizer, antioxidant, UV stabilizer, fungicide and colorants. The effectiveness of a UV stabilizer, fungicide, fiber type and content were determined.

Based on the results from the screening study, two formulations were selected for further analysis and two new formulations were identified for Phase II. Virgin HDPE was chosen to eliminate the high material variability inherent in recycled polymers. Two lignocellulosic fillers; wood flour and kenaf fiber were selected and added at 50% by weight. Specimens were injection molded into flexural and impact specimens. Flexural and impact specimens were subject to WeatherOmeter exposure according to International Conference of Building Officials (ICBO) AC07. It was determined that the orientation of the degraded layer is significant in flexure.

In Phase III, theoretical modeling and physical characterization of the degraded surface layer of NFTC composites from Phase II was performed. A two-layer model utilizing elementary mechanics was tested for predicting the flexural strength and modulus of NFTC exposed to accelerated weathering. It was found that the model reasonably predicts changes in strength but poorly predicts changes in modulus.

In Phase IV manufactured NFTC roofing panel were installed on a demonstration roof and exposed to 1 year of natural weathering. In addition, specimens were cut from an unexposed roofing panel and subjected to accelerated weathering. One year of natural weathering in Madison Wisconsin resulted in 125% to 175% greater change in color than 2000 hours of accelerated weathering.

Acknowledgments

The research presented in this thesis was completed in cooperation with the University of Wisconsin – Madison, United States Department of Agriculture Forest Products Laboratory (FPL), Teel – Global Resource Technologies (TGRT), the Wisconsin Department of Natural Resources (WDNR) Waste Reduction and Recycling program, and the Partnership for Advanced Technology and Housing Program (PATH). I greatly appreciate all of the time and effort of everyone who made this thesis possible.

I would like to mention a few. I am especially thankful to all of the thesis committee members for spending the time reading the drafts and providing valuable feedback. Dr. Robert Falk for serving as my primary advisor at FPL and for taking the time to help me through this entire process. Dr. Steven Cramer for serving as my advisor at the University of Wisconsin and for providing me with this wonderful opportunity. Additional thanks go to Dr. Lawrence Bank and Dr. Tim Osswald for serving on my thesis review committee.

I would like to thank the following people at FPL; Bill Nelson and all of the people at the FPL engineering mechanics laboratory for providing testing equipment and training, Sam Williams and everyone involved in the weathering group at FPL for making room and maintaining the weatherometer, Vicki Herian for statistical advice and analysis, Steve Hankel for helping in the manufacturing of test setups and machining, Craig Clemons and Nicole Stark for helping with molding of specimens and providing information on NFTC, and Doug Rammer for providing some of the more insightful conversations regarding research and methodology.

Finally I would like to thank everyone at TGRT especially Colin and Brad Felton. Their contributions and assistance throughout the entire compounding and manufacturing process made this project possible.

Table of Contents

Title Page		i
Abstract		ii
Acknowledgments		iii
Table of Contents		iv
List of Tables		viii
List of Figure		x
Chapter 1	**Introduction**	**1**
1.1	Background	1
1.2	Motivation for Research	2
1.3	Hypothesis and Objectives	2
1.4	Scope	3
1.5	Outline	4
Chapter 2	**Literature Review**	**5**
2.1	Introduction	5
2.2	Common Types of Thermoplastics	5
2.3	Mechanical Properties and Behavior of Thermoplastics	6
2.4	Failure Characteristics of Thermoplastics	7
2.5	Optical Properties of Thermoplastics	7
2.6	Weathering of Thermoplastics	7
	2.6.1 Photo-oxidation Process	8
	2.6.2 Effect of Wavelength	11
	2.6.3 Rate of Degradation	12
	2.6.4 Extent of Degradation	12
	2.6.5 Effect on Morphology	13
	2.6.6 Effect of Crystallinity	14
	2.6.7 Effect of Moisture	14
	2.6.8 Temperature Dependence	15
	2.6.9 Effect of Different Processing Conditions	15
2.7	Polymeric Additives	16
	2.7.1 Colorants	16
	2.7.2 Light Stabilizers	17
	2.7.3 Fungicides	18
	2.7.4 Coupling agents	18
	2.7.5 Process Stabilizers	19
	2.7.6 Fillers	19
2.8	Common Types of Lignocellulosics	19
2.9	Mechanical Properties of Lignocellulosics	20
2.10	Physical Characteristics of Lignocellulosics	20
2.11	Weathering of Lignocellulosics	21
	2.11.1 Photo-oxidation Process	21
	2.11.2 Effect of Wavelength	21
	2.11.3 Rate of Degradation	22

2.11.4 Extent of Degradation 22
2.11.5 Effect of Moisture 22
2.11.6 Photo-protection of lignocellulosics 23
2.12 Common Types of Natural Fiber Thermoplastic Composite 23
2.13 Mechanical Behavior of Fiber Composites 23
2.13.1 Effect of Lignocellulosic Concentration, Size, and Type 23
2.13.2 Effect of Processing Fiber Orientation 25
2.14 Weathering of Fiber Composites 25
2.14.1 Effects on Mechanical Properties 25
2.14.2 Effects on Optical Properties 26
2.15 Test Standards 26
2.15.1 Flexural Testing 26
2.15.2 Tensile Testing 26
2.15.3 Chromaticity Measurements 27
2.15.4 Ultra Violet Weathering Tests 27
2.16 Differences and Similarities Between Natural and Accelerated Weathering 28

Chapter 3. Phase I. Effects of Different Fillers and Additives on the Durability of Natural Fiber Thermoplastic Composites 31
3.1 Introduction 31
3.2 Experimental 31
3.2.1 Materials 31
3.2.2 Specimen Preparation 32
3.2.2.1 Testing 33
3.2.2.2 Accelerated Weathering 34
3.2.2.3 Color Fade Measurement 34
3.2.2.4 Flexural Testing 35
3.3 Results and Discussion 37
3.3.1 Effects of Accelerated Aging on Color Fade 37
3.3.1.1 Effect of UV Stabilizer 38
3.3.1.2 Effect of Fungicide 41
3.3.1.3 Effect of Wood Flour Content 44
3.3.1.4 Effect of Fiber Type and Content 46
3.3.1.5 Effect of Colorant 47
3.3.2 Effects of Accelerated Aging on Flexural Properties 50
3.3.2.1 Effect of UV Stabilizer 51
3.3.2.2 Effect of Fungicide 55
3.3.2.3 Effect of Wood Flour Content 56
3.3.2.4 Effect of Fiber Type and Content 58
3.3.2.5 Effect of Colorant 59
3.3.3 Effects of Accelerated Aging on Dimensional Changes 60
3.4 Conclusions 61

Chapter 4. Phase II. Effect of Length of Exposure on the Physical and Mechanical Properties of Natural Fiber Thermoplastic Composites **63**
4.1 Introduction 63
4.2 Experimental 63
4.2.1 Materials 63
4.2.2 Specimen Preparation 64
4.2.3 Testing 65
4.2.3.1 Accelerated Weathering 65
4.2.3.2 Color Fade Measurement 65
4.2.3.3 Flexural Testing 66
4.2.3.3.1 Static Bending Testing 66
4.2.3.3.2 Impact Testing 66
4.3 Results and Discussion 67
4.3.1 Effect of Accelerated Weathering on Color Fade 67
4.3.2 Effect of Accelerated Weathering on Flexural Properties 73
4.3.2.1 Load Deflection Curves 73
4.3.2.2 Orientation of Degraded Layer 76
4.3.2.3 Flexural Modulus 76
4.3.2.4 Flexural Strength 81
4.3.2.5 Impact Properties 86
4.4 Conclusions 89

Chapter 5 Phase III. Modeling and Characterization of the Degraded Layer of Natural Fiber Thermoplastic Composites **92**
5.1 Introduction 92
5.2 Surface Degradation 92
5.3 Visible Depth of Degradation 94
5.4 Analysis of Phase III Results 97
5.4.1 Relation Between Color Fade and Depth of Degradation 97
5.4.2 Relation Between Color Fade and Flexural Properties 99
5.4.3 Relation Between Depth of Degradation and Flexural Properties 99
5.4.4 Effect of Depth of Degradation on the Effective Moment of Inertia 103
5.4.5 Flexural Modulus Calculated Using the Effective Cross Section 105
5.4.6 Flexural Strength Calculated Using the Effective Cross Section 107
5.4.7 Flexural Modulus and Strength as a Function of Specimen Depth 109
5.4.8 Relations Between Milled and Specimens Exposed to Accelerated Weathering 110
5.5 Conclusions 112

Chapter 6	**Phase IV. Manufactured Roofing Panels**	**113**
6.1	Introduction	113
6.2	Experimental	113
	6.2.1 Materials	113
	6.2.2 Specimen Preparation	113
	6.2.3 Testing	114
	6.2.3.1 Accelerated Weathering	114
	6.2.3.2 Natural Weathering	114
	6.2.3.3 Color Fade Measurement	115
	6.2.3.4 Flexural Testing	115
6.3	Results and Discussion	115
	6.3.1 Effects of Accelerated Weathering on Color Fade	115
	6.3.2 Effects of Natural Weathering on Color Fade	116
	6.3.3 Effects of Accelerated Weathering on Flexural Properties	118
6.4	Conclusions	119
Chapter 7	**Summary**	**121**
7.1	Conclusions	121
7.2	NFTC Product Recommendations	123
7.3	Future Research	123
References		**125**
Appendices		**131**
A.1	Equations for Determining Chromaticity	131
A.2	ASTM D790 Equations and Comments	132
A.3	Equations for FPL Technique for Nonlinear Curve Fitting	133
A.4	Determination of the Sample Size Sufficient for Estimating the Mean by a Two-Stage Method	134
A.5	Manufactures Plastic Specifications Used in Phase II	134
A.6	Phase II Injection Molding Cycle Times	135
A.7	Phase II Injection Molding Pressures and Speeds	135
A.8	Tension and Three-Point Bending Stress-Strain Curves for Phase II Formulations 1-4	136
A.9	Three-Point Bending and Impact Testing Specimen Rotation for Phase II Accelerated Weathering	138
A.10	Nonlinear Least Squares Regression Fits	138

List of Tables

I. Chapter 2

Table 2.1 Standard Test Methods of Accelerated Weathering 27

II. Chapter 3

Table 3.1 Phase I Test Matrix 32

Table 3.2 Effects of UV Stabilizer and Accelerated Weathering on Unfilled HDPE and PP resin with 0.5% Fungicide 39

Table 3.3 Effects of Fungicide and Accelerated Weathering on Unfilled HDPE and PP resin 41

Table 3.4 Effects of Alternative Fibers and Accelerated Weathering on Total Color Difference for Thermoplastic Composites with 0.25% UV Stabilizer, and 0.5% Fungicide 47

Table 3.5 Effects of Colorants and Accelerated Weathering on Total Color Difference for 50% Wood Flour Thermoplastic Composites with 0.25% UV Stabilizer, and 0.5% Fungicide 48

Table 3.6 Effects of Colorants and Accelerated Weathering on Total Color Difference for 70% Wood Flour Thermoplastic Composites with 0.25% UV Stabilizer, and 0.5% Fungicide 49

Table 3.7 Effects of Colorants and Accelerated Weathering on Total Color Difference for 50% Wood Flour Thermoplastic Composites with 0.5% UV Stabilizer, and 0.5% Fungicide 49

Table 3.8 Effects of Colorants and Accelerated Weathering on Total Color Difference for 70% Wood Flour Thermoplastic Composites with 0.5% UV Stabilizer, and 0.5% Fungicide 50

Table 3.9 Effect of Fiber Type, Content, and Accelerated Weathering on Flexural Properties for Thermoplastic Composites with 0.25% UV Stabilizer, and 0.5% Fungicide 58

Table 3.10 Effect of Colorants and Accelerated Weathering on the Flexural Properties of HDPE & PP Specimens with 50% Wood Flour, 0.25% UV Stabilizer, and 0.5% Fungicide 60

III. Chapter 4

Table 4.1 Phase II Test Matrix 64

Table 4.2 Effect of Accelerated Weathering on Composite Chromaticity 68

Table 4.3 Effect of Accelerated Weathering on Composite Flexural Modulus 76

Table 4.4 Effect of Accelerated Weathering on Composite Flexural Strength 82

Table 4.5 Effect of Accelerated Weathering on Composite Impact Strength 87

IV. Chapter 6

Table 6.1 Roof Panel Formulation 113

Table 6.2 Effects of Accelerated Weathering on the Total Color Difference of Specimens Cut from Manufactured Panels 116

Table 6.3 Southeast Corner Color Fade Measurements 116

Table 6.4 Southwest Corner Color Fade Measurements 116

Table 6.5 Northeast Corner Color Fade Measurements 117

Table 6.6 Northwest Corner Color Fade Measurements 117

Table 6.7. Effect of Accelerated Weathering on Large Specimens Cut From Manufactured Roof Panels 118

Table 6.8. Effect of Accelerated Weathering on the Small Specimens Cut From Manufactured Roof Panels 119

List of Figures

V. Chapter 3

Figure 3.1 Specimens Attached to Screens Prior to Accelerated Weathering 34

Figure 3.2 Minolta CR-200 Chroma Meter 35

Figure 3.3 Phase I - Three-Point Bending Setup 36

Figure 3.4 HDPE Test Specimens with 50% Wood Flour Left, Weathered Specimen (1500 hours); Right, Unweathered Specimen 37

Figure 3.5 Surface Crazing of HDPE Specimen after 1500 Hours of Accelerated Weathering 38

Figure 3.6 Effects of UV Stabilizer and Accelerated Weathering on the Total Color Difference of 50% and 70% Wood Flour Composites with No Added Fungicide 40

Figure 3.7 Effects of UV Stabilizer and Accelerated Weathering on the Total Color Difference of 50% and 70% Wood Flour Composites with 0.5% Fungicide 40

Figure 3.8 Effects of UV Stabilizer and Accelerated Weathering on the Total Color Difference of 50% and 70% Wood Flour Composites with 2% Fungicide 41

Figure 3.9 Effect of Fungicide and Accelerated Weathering on the Total Color Difference of 50% and 70% Wood Flour Composites 42

Figure 3.10 Effect of Fungicide and Accelerated Weathering on the Total Color Difference of 50% and 70% Wood Flour Composites with 0.25% UV Stabilizer 43

Figure 3.11 Effect of Fungicide and Accelerated Weathering on the Total Color Difference of 50% and 70% Wood Flour Composites with 0.5% UV Stabilizer 43

Figure 3.12 Effect of Wood Flour Content and Accelerated Weathering on the Total Color Difference of Thermoplastic Composites 44

Figure 3.13 Effect of Wood Flour Content and Accelerated Weathering on the Total Color Difference of Thermoplastic Composites with 0.5% Fungicide 45

Figure 3.14 Effect of Wood Flour Content and Accelerated Weathering on the 45

Total Color Difference of Thermoplastic Composites with 0.25% UV Stabilizer and 0.5% Fungicide

Figure 3.15 Effect of Wood Flour Content and Accelerated Weathering on the Total Color Difference of Thermoplastic Composites with 0.5% UV Stabilizer and 0.5% Fungicide 46

Figure 3.16 Test Specimens with Red Colorant Added Left, Weathered (1500 hours); Right Unweathered Specimen 47

Figure 3.17 Load Deflection Curves for Unexposed 0%, 50%, 70% Wood Flour Composites of HDPE and Fitted Tanh Functions 51

Figure 3.18 Effect of UV Stabilizer and Accelerated Weathering on the Flexural Strength of Unreinforced Thermoplastics with 0.5% Fungicide 52

Figure 3.19 Effect of UV Stabilizer and Accelerated Weathering on the Flexural Modulus of Unreinforced Thermoplastics with 0.5% Fungicide 53

Figure 3.20 Effect of UV Stabilizer and Accelerated Weathering on Flexural Strength for 50% Wood Flour – Thermoplastic Composites 54

Figure 3.21 Effect of UV Stabilizer and Accelerated Weathering on Flexural Modulus for 50% Wood Flour – Thermoplastic Composites 54

Figure 3.22 Effect of Fungicide and Accelerated Weathering on Flexural Strength for 50% Wood Flour – Thermoplastic Composites 55

Figure 3.23 Effect of Fungicide and Accelerated Weathering on Flexural Modulus for 50% Wood Flour – Thermoplastic Composites 56

Figure 3.24 Effect of Wood Flour Content and Accelerated Weathering on Flexural Strength for Thermoplastic Composites with No Added UV Stabilizer and Fungicide 57

Figure 3.25 Effect of Wood Flour Content and Accelerated Weathering on Flexural Modulus for Thermoplastic Composites with No Added UV Stabilizer and Fungicide 57

Chapter 4

Figure 4.1 Granulated Polymer and Fiber after Compounding 64

Figure 4.2 30-Metric Ton Reciprocating-Screw Injection Molder 64

Figure 4.3 Inside of Weatherometer 65

Figure 4.4 Phase II Three – Point Bending Setup 66

Figure 4.5 Impact Bending Setup 67

Figure 4.6 Effect of Accelerated Weathering on the Total Color Difference of Formulation 1 – HDPE 70

Figure 4.7 Effect of Accelerated Weathering on the Total Color Difference of Formulation 2 – Additives 71

Figure 4.8 Effect of Accelerated Weathering on the Total Color Difference of Formulation 3 – Wood 71

Figure 4.9 Effect of Accelerated Weathering on the Total Color Difference of Formulation 4 – Kenaf 72

Figure 4.10 Comparison of The Mean Total Color Difference Between Specimens Exposed for the First and Last 1000 hours of Bulb 1 73

Figure 4.11 Typical Load Deflection Curves for Formulation 1 – HDPE 74

Figure 4.12 Typical Load Deflection Curves for Formulation 2 – Additives 74

Figure 4.13 Typical Load Deflection Curves for Formulation 3 – Wood 75

Figure 4.14 Typical Load Deflection Curves for Formulation 4 – Kenaf 75

Figure 4.15 Effect of Accelerated Weathering on the Flexural Modulus of Formulation 1 – HDPE Tested With Exposed Surface on Compression Side 78

Figure 4.16 Effect of Accelerated Weathering on the Flexural Modulus of Formulation 1 – HDPE Tested With Exposed Surface on Tension Side 79

Figure 4.17 Effect of Accelerated Weathering on the Flexural Modulus of Formulation 2 –Additives 79

Figure 4.18 Effect of Accelerated Weathering on the Flexural Modulus of Formulation 3 – Wood 80

Figure 4.19 Effect of Accelerated Weathering on the Flexural Modulus of Formulation 4 – Kenaf 80

Figure 4.20 Effect of Accelerated Weathering on the Flexural Strength of Formulation 1 – HDPE Tested with Exposed Surface on Compression Side 84

Figure 4.21 Effect of Accelerated Weathering on the Flexural Strength of Formulation 1 – HDPE Tested with Exposed Surface on Tension Side 84

Figure 4.22 Effect of Accelerated Weathering on the Flexural Strength of Formulation 2 – Additives 85

Figure 4.23 Effect of Accelerated Weathering on the Flexural Strength of Formulation 3 – Wood 85

Figure 4.24 Effect of Accelerated Weathering on the Flexural Strength of Formulation 4 – Kenaf 86

Figure 4.25 Effect of Accelerated Weathering on the Energy to Maximum Load for Formulation 2 – Additives 88

Figure 4.26 Effect of Accelerated Weathering on the Energy to Maximum Load for Formulation 3 – Wood 88

Figure 4.27 Effect of Accelerated Weathering on the Energy to Maximum Load for Formulation 4 – Kenaf 89

Chapter 5

Figure 5.1 Electron Micrograph of Unexposed Wood Flour Composite Surface 92

Figure 5.2 Electron Micrograph Wood Flour Composite Exposed for 2000 Hours 92

Figure 5.3 Unexposed Surface of Kenaf Fiber Composite 93

Figure 5.4 Surface of Kenaf Fiber Composite – 1000 Hours of Exposure 93

Figure 5.5 Unexposed Surface of Wood Fiber Composite 93

Figure 5.6 Surface of Wood Fiber Composite – 1000 Hours Exposure 93

Figure 5.7 Edge of Unexposed Specimen Formulation 3 – Wood 95

Figure 5.8 Edge of Formulation 3 – Wood 2000 Hours of Exposure 95

Figure 5.9 Edge of Formulation 3 – Wood 4000 Hours of Exposure 95

Figure 5.10 Edge of Unexposed Specimen Formulation 4 – Kenaf 95

Figure 5.11 Edge of Formulation 4 – Kenaf 2000 Hours of Exposure 95

Figure 5.12 Edge of Formulation 4 – Kenaf 4000 Hours of Exposure 95

Figure 5.13 Depth of Degradation as a Function of Distance from Edge 96

Figure 5.14 Effect of Accelerated Weathering on the Visible Depth of Degradation for Formulation 3 – Wood 96

Figure 5.15 Effect of Accelerated Weathering on the Visible Depth of Degradation Measurements for Formulation 4 – Kenaf 97

Figure 5.16 Effect of Accelerated Weathering on the Total Color Difference and Visible Depth of Degradation for Formulation 3 – Wood 98

Figure 5.17 Effect of Accelerated Weathering on the Total Color Difference and Visible Depth of Degradation for Formulation 4 – Kenaf 98

Figure 5.18 Effect of Accelerated Weathering on the Total Color Difference and Change in Flexural Modulus for Formulation 3 – Wood 99

Figure 5.19 Effect of Accelerated Weathering on the Total Color Difference and Change in Flexural Modulus for Formulation 4 – Kenaf 100

Figure 5.20 Effect of Accelerated Weathering on the Total Color Difference and Change in Flexural Strength for Formulation 3 – Wood 100

Figure 5.21 Effect of Accelerated Weathering on the Total Color Difference and Change in Flexural Strength for Formulation 4 – Kenaf 101

Figure 5.22 Effects of Accelerated Weathering on the Visible Depth of Degradation and Change in Flexural Modulus for Formulation 3 – Wood 101

Figure 5.23 Effects of Accelerated Weathering on the Visible Depth of Degradation and Change in Flexural Modulus for Formulation 4 – Kenaf 102

Figure 5.24 Effect of Accelerated Weathering on the Visible Depth of Degradation and Change in Flexural Strength for Formulation 3 – Wood 102

Figure 5.25 Effect of Accelerated Weathering on the Visible Depth of Degradation and Change in Flexural Strength for Formulation 4 – Kenaf 103

Figure 5.26 Effect of Accelerated Weathering on the Effective Moment of Inertia for Formulation 3 – Wood 104

Figure 5.27 Effect of Accelerated Weathering on the Effective Moment of Inertia for Formulation 4 – Kenaf 104

Figure 5.28 Predicted Flexural Modulus of Formulation 3 – Wood 106

Calculated using the Effective Cross Section

Figure 5.29 Predicted Flexural Modulus of Formulation 4 – Kenaf Calculated using the Effective Cross Section 106

Figure 5.30 Predicted Flexural Strength of Formulation 3 – Wood Calculated using the Effective Cross Section 108

Figure 5.31 Predicted Flexural Strength of Formulation 4 – Kenaf Calculated using the Effective Cross Section 108

Figure 5.32 Flexural Modulus as a Function of Depth of Specimen Removed for Formulation 4 – Kenaf 109

Figure 5.33 Flexural Strength as a Function of Depth of Specimen Removed for Formulation 4 – Kenaf 110

Figure 5.34 Relation between Flexural Modulus of Milled and Weathered Specimens using the Effective Cross Section 111

Figure 5.35 Relation between Flexural Strength of Milled and Weathered Specimens using the Effective Cross Section 111

Chapter 6

Figure 6.1 Typical Roofing Panel 114

Figure 6.2 Panels after Installation 114

Figure 6.3 Color Change of Roof Panels Exposed Outdoors and of Specimens Exposed Artificially 118

Chapter 1. Introduction

1.1 Background

It is estimated that six billion pounds of commingled plastic containers are landfilled each year in the United States, the majority thermoplastics (Lampo 1999). The Environmental Protection Agency estimates that 56 million tons of waste wood and paper are annually disposed of in landfills – a quantity three times the 1990 timber harvest on national forests (Backiel 1995). Finding uses for these large waste streams would minimize the demands placed on forests, petroleum resources, and landfill space.

The technology exists to manufacture building products from natural fiber thermoplastic composites (NFTC). Natural fibers are an attractive choice for use with thermoplastics because they are inexpensive, lighter than mineral fillers, and they can improve mechanical properties. NFTC products are potentially more resistant to moisture damage, splitting, insect attack, and fungal decay than conventional wood products. Waste from the production, and installation of NFTC products could potentially be collected and remolded into new NFTC products. The development of commodity building products from NFTC could create markets for waste materials. Currently, however, less than 5% of building materials utilize recovered materials from the solid waste stream (Backiel 1995).

NFTC products are currently produced commercially. Wood/thermoplastic composite lumber, products with 50% or less plastic by weight, have been accepted by the construction industry and home owners, primarily for decking applications and make up 3-10% of the decking market (Eckert 2000). Currently about 70 North American firms' produce approximately 16 to 24 million board feet of plastic lumber annually, lumber that is at least 50% plastic by weight, worth roughly $40 to $60 million in 1996 (Powell 1996). Wood/thermoplastic decking manufacturers claim that with little maintenance, superior performance over conventional wood decking can be achieved. To back these claims; the majority of wood/thermoplastic lumber is warranted for 10 – 20 years against splitting, checking, and decay. Disadvantages of these products lie in their relatively low structural properties compared to structural lumber, limiting their use to non-or semi-structural applications such as landscaping, piers and docks, wall panels, and outdoor furniture. Larger markets within the building industry could be developed; however, a lack of durability performance data, standards, and reluctance by homebuilders to utilize undemonstrated products has hampered market development.

The durability of NFTC products is dependant on the durability of the polymer matrix, fiber, and the interfacial bond between the polymer and fiber. Degradation of any of these components will ultimately affect the product's physical and mechanical properties.

Thermoplastics and natural fibers are susceptible to environmental stresses including temperature, moisture, light (UV), and chemical agents such as organic solvents, ozone, acids and bases. Degradation or the adverse change in physical or mechanical properties results from oxidation reactions that result from any combination of the following

processes; melt degradation, thermal oxidation, and photodegradation. Of particular importance for outdoor applications is the effect of photodegradation. Photodegredation or weathering of some thermoplastics can result in the embrittlement of otherwise ductile polymers and is confined to the surface. For lignocellulosics, photodegradation can result in the breakdown of lignin, hemicelluloses and cellulose. The effects of weathering on composites manufactured from these materials are largely unknown.

1.2 Motivation for Research

NFTC have the potential to be increasingly used for exterior building applications and to utilize recyclable materials. Currently, their use is limited by the availability of durability performance data and applicable standards. Artificial and natural weathering tests have been developed for materials intended for use in outdoor environments. These tests have been shown to adversely affect both physical and mechanical properties of polymers and lignocellulosics. The degree of degradation due to these tests and its impact on NFTC properties however has not been well documented, nor has any quantifiable correlation between degradation of physical and mechanical properties been made. Additionally there are questions as to how well these tests simulate actual service conditions.

1.3 Hypothesis and Objectives

The overall hypothesis of the research was that NFTC are suitable for severe outdoor applications such as roofing. To test this hypothesis the following specific hypotheses were tested:

1. The effects of natural weathering on NFTC can be reproduced using accelerated weathering devices.
2. An Ultra Violet light stabilizer is effective in reducing the effects of photodegradation due to accelerated weathering.
3. NFTC additives will affect the durability of composites exposed to accelerated weathering.
4. The content of lignocellulosic will affect the durability of composites exposed to accelerated weathering.
5. The changes in physical and mechanical properties due to the degradative effects of weathering are quantifiable.
6. The mechanical behavior of weathered NFTC products is influenced by the formation of a degraded layer.

The overall objective of this research was to evaluate the durability of NFTC intended for exterior roofing applications based on natural and accelerated weathering. To reach this objective the following specific objectives were investigated:

1. Evaluate the durability of different formulations of NFTC based on accelerated weathering tests.

2. Measure the physical changes of NFTC exposed to increments of accelerated weathering
3. Measure the mechanical behavior of NFTC exposed to increments of accelerated weathering
4. Determine if the orientation of the degraded layer from accelerated weathering affects the mechanical properties of NFTC
5. Investigate the correlation between changes to physical and mechanical properties due to accelerated weathering
6. Evaluate the durability of manufactured NFTC roofing panels subjected to natural and accelerated weathering

1.4 Scope

Products intended for outdoor applications must resist failure due to exposure during their intended service life. Failure can be defined as changes beyond an acceptable limit to either physical or mechanical properties and are to be determined by the potential manufacturer of these products. In this experimental study the relative durability of NFTC specimens were evaluated by measuring the changes to chromaticity and flexural properties due to both natural and accelerated weathering.

Polypropylene and high-density polyethylene, recyclable and commercially important thermoplastic polymers that are susceptible to weathering were investigated. Five different natural fibers were selected as fillers; coir, jute, kenaf, sisal, and wood flour. Additives were limited to a UV stabilizer, process stabilizer, compatibilizer, fungicide, and two colorants. The concentration of fillers and additives was predetermined. Two different methods of processing were used in this research. Compression and injection molded specimens were produced and exposed. The relative effects of additives, lignocellulosic fillers, polymer type, and length of exposure were determined.

The durability of a NFTC product would be best determined from actual exposure conditions that the product may experience. However, due to the long time involved in outdoor weathering and the variety of potential service environments, accelerated weathering tests were performed. A direct correlation between natural and accelerated weathering was beyond the scope of this research. Accelerated weathering tests were assumed to produce similar chemical and mechanical effects as natural weathering on NFTC. Photodegradation theory was compared for natural and accelerated weathering. Given the similarities between natural and accelerated weathering tests, favorable composite formulations were selected after accelerated weathering and further investigated under natural exposure.

A simple two-layer model utilizing elementary mechanics was used to evaluate the changes occurring due to accelerated weathering. This model includes the assumption that a degraded layer is identifiable and that it doesn't influence the mechanical properties of the undegraded layer. From this model, changes to mechanical properties were predicted from experimental data.

1.5 Outline

The thesis consists of a literature review and four phases of research. A relevant literature survey is presented in Chapter 2. The literature survey focuses on the changes occurring in the materials due to photooxidation, what factors influence the degradation, and how photooxidation differs in natural and accelerated weathering. It reviews polymeric additives, the mechanical properties of the materials individually and as composites, and what factors influence those properties. The research consists of four distinct phases: Chapter 3 (Phase I) presents the relative durability of two polymers, a variety of additives and lignocellulosic fillers; in Chapter 4 (Phase II) the effects of increasing length of exposure on mechanical and physical properties of a select number of formulations are presented; in Chapter 5 (Phase III) a degraded layer is identified and a mechanistic prediction of mechanical properties is presented; finally, in Chapter 6 (Phase IV) full size manufactured roof panels subjected to natural and accelerated weathering are evaluated. Materials in Phase I were chosen because of low cost, abundance, and recylability. Phase I was intended as a precursory study for determining the material formulations for Phase II and IV. Materials in Phase II and IV were chosen based on the relative durability of those specimens exposed in Phase I.

Chapter 2. Literature Review

2.1 Introduction

Polymeric materials are used for a variety of outdoor applications and the demand for these materials is increasing. Between 1980 and 1994 high-density polyethylene, a commercially important polymer, has displayed an average compound growth of 8% (Killough 1995). In particular, organic polymers are highly utilized due to favorable characteristics including moldability, low density, and low cost.

Recently there has been interest in compounding natural fibers with thermoplastics. This is done to reduce material cost and can improve mechanical properties. The properties of NFTC are dependant upon the polymer matrix, natural fiber, and interfacial bond between the fiber and the matrix. The processing conditions, strain, strain rate, time-scale, temperature, additives, and service environment further influence the properties. NFTC products must resist changes to physical and mechanical properties during their intended service life. Little is known about the effects of weathering, or outdoor exposure, on the properties of these composites.

The literature studied focuses on the changes to thermoplastics and lignocellulosics due to photooxidation, what factors influence photooxidation, and how photooxidation differs in natural and accelerated weathering. In addition polymeric additives, the mechanical properties of thermoplastics, lignocellulosics, and NFTC are discussed.

2.2 Common Types of Thermoplastics

Plastics can be distinguished from other materials by their high molecular weight and long chain length. There are two types of polymeric materials, thermoplastics and thermosets. In 1993 over 31 million tons of polymers were produced in the United States with thermoplastics accounting for 90% of the total (Osswald 1995). The majority of thermoplastics sold were high-density polyethylene and polypropylene accounting for approximately 35% of the thermoplastic resin market (Killough 1995). The difference between these two types of plastics is determined by their temperature response. Thermoplastics are those plastics that have the ability to remelt after they have solidified. Thermosets are those that solidify due to chemical reactions that result in cross-linking and cannot be remelted after solidification. Due to cross-linking, thermosets cannot be easily recycled. This research focused solely on thermoplastics.

There are two main types of thermoplastics, amorphous and semi-crystalline. The most significant difference between amorphous and semi-crystalline polymers can be explained by their morphology or the arrangement of the polymer structure. A true amorphous polymer is defined as a polymer with purely random structure. Crystalline polymers are those with regular, repeating structural patterns called crystals. A semi-crystalline polymer is one that contains both amorphous and crystallites or ordered regions. Amorphous polymers are those that do not exhibit a sharp transition between

liquid and solid states, while semi-crystalline polymers do exhibit a sharp transition between the melting temperatures, T_m, and solid state.

A commercially important group of thermoplastics are polyolefins. Polyolefins are semi-crystalline polymers that include, high-density polyethylene (HDPE), low-density polyethylene (LDPE), polypropylene (PP) and polystyrene (PS). An olefin is a hydrocarbon structure containing one or more unconjugated carbon-carbon double bonds.

2.3 Mechanical Properties and Behavior of Thermoplastics

The mechanical properties of polymers are not homogeneous. The mechanical properties of thermoplastics are dependant upon the processing conditions, strain, strain rate, time scale and temperature. The processing conditions will affect the morphology or the arrangement and flexibility of solid polymers chains, crystallites, over the surface and though the depth of the product due to flow through the mold and cooling effects. Processing will also determine the degree of crystallinity in a product. A wholly crystalline polymer would be brittle due to the weakness of the crystal-to-crystal bonds while a wholly amorphous polymer would be rubbery. Generally polymers with higher degree of crystallinity have greater strength. Polyethylene (PE) has a linear chain structure, and therefore a higher degree of crystallinity than PS and PP. The tensile and flexural strength of polyolefins generally decrease in the order PS, PP, HDPE, Low – density polyethylene (LDPE), however the elongation at break and izod impact strength decreases in the opposite order (Osswald 1995). The degree of crystallinity increases with increasing crystallization temperature (Allen 1983). Rapidly cooled material may only reach 50% crystalline while cooling at close to the melting point can produce crystallinities approaching 100% (Allen 1983). The fraction of crystalline material is generally lower near the surface than in the middle of the specimen (Hoekstra 1997).

Thermoplastics may behave as solids or liquids depending on the speed that the molecules are deformed. This behavior is referred to as viscoelastic behavior or material response. For small deformations thermoplastics behavior can be described by linear viscoelastic theory and for large deformations a non-linear viscoelastic analysis may be required. The viscoelastic behavior of oriented, anisotropic polymers would be different in different directions (Ferry 1980).

The glass transition temperature is a softening temperature dependant on the size and stiffness of the pendent groups, groups of atoms attached to the main polymer backbone. The glass transition temperature can be described as a temperature or narrow region were the thermal expansion coefficient undergoes a discontinuity and below which the mobility of the polymer chains is limited. Below T_g the plastic is brittle, above T_g the plastic is relatively flexible. The modulus of a polymer is dependent on the crystallinity at temperatures between the glass transition and melting point, below T_g the amorphous regions within the semi-crystalline structure determine the modulus (Allen 1983).

2.4 Failure Characteristics of Polyolefins

The failure behaviors of polyolefins are influenced by the loading conditions and service environment. More specifically the failure can be predicted based upon strain rate and temperature (Hoekstra 1997). At low strain rates/high temperature a ductile failure ($\varepsilon_{failure} < \varepsilon_{yield}$) can be expected and the failure stresses will be low. At high strain rates/low temperatures a brittle failure process will be found with relatively high failure stresses. At intermediate strain rates/intermediate temperatures, a necking or localized reduction in cross-section, process resulting in ductile failures ($\varepsilon_{failure} > \varepsilon_{yield}$) at intermediate stresses follows yielding.

The failure behaviors of weathered polyolefins are determined by many of the same factors as unweathered thermoplastics such as strain rate and temperature. Weathered polymers however exhibit a brittle surface layer that can influence the failure behavior. Cracks may form in the brittle layer and depending upon the dimensions, mechanical properties, and loading conditions, the crack will propagate into the ductile material (Bruijn 1992).

2.5 Optical Properties of Thermoplastics

The optical properties of thermoplastics are influenced by molecular structure of the polymer. The optical properties of a polymer are dependent on the size of the crystalline domains. The crystalline domain is the region with ordered molecular structure. The size of crystalline domains is larger than the wavelengths of visible light making polyolefins translucent. How rays of light bend when they enter a media is determined by the index of refraction. The index of refraction is dependent on the density of the media and the wavelength of light. Generally the physical appearance of polymer parts is modified through the use of pigments.

2.6 Weathering of Thermoplastics

Thermoplastics undergo degradation reactions in the presence of oxygen. Oxidative reactions are influenced by heat, light, and water, all of which are present throughout many polymers life cycle. During processing the polymer is subjected to heat and mechanical shear that assist oxidative degradation reactions. During service, a product can be exposed to terrestrial light and water.

The two major categories of degradation involving a reactant from the atmosphere or environment are oxidation and hydrolysis, though most polymers are primarily degraded by oxidation (Gillen 1986). When exposed to terrestrial sunlight, physical and chemical processes can damage the polymer through a process referred to as weathering. Weathering can result in discoloration or the formation of microcracks (crazes), embrittlement, and checking that will further expose underlying polymer to weathering and could possible reduce mechanical properties. Outdoor weathering is a common case of oxidation enhanced by photochemical reactions. This degradation process is referred to as photooxidation.

Photooxidation of polymers produces a complex mixture of different products. Degradation reactions can result in the formation of, peroxides, alcohols, ketones, aldehydes, acids, peracids, and peresters. The molecules that connect crystallites through amorphous regions can undergo scissions during the oxidation process, resulting in a decrease in the elongation or ductility and changes in the physical properties (Rabek 1996).

PE crystallized from the melt consists of a skeletal structure of crystalline lamellae interlaced with tie chains in a disordered arrangement. Exposure of this type of polymer to oxygen at elevated temperatures or under UV radiation produces a rapid rise in crystallinity (Davis 1983). As chains break in amorphous regions, the freed fragments relax into a more compact arrangement. The relaxation process is inhibited by branching or cross-linking, and is therefore a function of polymer structure and reactions conditions. Inhibition of crystallization by cross-links formed during photo-oxidation increases the fraction of polymer ultimately accessible to oxygen, thereby increasing the level of oxygen consumption associated with embrittlement (Davis 1983).

2.6.1 Photo-oxidation Process

In general terms, photooxidation can be described as a branched chain reaction where the initiation is a photolytic process. For photooxidation to occur radiation must be absorbed by a molecule and must be strong enough to dissociate bonds in a molecule to form free radicals (Rabek 1996). Photooxidation of most polymers proceeds by a radical chain mechanism composed of the following steps, initiation, propagation, possibly branching and termination (Davis 1983). The steps of propagation and branching and termination for photooxidation are believed to closely parallel those of thermal-oxidation even though the inherent differences between the initiation steps (Davis 1983). The sequence of photo-oxidation reactions is the abstraction or removal of the hydrogen atom at the tertiary carbon atom, leaving a free radical at the carbon atom. Free radicals, which are unstable and highly reactive, react with oxygen and in other ways lead to polymer degradation (Ezrin 1996).

It is generally accepted that photooxidation processes are initiated at the surface, which gives rise to a gradient of deteriorated material through the specimen thickness (Rabek 1996). For most polymers there are sufficient imperfections in the molecular chains that act as chromophores (centers that absorb light). These will cause localized bond rupture by a free radical mechanism, and subsequent auto-oxidative reactions (Mascia 1982). Photo-oxidation is essentially a problem of impurities, as hydrocarbons do not absorb light above 200nm that is well below the wavelength of terrestrial sunlight (Allen 1983). All radiation-induced processes start at chromophoric groups that are radiation sensitive sites (Rabek 1996). Chromophoric groups are formed in several polymers including polyolefines as internal and external impurities (Rabek 1996).

Several internal impurities that may contain chromophoric groups include; hydroperoxides, carbonyl and unsaturated bonds, branching due to the polymerization

process, catalyst residues attached to the chain ends of macromolecules, and charge transfer complexes with oxygen (Rabek 1996). Carbonyl groups and hydroperoxides are commonly investigated as principal photo-initiators of oxidation. Carbonyl groups have higher extinction coefficients than peroxide groups yet their quantum efficiency for producing radicals is extremely low. Hydroperoxides are weaker UV absorbers than carbonyl groups but decompose on excitation with nearly 100% efficiency to yield mobile radicals (Allen 1983). Gijsman cites several articles that discuss the initiation of photooxidation. The initiating capacities of added ketones in PE and of hydroperoxides formed by thermal oxidation are low because hydroperoxides decompose without forming radicals (Gijsman 1996). An alternative mechanism for radical formation is postulated by Gugumus where he suggests that the main source of new radicals is hydroperoxide, which is formed from a charge transfer complex (CTC) of the polymer with oxygen (Gijsman 1996). The formation of a trans-vinylene group and hydrogen peroxide is a result of the reaction of the CTC (Gijsman 1996). Oxidation is than initiated by thermal or photochemical decomposition of hydrogen peroxide (Gijsman 1996).

Several external impurities that may contain chromophoric and/or photo-reactive groups include; traces of catalysts, solvents, additives such as pigments and stabilizers, compounds from polluted urban atmosphere and smog, and traces of metals, metal oxides, and metal salts from processing (Rabek 1996). The presence of copper remaining in polyethylene has been known to accelerate oxidation by an ionic mechanism (Davis 1983). Regardless of the initiation of photodegradation, hydroperoxides do accumulate and the concentration increases with time (Hoekstra 1997). The origin of the initiating primary alkyl radical R^* for the chain reaction is still controversial (Zweifel 1998).

Propagation:

$$R^\bullet + O_2 \rightarrow RO_2^\bullet \quad (2.1)$$

$$RO_2^\bullet + RH \rightarrow RO_2H + R^\bullet \quad (2.2)$$

Chain Branching:

$$ROOH \rightarrow RO^\bullet + HO^\bullet \quad (2.3)$$

$$2ROOH \rightarrow RO_2^\bullet + RO^\bullet + H_2O \quad (2.4)$$

$$RO^\bullet + RH \rightarrow ROH + R^\bullet \quad (2.5)$$

$$HO^\bullet + RH \rightarrow R^\bullet + H_2O \quad (2.6)$$

$$RO^\bullet \rightarrow \textit{chain scission processes} \quad (2.7)$$

Termination:

$$R^\bullet + R^\bullet \rightarrow \textit{crosslinking reactions to inactive products} \quad (2.8)$$

$$R^\bullet + RO^\bullet \rightarrow \textit{crosslinking reactions to inactive products} \quad (2.9)$$

$$R^{\bullet} + RO_2^{\bullet} \rightarrow crosslinking\ reactions\ to\ inactive\ products \quad (2.10)$$

$$RO_2^{\bullet} + RO_2^{\bullet} \rightarrow crosslinking\ reactions\ to\ inactive\ products \quad (2.11)$$

$$2R^{\bullet} \underset{Disproportionstion}{\rightarrow} RH + Olefin \quad (2.12)$$

Where RH is the polymer, $R^{\bullet}$ is the polymer alkyl radical, $RO^{\bullet}$ is the polymer oxy radical (polymer alkoxy radical), $ROO^{\bullet}$ is the polymer peroxy radical (polymer alkylperoxy radical), ROOH is the polymer hydroperoxide, and $HO^{\bullet}$ is the hydroxy radical. Equation 1 shows the reaction of a radical initiator and oxygen to form peroxy radicals. Peroxy radicals then abstract hydrogen from the polymer to form an alkyl radical (Equation 2.2). The abstraction of hydrogen by a peroxy radical (Equation 2.2) requires the breaking of the C-H bond (Zweifel 1998). This reaction (Equation 2.2) requires activation energy and is the rate-determining step in auto oxidation (Zweifel 1998).

Hydroperoxides are formed during the first processing steps of the melt (Equation 2.2). Under the combined actions of heat and mechanical shear in combination with oxygen during extrusion, peroxide radicals are formed that can further abstract hydrogen from the polymer and form hydroperoxides (Zweifel 1998). Hydroperoxides decompose to alkoxy and hydroxyl radicals and the rate increases with increasing temperature, however the decomposition reactions can proceed under the influence of light and metal ions in the presence of molecular oxygen (Zweifel 1998).

Once a free radical is formed on a polymer chain, C-H and C-C bonds on the carbon adjacent to the radical site are subject to cleavage as they have much lower bond dissociation energies than those associated with primary polymer molecule. The reduction in the energy required to break these bonds results from the gain in energy when a new double bond is formed either to carbon or to oxygen (Davis 1983).

Equation 2.3 is the ROOH photolysis. After initiation the subsequent chemical reactions result in hydroperoxides that in tern act as further initiators (Equations 2.3-2.4). After prolonged exposure carbonyl groups will form due to secondary reactions and will act as initiators above a certain level (Schoolenberg 1988). ROOH photolysis (Equation 2.3), hydrogen abstraction (Equation 2.5), β-scission of alkoxyls (Equation 2.7), and hydrogen abstraction (Equation 2.6) all have the same reaction rate k_1. Where k_1 is the equal to the quantum yield times the light intensity.

The main chain scission involves the breaking of the C-C bonds in the polymer backbone. It occurs as a consequence of primary photophysical processes or as secondary processes and results in a decrease in the average molecular weight (Rabek 1996). In addition, high mechanical forces as a result of extrusion, particularly in the amorphous region of the polymer, lead to C-C chain scission resulting in macroalkyl radicals (Zweifel 1998). If a polymer is cross-linked, its molecular weight is practically infinite (Ezrin 1996). Crosslinking is the formation of new intermolecular bonds resulting in the binding together of macromolecules (Rabek 1996).

Chain termination proceeds by the recombination of peroxy radicals when sufficient oxygen is available and the temperature is not too high (Zweifel 1998). When oxygen is the controlling reactant, the concentration of the primary alky radical is much higher than the concentration of the peroxy radical; chain termination is caused by the recombination of alkyl radicals with other available radicals (Equation 2.8 – 2.11). Equation 2.12 is an important termination reaction depicting the disproportionation of alkyl radicals (Zweifel 1998).

The formation of Ketones during photodegradation are especially important because they can lead to initiation via the Norrish I Reaction and further propagation or can contribute to chain scission by Norrish I or II reactions (Hoekstra 1997). It is believed that Ketone photolysis and β-scission of alkoxyls (Equation 2.7) are the most important processes of chain scission. The preceding reactions are all diffusion dependent because the reactions occur between a high viscosity melt or solid plastic phase and a gas – oxygen (Zweifel 1998).

Acid groups are formed from the Norrish type I reactions on ketone groups and may come from hydroperoxides (Tidjani 1993b). Vinyl groups may come from Norish type II reactions on ketones with significant amounts of this species possible formed from hydroperoxide decomposition (Tidjani 1993b).

Photochemical reactions in polymers are those connected with changing chemical structure of the system and can be divided into three stages; the absorptive act that produces an electronically excited state, the primary photochemical process that involves electronically excited states, and the secondary or dark (thermal) reactions of the radicals, radical ions, ions and electrons produced by the primary photochemical process (Rabek 1996). Bond dissociation is a direct photochemical process that causes polymer degradation (Rabek 1996). Photodegradation is a result of primary (photo-) and secondary (dark-) reactions that change a primary structure of the polymer by chain-scission, cross linking and oxidative processes (Rabek 1996)

2.6.2 Effect of Wavelength

The wavelength of absorbed light will determine the effectiveness for initiating photo oxidation. The critical wavelengths can be understood through the following equation

$$E = h\nu \qquad (2.13)$$

where h is Planck's constant and ν is the frequency. The energy of a photon increases as the wavelength decreases. Therefore it makes sense that higher frequencies are generally more harmful to polymers.

Ultra Violet light is the most significant factor in degrading polymers and results in photochemical reactions when either one of the following two conditions are met; the wavelength of the incident light is such that it can be absorbed by the polymer molecule (The energy of the photon is at least equal to the difference between any two energy

levels that a molecule can occupy), or that the energy of the absorbed photons is sufficient to dissociate bonds in the polymer molecules (the vibrational energy is at least that of dissociation) (Schoolenberg 1988).

One of the controlling factors of a polymers' resistance to outdoor weathering or photolytic stability, is the bond strength of the R group to the carbon atom to which it is attached (Ezrin 1996). In polyethylene a tertiary carbon atom exists at each polymer branch and is the site of rather poor photo-stability (Ezrin 1996). Based on the bond strength of 98 kcal/mole for the methane group (C-H) polyethylene would appear to resist outdoor exposure using the lower limit of the solar spectrum at sea level to be 295 nm or equivalently 97 kcal/mole, however this is not the case (Davis 1983). Some polymers do photodegrade because they have chemical bonds that can be broken by the more energetic wavelengths of the solar spectrum (Davis 1983). The critical wavelengths for polymers can be thought of as wavelengths less than 400 nm and greater than 295 nm, 295 nm being the shortest wavelength that is not filtered out by the atmosphere. It has been found that the wavelengths between 280 nm and 315 nm (UVB) are most damaging to polymer materials (Torikai 1995), with those found to be particularly effective in degrading polyethylene are those less than 300 nm (Davis 1983).

2.6.3 Rate of Degradation

The rate of photodegradation is influenced by the rate that oxygen diffuses into the polymer. The rate of diffusion of oxygen into a solid polymer is a relatively slow process and beyond a certain thickness it can become a rate controlling process (Bruijn 1992) and is altered by the wavelength distribution and intensity of light (Davis 1983). Oxygen deficient conditions generally occur during processing of the melt, and oxygen saturation occurs at the end of a products use (Zweifel 1998). The diffusion of oxygen occurs exclusively in the amorphous phase in polyolefins (Zweifel 1998).

In polyolefins, Cunliffe and Davis have quantitatively described the degradation profiles found experimentally using standard equations for oxygen diffusion and photo-oxidation kinetics (Cunliffe 1981). For artificial weathering with a constant light source, a steady state of oxygen diffusion is reached in which the oxygen concentration at each point attains constant value where the rate of removal of oxygen by photoreaction is balanced by the diffusion of oxygen in to the sample, and thus the oxygen profile does not change with time, though the level of degradation does. This assumption has proved valid by Ferneaux, Ledbury and Davis for a 3mm thick LDPE sample (Schoolenberg 1991). Schoolenberg did find however that up to a time of t_{50} (the time after which the fracture energy is reduced to 50% of the original value) the steady state condition does not occur (Schoolenberg 1991). It was also found that after prolonged exposure the shoulder in the profile does not remain at the same depth but rather shifts to deeper layers at longer exposure times (Schoolenberg 1991).

2.6.4 Extent of Degradation

Limited oxygen diffusion (Furneaux 1981) and or limited UV intensity (Ashbee 1993) will limit the effect of weathering in thick (> 1 mm) polymer parts to the surface (< 0.5 mm (Schoolenberg 1991)). Consider a monochromatic (one-wavelength) beam propagating through matter of any kind (solid, liquid, gas). Due to the absorption, μ, the intensity *I* is diminished by *dI* in distance *dx*. *dI/I* is linearly proportional to *dx* (Ashbee 1993),

$$\frac{dI}{I} = -\mu dx \qquad (2.17)$$

where the constant of proportionality μ is known as the linear absorption coefficient and its magnitude is dependent of the wavelength of the material. Integrating the above equation we are left with

$$I = I_o e^{-\mu x} \qquad (2.18)$$

Equation 2.18 says that the intensity falls off exponentially with thickness of material traversed.

The degradation depth is proportional to the square root of the oxygen diffusion coefficient (which decreases with increasing crystallinity) and inversely proportional to the square root of the oxidation rate. Equation 2.19 illustrates this relationship according to the theory of oxygen-limited photooxidation, the degradation depth, a_i, depends on D and r, the reaction rate (Bruijn 1996).

$$a_i \propto \sqrt{\frac{D}{r}} \qquad (2.19)$$

2.6.5 Effect to Morphology

The morphology of HDPE changes with UV-exposure. UV-exposure will lead to increased oxygen uptake increasing the density. At the same time chain scission will result in decrease in molecular weight. Hoekstra notes that in some cases the crystallinity can increase because of the phenomenon that free ends of polymer chains, originated from chain scission, can reenter the crystal lamella and is called chemicrystallisation that can increase the density (Hoekstra 1997). The change in morphology can affect the rate of oxidation. The increase in oxide groups can lead to an increase in the photooxidation rate if they act as chromophores. An increase in density and crystallinity could reduce the oxygen diffusion coefficient.

Photo oxidation of HDPE leads to a decrease in the molecular weight and mechanical properties due to chain scission and can lead to the localized micro cracks (Hoekstra 1997). The formation of micro cracks would require the strain rate to be decreased for ductile failure.

2.6.6 Effect of Crystallinity

Crystallinity imposes certain constraints on photo-degradation of polymers. The constraints due to crystallinity do not generally apply to absorption of UV irradiation and formation of excited singlet and/or triplet states, but rather to subsequent secondary reaction such as the nature and stability of radicals and diffusion rate of oxygen to these radicals (Rabek 1996). Crystallites, ordered chemical chains, behave similarly to chemical crosslink in that the greater the density of the crystallites, the less mobile are the chains in the amorphous or noncrystalline regions will be. This lack of mobility means that radicals that are formed in crystalline regions are essentially trapped and are not allowed to progress (Rabek 1996). Most photochemical reactions cannot occur in the crystalline state due to; the possible delocalization of the excitation through the crystal, the rigidity of the crystal lattice, the high symmetry and close packaging of the polymer molecules that reduces the free volume with a consequent reduction of chemical reactivity, or the lack of oxygen in the crystalline lattice (Rabek 1996). Higher degrees of crystallinity also increase thermomechanical stability (Rabek 1996). High density, i.e., high crystallinity, does however contribute to failures because it is more susceptible to stress cracking than lower density PE (Ezrin 1996).

Oxidation of semi-crystalline polymers such as polyolefins is generally considered to occur in the amorphous region or boundary phase between neighboring crystalline phases (Rabek 1996). Rabek cites several studies that have shown that crystalline regions of polyethylene are impenetrable to oxygen (Rabek 1996).

The ratio of chain scission to cross-linking during photo-oxidation depends on oxygen concentration and therefore varies with both crystallinity and specimen thickness (Davis 1983).

2.6.7 Effect of Moisture

Polymeric materials in the presence of water undergo several chemical and physical processes that seriously affect the mechanical properties of the material. Moisture can influence degradation reactions by extractive or hydrolytic processes. As water permeates into the polymer matrix, it behaves as a plasticizer resulting in a reduction in tensile strength and often an increase in ultimate elongation (Rabek 1996). During water absorption, compressive stresses dominate externally while tensile stresses dominate internally. The opposite holds true for desorption (Rabek 1996). Water absorbed will cause swelling in plastics. A subsequent dry period will then entail the loss of water leading to contraction of the surface layers, but since the underlaying layers may still be swollen, tensile stresses could arise on the surface that could result in cracking (Rabek 1996). Additionally moisture can participate in photochemical reactions involving pigments such as titanium dioxide (Gugumus 1990)

Water absorption is a diffusion-controlled process (Rabek 1996). The time determining factor for plastics is the diffusion coefficient, which is of the order of magnitude 10^{-8} cm^2

s^{-1} which means that it could take weeks or even months before moisture equilibrium is reached (Rabek 1996)

2.6.8 Temperature Dependence

Oxidation may occur in conjunction with radiation (UV, nuclear) or in air alone. In all cases, rate of reaction is faster at high temperatures (Ezrin 1996). The mobility of any polymer chain is the sum of all realized motions of the chain over a given time interval (Hoekstra 1997). The mobility of the polymers chain segments determines its mechanical properties. The mobility of the chains is described for local rotational motions by Arrhenius kinetics. The logarithm of the time in which an event (jump or movement of a chain segment) occurs is proportional to the inverse of the temperature. That is at high temperatures shorter times are needed for a polymeric material to relax than at low temperatures. This can be further explained because at high temperatures molecular chains move easier than at low temperatures. If the photon energy is great enough to sufficiently increase the temperature of the polymer resulting in melting of the crystal lattice, the necessary free volume could be present for significant photo-oxidation (Rabek 1996). Bruijn derived a relation stating that an increase in exposure temperature of 10 °C reduces the time to failure to less than half of its original value, while a decrease in exposure temperature by 10 °C will more than double the time to failure (Bruijn 1992). Time to failure is defined as the exposure time at which the average value of the total absorbed energy for HDPE specimens tested in bending equals the absorbed energy up to the peak for unexposed samples. From experimental results the temperature dependence of the reaction rate appeared to be small, but could be attributed to the small variations in exposure temperature (Bruijn 1996).

2.6.9 Effect of different Processing Conditions

Two common methods of processing polymers are injection and compression molding. Injection molding consists of melting the polymer and forcing it into the cavity of a closed mold. Injection molding is attractive because there is little variability between parts. Compression molding consists of placing a charge of polymer into the mold cavity that is closed under pressure so that the resin uniformly fills the mold. A significant difference between compression and injection molding is the temperature of the mold. In compression molding the mold is heated while in injection molding the mold is cold so that the polymer will cool much faster.

The processing of a polymer component can significantly affect mechanical properties or more specifically the density, the crystalline fraction, and the orientation of the polymer and fillers (Hoekstra 1997). Orientation results from the entanglement of the polymer chains due to cooling before they can relax. Orientation will influence the strength and stiffness of a polymer and will also affect the refraction of light. Orientation generally increases from the place in the mold that fills last to the entry location of the mold or gate. Additionally the processing of thermoplastics along with structural factors can dictate the degradation reactions during service conditions (Zweifel 1998). During processing the temperature required can be high enough to cause oxidative thermal

degradation. In addition the elastic stresses induced during the melt can result in the chain scission. Both degradation processes result in the formation of additional chromophores hence enhancing the photooxidation process. Cooling can result in variations in crystallinity with depth. Frozen in stresses at the surface could further lower the activation energy needed for radical formation (Hoekstra 1997).

For a thermoplastic material injection molding specimens is attractive, however some question must be raised about the degree of molded in stress. High local stresses can result in surface cracking of the specimens. To minimize frozen in stress, molding is done at as high a temperatures as possible, and cycle time is made as long as possible to allow the orientated polymer molecules to relax before cooling (Ezrin 1996). Another option is the use of compression molded specimens. Compression molded specimens can be expected to be practically free from residual stress (Davis 1983) and can be expected to have a more homogeneous morphology than injection molded specimens (Bruijn 1992). High stresses in natural HDPE have been shown to accelerate the physical deterioration of aged specimens. Similarly the residual internal stresses from molding can show up in weathering (Davis 1983). Stress can facilitate the rupture of polymer chains since it cause a distortion of the bond angles and an increase in interatomic distances. An applied stress increases the potential energy of the system and this has the effect of decreasing the energy required to cause degradation (Davis 1983).

Bruijn found that compression molded specimens had shallower degradation depths than injection-molded specimens (Bruijn 1992). He attributed this to the lower diffusion coefficient of the more crystalline compression molded specimens. The formation of surface cracks due to weathering has been found to be affected by processing. Surface cracks are formed by internal stresses between amorphous regions of varying oxidation degradation. The mobility of broken polymer chains in the more oxidized layer will be hindered by the less oxidized layer resulting in stresses. Compression-molded specimens usually have randomly oriented cracks while injection-molded specimens generally have cracks oriented perpendicular to the flow direction (Schoolenberg 1991).

2.7 Polymeric Additives

Additives are commonly used in the manufacture of polymeric products. Additives are used for a variety of reasons including; modifying optical properties, light and thermal stabilization, fungal control, and reducing cost.

2.7.1 Colorants

Colorants or pigments are added to polymers for aesthetic reasons. Pigments may influence the light stability of plastics both favorable and unfavorable. Pigments may act as chromophores, and may reduce the UV stability. Pigments that may reduce the photstability include organic yellow and organic red pigments. Pigments may also act as UV absorbers in thick products, effectively reducing the depth that UV light is absorbed. Predictions of the life of HDPE containing 2 –5 % carbon black (<19mμ) from weathering studies suggest that the material will resist photo-oxidation for at least 40

years (Davis 1983). Pigments in the blue-violet range give poorer protection than those in the red range probably because of the greater opacity of the latter to ultraviolet radiation (Davis 1983). The use of iron oxide, a smoke suppressant will additionally aid fire tests that are to be performed (Pritchard 1998).

2.7.2 Light Stabilizers

Light stabilizers are chemical compounds that can reduce the chemical and physical effects of light-induced degradation. Stabilizers are grouped according to their intended function, UV absorbers, quenchers of free radicals, hydroperoxide decomposers, and free radical scavengers.

UV absorbers protect polymer materials by absorbing harmful radiation and dissipating the energy as heat. Common types include hydroxybenzophenones and hydroxyphenyl benzotriazoles. A disadvantage of UV absorbers is that they require an absorption thickness to fully absorb UV light making them not suitable for thin films and polymer fibers.

Light stabilization by quenching of free radicals occurs when the energy absorbed by chromophores is dissipated either as heat or as fluorescent or phosphorescent radiation. These reactions occur when the quencher has a lower energy state than the chromophore. Quenchers are useful in the stabilization of thin films because their action is independent of specimen thickness.

Hydroperoxide decomposers reduce the hydroperoxide concentration of polymers effectively reducing the amount of free radicals than can be formed from phtolysis. Common types are metal complexes of sulfur-containing compounds.

Free radical scavengers work by reducing the number of free radicals that can generate hydroperoxides. An important group of scavengers are hindered amine light stabilizers (HALS). Though the mechanisms of HALS stabilization is still uncertain the process is thought to consist of the scavenging of radicals by a nitroxide formed during degradation. HALS have been shown to extend the lifetime of thin PE films from 3 months to over 5 years (Gugumus 1990).

Stabilizers tend to concentrate in the amorphous regions giving greater protection to these areas (Davis 1983). Degradation is most marked in the amorphous phase as opposed to the crystalline phase presumably because of the lower solubility and rate of diffusion in the latter and so stabilizer is most concentrated in the region it is most needed. It has been found that for PE stabilized with a hindered amine light stabilizer (HALS), the major part of the oxygen uptake was converted into gaseous products while the degradation of unstabilized PE resulted in many different products (Gijsman 1996). Hindered amines are organic optical brighteners that absorb ultraviolet radiation below 300 nm and emit it as visible radiation below about 550 nm (Pritchard 1998).

Optimum light stabilization of polyolefins can be achieved through the use of a combination of light stabilizers, specifically HALS and UV absorbers (Gujumus 1995).

2.7.3 Fungicides

Many environments that NFTC are used are conducive to fungal growth. Fungal growth could lead to the decay of the composites organic components resulting in the loss of mass and mechanical properties ultimately leading to possible failure of the system. A common fungicide is zinc borate which is an excellent after-glow suppressant, flame retarded and char promoter (Pritchard 1998)

2.7.4 Coupling agents

Mechanical behavior of NFTC is determined by the fracture strength of NFTC and is caused by the delamination of the fiber from the polymer matrix (Razi 1999). Delamination is controlled by the interfacial adhesion between the matrix and fiber reinforcement. Thermoplastics are non-polar (hydrophobic) substances that are generally not compatible with polar (hydrophilic) natural fibers. Processing of these two incompatible materials could result in poor interfacial bond. In order to resist delamination and improve on the poor compatibility between natural fibers and thermoplastics, a chemical coupling agent or electron irradiation can be used.

Coupling agents can be classified as bonding agents or surfactants that include compatibilizers and dispersing agents. Bonding agents' bridge natural fibers to thermoplastic polymers through chemical bonding and entanglement. Compatibilizers improve compatibility by modifying the solubility parameters of the fiber surface to more similar to the polymer matrix. Dispersing agents function by reducing interfacial energy between the fiber and matrix promoting more uniform dispersion in the polymer matrix

Over forty chemical coupling agents have been used in wood fiber plastic composites (Lu 2000). Coupling agents are generally added at 1-3% of the total weight of the composite with the concentration generally determining the coupling effectiveness in the composite (Lu 2000).

The most popular chemical coupling agents are isocycnates, anhydrides, silanes, and anhydride-modified copolymers such as poly[methylene(polyphenyl isocyanate)] (PMPPIC) and Maleated Polypropylene MAPP. MAPP and maleated polyethylene (MAPE) bonding agents act as compatibilizers that provide compatibility between otherwise immiscible polymers by reducing interfacial tension (Lu 2000). It has been shown that MAPP is effective in improving processing and impact strength for conifer (Chuai 2001) and wood flour PP composites (Li 2001). Chuai not only found an improvement in the mechanical properties of PP-conifer composites but improvement in processability with the addition of MAPP (Chuai 2001). Li additionally showed that composites with 30% and 40% wood flour had greater impact strength than even neat PP resin (Li 2001). Chemical coupling agents have also been shown to increase high temperature modulus, and softening temperature over uncoupled systems (Feng 1995).

In addition to using chemical coupling agents, Xu presents the use of electron beam irradiation for improving interfacial bond with hydrophilic reinforcement (Xu 2000). Through irradiation in air, some oxygen containing groups can be introduced on the HDPE molecular chain and the interface compatibility can be improved. Xu showed that the tensile and impact strength of irradiated HDPE and sericite-tridymite-cristobalite (STC), a natural flaky sericite, composites were improved after irradiation. Xu concluded that the strong interfacial adhesion between irradiated HDPE and STC minimized the propagation of cracks. Care must be taken however to avoid excessive degradation of the polymer during irradiation.

2.7.5 Process Stabilizers

Process Stabilizers or antioxidants are used to minimize the effects of degradative reactions that occur during the processing or compounding of polymer parts. There are two classifications of antioxidants primary and secondary. Primary antioxidants act as radical scavengers and consist of hindered phenols and aromatic amines. Secondary antioxidants act as hydroperoxide decomposers and consist of thioesters and phosphites. Processing stabilization is usually achieved with combinations of high molecular mass phenolic antioxidants with phosphites or phosphonites (Gugumus 1995). It has been shown that some processing antioxidants do not have a significant effect of the photoxidation rate (Tidjani 1993b). Process stabilizers are important because they will limit the formation of hydroperoxide chromophores during processing that could influence photooxidation during service.

2.7.6 Fillers

Fillers are used with polymeric materials for reinforcement and or to reduce the cost of a product. Composites are polymers that contain fillers that improve the mechanical properties. Typically inorganic materials including calcium carbonate and glass fibers are used as fillers. Recently organic materials, predominantly wood flour (wood ground in a very fine particle form) and other natural fibers (lignocellulosics) are being used as fillers. Wood flour performs similarly to talc and other mineral fillers with the advantage of reduced weight due to lower specific gravity. Natural fibers fillers are relatively non-abrasive to processing equipment and less expensive than synthetic or inorganic fillers. Additionally the popularity of these fillers has increased as interest in using renewable resources has increased.

2.8 Common Types of Lignocellulosics

Natural fibers are readily available renewable resources that are pervasive throughout the world in plants. These fibers are generally referred to as lignocellulosic or cellulosic fibers because of the principal chemical components lignin, a polyphenolic polymer and cellulose the principal chemical component of the fiber. The lignin, hemicellulose, and surface of the cellulose are amorphous regions while interior of cellulose is crystalline in

nature. The properties of these fibers are dependant upon the fibrillar structure and lamellae matrix.

A variety of cellulosic fibers have been studied as fillers in thermoplastic composites. These fibers include but are not limited to, bagasse, cereal straw, cornstalks, jute, kenaf, nettles, peanut hulls, rice husks, ricestraw, sisal, wood and wood flour. Cellulosic fibers have similar advantages to thermoplastics such as low cost, low density, high specific strength and modulus, availability, and pose limited health problems to humans. Disadvantages of natural fibers include low processing temperatures, and are generally incompatible with thermoplastics without surface treatment.

2.9 Mechanical Properties of Lignocellulosics

The mechanical properties of some lignocellusic materials (particularly lumber and timber) have been studied extensively. A variety of mechanical properties of structural wood products have been determined through exhaustive testing and are well documented and published in building standards. Difficulties arise when determining mechanical properties of individual fibers and fiber components due to the relative scale of the fibers in question.

The mechanical properties of lignocellulosics are generally superior to those of thermoplastics. The tensile strength and modulus of elasticity for HDPE can range from 18 – 35 N/mm^2 and 700 - 1400 N/mm^2 respectively. The tensile strength and modulus for individual virgin wood fibers ranges from 350 – 900 N/mm^2 and 14000 – 42000 N/mm^2 respectively (Groom 95). Groom 1995 found that the mechanical properties of individual virgin fibers from plantation loblolly pine were superior to those from either agricultural or recycled fibers. The average tensile strength of some other lignocellulosics fibers are; kenaf = 1190 N/mm^2, hemp = 900 N/mm^2, sisal = 610 N/mm^2, cotton = 350 N/mm^2 (Rowell 2000). The mechanical properties of lignocellulosic are greatly influenced by the moisture content.

2.10 Physical Characteristics of Lignocellulosics

The physical characteristics of lignocellulosic are as varied as the sources from which they are obtained. The fiber aspect ratio (L/D) of lignocellulosic fibers is highly variable and depends on the processing conditions and source. Lignocellulosics also come in a variety of colors, densities and specific gravities, which are dependant upon the type, age and season at harvest, and what part of the plant the fiber came from.

A popular lignocellulosic filler is wood flour. Wood flour is produced from dry wood waste through grinding and sized by mechanical screening. Variation in resin content occurs within a species and will therefore occur in the flour. Variation in manufacturing methods results in wood flour particles that are different in structure and shape. In dry mechanical production of wood flour, the wood particles are generally fragmented cell bundles or single cells.

2.11 Weathering of Lignocellulosics

The weathering of lignocellulosics materials is primarily caused by the combined actions of ultraviolet (UV) light, water, heat, and abrasion. Weathering mainly results in the loss of lignin and hemicelluloses resulting in weight loss (Evans 1992). Almost every chemical constituent (cellulose, hemicelluloses, lignin, and extractives) is sensitive to UV light with consequential deterioration effects. Of the chemical constituents, lignin is oxidized and degraded by UV light most rapidly and leads to radical induced depolymerisation of both lignin and hemicellulose (Evans 1996). It has been reported that lignin absorbs 80 –95% of the total absorbed light (Hon 2001). However due to the strong ultraviolet-absorbing characteristics of lignin, it may also function as a shielding agent to protect cellulosic material. Again photodegradation is a free radical driven series of reactions. Defiberization, or loss of surface wood cells, occurs more rapidly in the thin-walled fibers of springwood than summerwood.

2.11.1 Photooxidation Process

Photooxidation of wood is similar to the radical chain reactions in other polymers in that it can be divided into three separate processes: initiation, propagation, and termination.

Initiation:

$$RH \rightarrow R^{\bullet} + H^{\bullet} \qquad (1)$$

Propagation:

$$R^{\bullet} + O_2 \rightarrow RO_2^{\bullet} \qquad (2)$$

$$RO_2^{\bullet} + RH \rightarrow ROOH + R^{\bullet} \qquad (3)$$

Termination:

$$RO_2^{\bullet} + RO_2^{\bullet} \rightarrow non-radical\ product \qquad (4)$$

$$R^{\bullet} + RO_2^{\bullet} \rightarrow non-radical\ product \qquad (5)$$

$$R^{\bullet} + R^{\bullet} \rightarrow non-radical\ product \qquad (6)$$

Where RH are the chemical components cellulose, hemicelluloses, and lignin at the wood surface. Initiation consists of the formation of free radicals due to irradiation of UV light (1). Oxygen in the system will react with the free radicals to form hydroperoxy radicals (2), and hydroperoxides (3). The photooxidation process ends when the radicals and hydroperoxides further react to form non-radical products.

2.11.2 Effect of Wavelength

The rate and type of radicals formed due to photooxidation are dependant upon the wavelength. When the wavelength is longer than 340 nm, cellulose in the presence of oxygen will form alkoxy and carbon radicals. When the wavelength is longer than 280 chain scission and dehydrogenation occur (Hon 2001).

Lignocellulosics contain functional groups called chromophores that will absorb light. The amorphous regions of cellulose absorb light strongly between 200 – 300 nm, with a tail of absorption extending to 400 nm (Hon 2001). Lignin and polyphenols absorb light strongly below 200 nm and also have a strong peak at 280 nm, with absorption extending through the visible spectrum (Hon 2001). The crystalline regions of cellulose are completely impervious to light (Hon 2001).

2.11.3 Rate of Degradation

The rate of photodegradation of cellulose is dependent on the intensity and energy distribution of light and on the species of lignocellulosic. The rate of oxidation can be accelerated by UV light, heat, and metal ions (Hon 2001).

2.11.4 Extent of Degradation

The extent of degradation in wood is generally limited to the surface, either due to limited light penetration and or protection of deeper layers by already degraded fibers. Microscopic changes can be observed in degraded wood. In softwood degradation results in the enlargement of bordered pits in the radial wall of earlywood tracheids (Hon 2001).

The depth of degradation of solid wood is limited to 0.2 – 0.5 inches per 100 years. The most significant changes occur in the first several years, and can be attributed to both the limited depth of ultraviolet penetration (75μm) and the shielding of all ready damaged fibers (Hon 2001).

2.11.5 Effect of Moisture

Lignocellulosic materials are naturally hydrophilic meaning they have an affinity towards water, however moisture is not accessible to the crystalline regions of cellulose. This attraction results in dimensional instabilities that can lead to changes in stresses. Water may penetrate into and swell cell walls leading to a reduction in hydrogen bonding (Hon 2001). It has been shown that when wood was exposed to fluorescent light, the concentration of free radical increased as the moisture content increased from 0 – 3.2% and reached a peak at 6.3% (Hon 2001). It has been suggested that the principal role of water is to facilitate light penetration into previously inaccessible regions (Hon 2001). It has been reported that the loss in weight of wood due to photodegrdation is much greater in the presence of water possibly indicating that water-soluble products are formed (Hon 2001).

Generally synthetic polymers such as thermoplastics are less influenced by moisture than naturally occurring polymers such as wood. The amount of moisture that wood will

absorb is dependent upon the relative humidity and influence most properties. The diffusion coefficient in the transverse direction of solid sawn wood is of the order of 20 x 10^{-8} cm^2s^{-1}, and an order of magnitude higher in the longitudinal direction (Tarkow 1981).

2.11.6 Photo-protection of lignocellulosics

A considerable amount of research has been conducted on the protection of wooden decking and siding. Research has examined the use and application of various stains and paints on the life of these products of which two inorganic salts, chromic acid and ferric chloride, appear to protect wood finishes against UV irradiation (Chang 1982).

2.12 Common Types of Natural Fiber Thermoplastic Composites

A wide variety of NFTC exist and are currently manufactured. NFTC can generally be processed using the same techniques as unfilled thermoplastics. Polyolefins are attractive for use in NFTC due to low meting point and relatively inexpensive cost. The low melting temperature allows for the mixing of the fiber and polymer with minimal thermal fiber damage. There is a wide variety of commercially available NFTC parts and products. Applications include interior automotive panels, interior trim, molding and flooring, exterior decking and inexpensive packaging and small appliance housings. Generally these composites are intended for non – or semi – structural applications.

2.13 Mechanical Behavior of Fiber Composites

The performance of any composite is based on its constituents and how they interact. Specifically for fiber based thermoplastic composites, the performance and properties are governed by the interaction and adhesion between the polymer matrix and the strengthening fiber. The transfer of load occurs, assuming perfect interfacial bond between the fiber and matrix, along the entire length of the fiber through the shear strength in the direction of the fiber of the matrix. More specifically the properties depend on the physical and mechanical properties of the fiber, fiber distribution, orientation and concentration, the polymer and its polymerization process, and stress transfer between fibers and the fiber matrix interface. Generally failure of such composites is a direct result of the delaminating of the fiber from the polymer matrix.

2.13.1 Effect of Lignocellulosic Concentration, Size, and Type

A variety of studies have evaluated the effects of flour or fiber concentration and size on the mechanical properties of NFTC (Berger 1997, Chuai 2001, Keruvilla 1993, Li 2001, Razi 1997, 1999, Sanadi 1995, Simonsen 1997, Stark 1997).

The flexural strength of NFTC is generally greater than that of unfilled thermoplastics but does decrease with increasing flour or fiber content. The flexural modulus is generally greater than unfilled thermoplastics and generally increases with increasing fiber content. The flexural strength decreased 7% - 18% when the content of wood flour increased from

20% - 60% (Berger 1997). Berger found a nearly linear relationship between the increase in flexural modulus and increasing filler content for wood flour PP composites (Berger 1997). The flexural modulus of 20% PP composites was found to increase 200% - 250% when 60% wood flour was added, depending on the type of flour used (Berger 1997). Razi found that both the size and concentration of the fiber reinforcement had an effect on the mechanical properties of wood chip - HDPE composites (Razi 1997). It was found that the flexural strength and stiffness of composites with the same percent of wood chips by volume decreased 15% to 40% as the size increased from 0.32 cm (0.125 in) to 1.27 cm (0.5 in), depending on the content. These results were attributed to larger continuous interface between the wood chips and polymer matrix over which the crack can propagate. He also found that the bonding strength on the interface to be lower than the strengths of the individual polymer or wood and is likely the result of residual stresses on the interface and poor bonding.

The tensile modulus of NFTC generally increases with increasing fiber content but the tensile elongation generally decreases with increasing flour or fiber content. Li showed that the tensile modulus increased as the content of wood flour increased from 5% to 40% (Li 2001). The maximum tensile strength of 60% uncoupled PP wood flour composites was 70% - 75% that of 20% uncoupled PP wood flour composites and depended on the type of flour used (Berger 1997). Li showed that tensile strength of 40% wood flour – MAPP – PP composites was 15% greater than similar composites with 5% wood flour (Li 2001). It was also reported that necking was not observed when the filler content was equal to or higher than 10% (Li 2001). Sanadi showed that the tensile strength of 60% kenaf fiber PP – MAPP composites was nearly 200% greater than unfilled PP composites (Sanadi 1995). Stark found that the percentage of tensile elongation increased as the size of wood flour increased for PP wood flour composites (Stark 1997).

The notched impact strength of NFTC generally increases and unnotched strength generally decreases with increasing percentage of flour or fiber filler. The notched impact strength is generally greater than unfilled thermoplastics but the unnotched impact strength is generally less than unfilled thermoplastics. Chuai 2001 found that the notched impact strength of PP composites increased between 14% and 70% when the concentration of conifer fibers increased from 0 – 50% and was dependent upon the compatibilizer used. Likewise Berger 1997 found that the impact energy of PP composites increased 15% to 40% when the concentration of wood flour increased from 20 – 60%. The notched impact energy of PP composites with 20% and 30% wood flour was less than that of the unfilled PP but greater than unfilled PP when the flour concentration was greater than 40% wood flour. The unnotched impact energy decreased for PP wood flour composites between 60% and 70% for fiber concentrations between 20% and 60%. The unnotched impact strength was between 15% and 20% that of the unfilled PP. Li 1997 found that the notched impact strength increased 20% when the content of wood flour increased from 5% to 40% for PP composites with MAPP. Conversely he found that the notched impact strength decreased 10% when the content of wood flour increased from 5% to 30%, but increased from 30% to 40% for uncoupled PP composites. PP composites filled with ponderosa pine wood flour outperformed composites of oak and maple flour in impact (Berger 1997). Stark 1997 found that the

unnotched impact strength decreased 40% and notched impact strength increased as the average size of wood flour increased for 40% wood flour filled PP composites without a coupling agent.

2.13.2 Effect of Processing on Fiber Orientation

The orientation of fibers in the polymer matrix influences the mechanical properties of the composite. Mechanical properties are generally greatest in the direction of fiber reinforcement. Fiber composites are generally anisotropic. Anisotropy is introduced during processing due to the orientation of molecules, fillers, and fibers in the flow of the mold cavity or die. The degree of fiber orientation increases with decreasing wall thickness (Osswald 1995). Generally fiber orientation is more complex in injection-molded parts than in compression-molded parts

The orientation of particles in injection-molded parts can be complex. It is accepted that injection molded parts can be divided into seven layers with different fiber orientations due to the velocity gradient in the mold (Osswald 1995). The seven Layers are: Two thin outer layers with a biaxial orientation, random in the plane of the mold surface, two thicker layers next to the outer layers with a main orientation in the mold direction, two thin randomly oriented transition layers next to the central core, and a thick central layer with orientation perpendicular to the mold direction. The orientation of these layers can be attributed to a phenomenon referred to as the *fountain flow effect*. The fountain flow effect is caused by a no-slip condition on the mold walls. As material enters the mold cavity, material is forced from the center to the mold surface. This material is frozen instantly upon contact with the walls.

During compression molding the material is deformed uniformly through the thickness with slip occurring at the mold surface (Osswald 1995). In compression-molded parts, fibers align themselves parallel to the direction of flow throughout the thickness of the specimens. Orientation is again increased in thinner specimens and as the percentage of charge mold coverage is increased. In compression molded parts a phenomenon can occur referred to as knitlines. Knitlines are regions in a part where few or no fibers bridge. Knitlines are common when multiple charges are placed in the mold cavity, and are located where two flowlines meet.

2.14 Weathering of Fiber Composites

2.14.1 Effects on Mechanical Properties of NFTC

Dash found that the flexural strength decreased 30% - 40% after 45 days of outdoor weathering depending on the fiber surface treatment for 60% jute polyester composites (Dash 2000). He also found that the flexural stiffness decreased 18% for the same composites exposed for 45 days.

Dash found that the tensile strength of 60% jute-polyester composites decreased 30% after 45 days of outdoor weathering (Dash 2000). He also found that the tensile modules

increased 20% for these same composites. It is suggested that moisture absorbed during weathering weakens the interface due to void formation and further acts like a plasticizer for accelerating delamination.

2.14.2 Effects on Optical Properties of NFTC

Rowell found that a combination of accelerated UV exposure and water spray results in increasing brightness of PP-aspen fiber composites (Rowell 1998). It was found that the increase in brightness was also non-linear for the 2000 hours of exposure with the most significant whitening occurring during the first 1000 hours. It was reported that the surface of these composites became rough and chalky after the exposure.

Falk found that increasing the concentration of wood flour increased the brightness of exposed HDPE and PP-wood composites (Falk 2000). It was also reported that the addition of red and black colorants reduced the effects of accelerated weathering. Matuana similarly found that the addition of titanium dioxide photoactive pigment reduced the color changes associated with accelerated UV weathering (Matuana 2001). Matuana suggests that the incorporation of wood fibers with PVC negatively affects the ability of the matrix to resists accelerated UV weathering (Matuana 2001).

Kiguchi found that grafting of benzophenone type UV absorber to the wood fiber reduced the discoloration associated with accelerated weathering in ethylene vinyl acetate composites (Kiguchi 2000).

2.15 Test Standards

2.15.1 Flexural Testing

Flexural testing is commonly used in the evaluation of building materials. The flexural properties of a product are dependent upon the test setup, orientation, and speed. Two types of flexural tests that are used are static bending and impact testing. These tests differ by the rate of crosshead motion. ASTM has published standards outlining test methods for both static bending and impact tests for plastics; ASTM D-790 Flexural Properties of Unreinforced and Reinforced Plastics and Electrical Insulating Materials, ASTM D256 Impact Resistance of Plastics and Electrical Insulating Materials and, ASTM D6109 Standard Test Methods for Flexural Properties of Unreinforced and Reinforced Plastic Lumber.

2.15.2 Tensile Testing

When determining the mechanical properties of plastics a common test method is the tensile test. The tensile test is valuable for generating stress-strain data that can be used for determining properties. ASTM D638 outlines a test method for tensile testing of plastics.

2.15.3 Chromaticity Measurements

Previous research has shown that the change in color is an effective tool for measuring the affects of accelerated weathering (Falk 2000, Kiguchi 2000, Matuana 2001). One method for determining a products color is through the use of a tristimulus color analyzer. A tristimulus color analyzer is used to measure reflective colors of surfaces. One commercially available tristimulus color analyzer is the Chroma Meter, manufactured by Minolta. The Meter has a 8mm-diameter measuring area and uses diffuse illumination and a 0^0 viewing angle (specular component included). The Meter encompasses a pulsed xenon arc lamp in a mixing chamber that provides diffuse, even illumination over the specimen surface. Six high-sensitivity silicon photocells filtered to match the Commission Internationale de I'Eclairage (CIE) Standard Observer Response, were used to measure both incident and reflected light and compose the optical cable. The optical-fiber cable for color analysis collects only light reflected perpendicular to the surface. For the purpose of this study, a color system was chosen for measurement that closely represents human sensitivity to color. The CIE L^*, $a^*$and, b^* Cartesian color system was chosen to measure absolute chromaticity (hue and chroma) along with a third factor of lightness to describe the color precisely. The lightness factor, L^* is expressed as a percentage based upon perfect reflectance. Formulas for calculating L^*, a^*, b^* are shown in Appendix 1. ASTM D2244 Calculation of Color Differences From Instrumentally Measured Color Coordinates outlines a test method for evaluating the affects of a particular treatment on the daylight illumination of small color differences.

2.15.4 Ultra Violet Weathering Tests

ASTM has published a variety of standards that discuss the basic principals and operating procedures for accelerated weathering apparatus (Table 2.1)

Table 2.1 Standard Test Methods of Accelerated Weathering	
ASTM G23	Operating Light-Exposure Apparatus (Carbon-Arc Type) With and Without Water for Exposure of Nonmetallic Materials,
ASTM G26	Operating Light-Exposure Apparatus (Xenon-Arc Type) With and Without Water for Exposure of Nonmetallic Materials
ASTM G53	Operating Light-Exposure Apparatus (Fluorescent UV-condensation type) With and Without Water for Exposure of Nonmetallic Materials
ASTM G141	Addressing Variability in Exposure Testing on Nonmetallic Materials
ASTM G147	Conditioning and Handling of Nonmetallic Materials for Natural and Artificial Weathering Tests
ASTM G151	Exposing Nonmetallic Materials in Accelerated Test Devices that Use Laboratory Light Sources
ASTM G155	Operating Xenon Arc Light Apparatus for Exposure of Nonmetallic Materials
ASTM D2565	Xenon-Arc Exposure of Plastics Intended for Outdoor Applications.
ASTM D4364	Practice for Performing Accelerated Outdoor Weathering of Plastics Under Concentrated Natural Sunlight

2.16 Differences and Similarities Between Natural and Accelerated Weathering

Several options are available for artificial weathering light sources but the xenon-arc source provides a better simulation of the solar spectrum than the carbon-arc source (Davis et. al. 1983). Xenon arcs require filters to remove unwanted radiation however it is important to determine the solar cut off of the filter. As xenon-arc lamps age, they experience light output decay that must be monitored to provide consistent irradiance. Two common irradiance settings are 0.35 W/m^2 and 0.55 W/m^2 at 340 nm. 0.35 W/m^2 compares with winter sunlight while 0.55 W/m^2 compares more closely with summer sunlight. Brennen suggests that for simulations of exposure to direct sunlight, artificial light sources should be compared to the solar maximum condition (Brennen 1988). The solar maximum condition is global noon sunlight on the summer solstice. The solar maximum is the most severe condition that a material will be subject to leading to a better indication of the relative performance of materials.

Though weathering tests can provide an indication of which materials may perform better in service conditions, the durability of a material weathered naturally may be significantly different from those exposed to accelerated weathering. It has been presented that the degradation of polymers is dependent upon temperature, spectral distribution, and light intensity. So to develop good correlation between accelerated and natural weathering the different factors need to be accelerated consistently from those in natural environments.

If methods of accelerated aging use too high of a temperature range, primary degradation of the surface layer will be caused by high reaction rate of oxidation and relatively low diffusion rate of the oxygen (Zweifel 1998). Differences in the infrared region between natural and accelerated weathering can cause the surface temperature of specimens to be quite different resulting in differences in the oxidative processes. If the output of the accelerated aging lamp extends below 295 nm (the cut off of solar radiation), it is possible that reactions could occur in the chamber that are not possible outdoors.

UV is easily filtered. Therefore, cloud cover, pollution, moisture can all affect the amount of spectra a material will see. In the winter the sun is lower in the sky resulting in a greater air mass that the light must pass through. This increase in distance results in a decrease in the lower more damaging UV wavelengths. In Cleveland Ohio for example, the intensity of UV at 320 nm changes by a factor of 8 from summer to winter (Brennen 1988). As a result, the solar cut off, the shortest wavelength not absorbed or scattered by the earths atmosphere, shifts from about 295 nm in the summer to 310 nm in the winter making materials that are sensitive to wavelengths below 310 nm relatively stable in the winter.

A significant amount of durability research has been conducted evaluating the effects of both accelerated and natural weathering (Cunliffe 1982, Bruijn 1992, Feist 1978, Furneaux 1981, Gijsman 1996, Gugumus 1995, Tidjani 1993a, Tidjani 1993b). These studies have looked at the differences between accelerated and natural weathering for, elongation at break, erosion rate, degradation profiles, stabilizer performance, oxygen

uptake, and chemical composition. Care should be taken when comparing durability results from different natural and accelerated weathering conditions. Samples exposed in Florida for example, would be subjected to different levels of UV radiation and temperatures than specimens exposed in Alaska. Likewise, specimens irradiated with Xenon – arc lamps would be exposed to different spectral distributions than those irradiated using fluorescent lights.

It has been shown that the changes in elongation at break for naturally weathered Linear low density polyethylene (LLDPE) specimens occurred more rapidly than those specimens exposed to artificial accelerated weathering (Tidjani 1993a). Gijsman also showed that for significant loss in elongation at break, there was twice the oxygen uptake for specimens weathered in sunlight than those specimens exposed to accelerated conditions (Gijsman 1996).

Feist showed that erosion rate of vertical grained western redcedar exposed to 15 weeks of accelerated weathering decreased in relation to the erosion rate of specimens naturally weathered outdoors for two years (Feist 1978).

Bruijn found that for samples exposed to different conditions, the depth of degradation and the slope at which the degree of degradation decreases from the surface varied, with those samples exposed outdoors having the greatest depth of degradation (Bruijn 1992). He also found that the degradation profiles of samples exposed by both accelerated aging devices and in natural conditions in Miami, Florida showed a constant degradation depth with exposure time.

Most accelerated weathering devices show poor correlation between UV stability measured with them and those measured outdoors (Gijsman 1996). The difference in UV stability has been explained by Fourier Transform IR (FTIR) studies that have suggested that the lack in correlation may be due to the differences in degradation mechanisms. Gijsman found that for PE specimens weathered outdoors, the ratio of end unsaturation to carbonyl groups was higher than for specimens that underwent accelerated weathering (Gijsman 1996). One explanation for the higher ratio of end unsaturation to carbonyl groups for PE samples weathered outdoors than accelerated is that the initiation by a CTC is more efficient in outdoor weathering because the stability of a CTC increases with decreasing temperature. The mean monthly temperature was lower for specimens exposed outdoors than accelerated. It was finally concluded that in accelerated weathering, oxygen was predominantly consumed via the propagation reaction and results in ketones and chain scission. In outdoor weathering, most of the oxygen absorbed was converted through a CTC into water with only a minor part consumed during propagation. Tidjani found that chain scission reactions outnumber crosslinking reactions during early exposure of naturally exposed LLDPE specimens while crosslinking reactions tend to outnumber chain scission reactions for artificially weathered specimens (Tidjani 1993a). Gijsman suggests that an increase in oxygen pressure in accelerated weathering or decrease in temperature should lead to more initiation through a CTC and better correlation with outdoor weathering (Gijsman 1996).

It is reasonable to assume that the day/night cycle experienced by samples exposed under natural conditions can result in a weathering process that is significantly different from that induced by continuous exposure to an artificial source. Thermal oxidative processes catalyzed by active intermediates remaining after sunset, such as hydroperoxides, the diffusion of additives or degradation products, and the opportunity for oxygen replenishment are some of the processes that could occur during the dark periods of natural weathering that would not occur in continuous artificial exposure. Bruijn suggests that long dark periods enable oxygen diffusion into deeper layers of the polymer and can explain the increasing degradation depth with time of samples exposed in Delft as compared to samples exposed in Florida and in the weatherometer were degradation depth showed a horizontal plateau with time (Bruijn 1996). It is also reasonable to assume that different seasons would result in different degradation processes. Gijsman found that LDPE films did not degrade during autumn and winter (Gijsman 1996). It was concluded that the outdoor oxidation rate during the summer period is comparable to that in accelerated weathering if degradation only occurred for 9.6 hours a day (daylight hours).

The most direct way of studying the oxidation of polymers is to measure the oxygen uptake, however, it has been found that oxygen uptake curves for accelerated and natural exposure conditions in the Netherlands were totally different (Gijsman 1996). During accelerated aging the oxygen uptake started immediately and was essentially linear with time. During natural weathering the oxygen uptake varied seasonally. During autumn and winter there was almost no oxygen uptake, an increase in spring until summer when the rate of oxygen uptake became constant (Gijsman 1996).

One proposed method for predicting the service life of accelerated parts is to use an acceleration factor. An acceleration factor uses the difference in the time between weathering conditions required to reach a change in a particular property. Measured acceleration factors have been shown to be different depending on the property selected. Tidjani showed that the acceleration factor for the change in elongation at breaks for LLDPE was half of that required for the change in absorbance (Tidjani 1993a). Due to these differences it is suggested that a useful acceleration factor be a combination of changes to both mechanical and physical properties.

A simple method to relate accelerated weathering conditions to natural accelerated conditions would be to equate the total radiant exposure of the product. Vincent found that the radiant exposure at 340 nm was not a unique value for the time to failure, similarly Bruijn found that for the radiant exposure between 300-400 nm and 295-385 nm time to failure was not the same for the same radiant exposure (Bruijn 1992).

The relationship between accelerated and natural weathering is not direct. Accelerated weathering does however provide a practical option for determining the relative durability of materials intended for outdoor applications. Further research is needed if accurate predictions of material durability are desired from accelerated tests.

Chapter 3. Phase I. Effects of Different Fillers and Additives on the Durability of Natural Fiber Thermoplastic Composites

3.1 Introduction

The research presented in this chapter served as a screening study to evaluate several NFTC formulations to be used in the roofing product described in Chapter 6. The results presented in this chapter were also used to design the NFTC formulations and test matrix in Chapter 4 and 5.

The objective of the research presented in this chapter is to determine the relative effects of accelerated UV weathering between NFTC compounded with different concentrations of fillers and additives. Specimen durability was evaluated based on measurable changes in physical and mechanical properties including, chromaticity, flexural strength and modulus. Test methods where chosen to satisfy the objectives of evaluating and demonstrating the use of NFTC roofing panels intended for commercial production.

3.2 Experimental

3.2.1 Materials

For this screening study, a test matrix was developed that included eighty-eight (88) different NFTC formulations (Table 3.1). All Formulations tested in Phase I are denoted by the formulation number followed by – I (e.g. 34 – I, Formulation 34 – Phase I). Table 3.1 shows the percent by weight of the different fibers and additives. Two thermoplastic types, High Density Polyethylene (HDPE) and Polypropylene (PP) were used. The HDPE was from chipped recycled 1-gallon milk jugs. For HDPE composites that contained 70% fiber, the recycled HDPE was supplemented with 30% 44-melt virgin HDPE. The PP copolymer used was recycled 46-melt Bamberger high impact. Five different natural fibers, wood, coir (coconut), jute, and sisal agava (mattress fibers) were used. The fiber contents ranged from 0 to 70 percent by weight. The wood flour used was 425 μm (#40 mesh) maple from American Wood Fiber. The coir, jute, and sisal fiber was 9.5 mm (0.375" mesh).

Additives included an antioxidant, two compatibilizers, two colorants, a fungicide, and an UV stabilizer. All of the additives except the antioxidant and compatibilizers were added at two different levels. The antioxidant used was Irganox B225 and was added at 0.1% by weight for all formulations. The colorants used were iron oxide (red) and Manganese Ferrite (black). Red colorant was added at concentrations from 0.5% – 0.9% by weight. Black colorant was added at 2.7% – 4.5% by weight. The Fungicide was zinc borate and was added at 0.5% and 2% by weight. The UV stabilizer used was Tinuven 783, a hindered amine, and was added at 0.25% or 5% by weight. Maleated polypropylene (MAPP) and maleated polyethylene (MAPE) bonding agents were used as compatibilizers for the PP and HDPE thermoplastics respectively. MAPP and MAPE were purchased as pellets and melt blended with the fibers and thermoplastics at 2.0% by weight.

3.2.2 Specimen Preparation

Teel-Global Resource Technologies (TGRT), a natural fiber thermoplastic compounder located in Baraboo, Wisconsin compounded all formulations using a proprietary process. The formulations were compression molded into test specimens by TGRT into 150 mm. x 150 mm. x 3 mm. (6 in. x 6 in. x 1/8 in.) flat plates. Two plates were molded for each formulation.

Table 3.1 Phase I Test Matrix
All percentages are by weight

Formulation	Polymer	% Wood Flour	% Coir	% Jute	% Sisal	% Red	% Black	% Stabilizer	% Fungicide	Replications Tested
1 – I	HDPE	0	0	0	0	0	0	0	0	8
2 – I	HDPE	0	0	0	0	0	0	0	0.5	8
3 – I	HDPE	0	0	0	0	0	0	0.25	0.5	8
4 – I	HDPE	0	0	0	0	0	0	0.5	0.5	8
5 – I	HDPE	50	0	0	0	0	0	0	0	8
6 – I	HDPE	50	0	0	0	0	0	0	0.5	8
7 – I	HDPE	50	0	0	0	0	0	0	2	8
8 – I	HDPE	50	0	0	0	0	0	0.25	0	8
9 – I	HDPE	50	0	0	0	0	0	0.5	0.5	4
10 – I	HDPE	50	0	0	0	0	0	0.25	2	4
11 – I	HDPE	50	0	0	0	0	0	0.5	0	8
12 – I	HDPE	50	0	0	0	0	0	0.5	0.5	4
13 – I	HDPE	50	0	0	0	0	0	0.5	2	4
14 – I	HDPE	70	0	0	0	0	0	0.5	0	8
15 – I	HDPE	70	0	0	0	0	0	0	0.5	4
16 – I	HDPE	70	0	0	0	0	0	0	2	4
17 – I	HDPE	70	0	0	0	0	0	0.25	0	4
18 – I	HDPE	70	0	0	0	0	0	0.25	0.5	4
19 – I	HDPE	70	0	0	0	0	0	0.25	2	4
20 – I	HDPE	70	0	0	0	0	0	0.5	0	4
21 – I	HDPE	70	0	0	0	0	0	0.5	0.5	4
22 – I	HDPE	70	0	0	0	0	0	0.5	2	4
23 – I	HDPE	0	50	0	0	0	0	0.25	0.5	8
24 – I	HDPE	0	70	0	0	0	0	0.25	0.5	8
25 – I	HDPE	0	0	50	0	0	0	0.25	0.5	8
26 – I	HDPE	0	0	70	0	0	0	0.25	0.5	8
27 – I	HDPE	0	0	0	50	0	0	0.25	0.5	8
28 – I	HDPE	0	0	0	70	0	0	0.25	0.5	8
29 – I	HDPE	50	0	0	0	0.5	0	0.25	0.5	8
30 – I	HDPE	50	0	0	0	0.75	0	0.25	0.5	8
31 – I	HDPE	50	0	0	0	0	2.7	0.25	0.5	8
32 – I	HDPE	50	0	0	0	0	4.0	0.25	0.5	8
33 – I	HDPE	50	0	0	0	0.5	0	0.5	0.5	4
34 – I	HDPE	50	0	0	0	0.75	0	0.5	0.5	4
35 – I	HDPE	50	0	0	0	0	2.7	0.5	0.5	4
36 – I	HDPE	50	0	0	0	0	4.0	0.5	0.5	4
37 – I	HDPE	70	0	0	0	0.6	0	0.25	0.5	4
38 – I	HDPE	70	0	0	0	0.9	0	0.25	0.5	4
39 – I	HDPE	70	0	0	0	0	3.0	0.25	0.5	4
40 – I	HDPE	70	0	0	0	0	4.5	0.25	0.5	4
41 – I	HDPE	70	0	0	0	0.6	0	0.5	0.5	4
42 – I	HDPE	70	0	0	0	0.9	0	0.5	0.5	4
43 – I	HDPE	70	0	0	0	0	3.0	0.5	0.5	4
44 – I	HDPE	70	0	0	0	0	4.5	0.5	0.5	4
45 – I	PP	0	0	0	0	0	0	0	0	8
46 – I	PP	0	0	0	0	0	0	0	0.5	8
47 – I	PP	0	0	0	0	0	0	0.25	0.5	8
48 – I	PP	0	0	0	0	0	0	0.5	0.5	8
49 – I	PP	50	0	0	0	0	0	0	0	8

50 – I	PP	50	0	0	0	0	0	0	0.5	8
51 – I	PP	50	0	0	0	0	0	0	2	8
52 – I	PP	50	0	0	0	0	0	0.25	0	8
53 – I	PP	50	0	0	0	0	0	0.5	0.5	4
54 – I	PP	50	0	0	0	0	0	0.25	2	4
55 – I	PP	50	0	0	0	0	0	0.5	0	8
56 – I	PP	50	0	0	0	0	0	0.5	0.5	4
57 – I	PP	50	0	0	0	0	0	0.5	2	4
58 – I	PP	70	0	0	0	0	0	0.5	0	8
59 – I	PP	70	0	0	0	0	0	0	0.5	4
60 – I	PP	70	0	0	0	0	0	0	2	4
61 – I	PP	70	0	0	0	0	0	0.25	0	4
62 – I	PP	70	0	0	0	0	0	0.25	0.5	4
63 – I	PP	70	0	0	0	0	0	0.25	2	4
64 – I	PP	70	0	0	0	0	0	0.5	0	4
65 – I	PP	70	0	0	0	0	0	0.5	0.5	4
66 – I	PP	70	0	0	0	0	0	0.5	2	4
67 – I	PP	0	50	0	0	0	0	0.25	0.5	8
68 – I	PP	0	70	0	0	0	0	0.25	0.5	8
69 – I	PP	0	0	50	0	0	0	0.25	0.5	8
70 – I	PP	0	0	70	0	0	0	0.25	0.5	8
71 – I	PP	0	0	0	50	0	0	0.25	0.5	8
72 – I	PP	0	0	0	70	0	0	0.25	0.5	8
73 – I	PP	50	0	0	0	0.5	0	0.25	0.5	8
74 – I	PP	50	0	0	0	0.75	0	0.25	0.5	8
75 – I	PP	50	0	0	0	0	2.7	0.25	0.5	8
76 – I	PP	50	0	0	0	0	4.0	0.25	0.5	8
77 – I	PP	50	0	0	0	0.5	0	0.5	0.5	4
78 – I	PP	50	0	0	0	0.75	0	0.5	0.5	4
79 – I	PP	50	0	0	0	0	2.7	0.5	0.5	4
80 – I	PP	50	0	0	0	0	4.0	0.5	0.5	4
81 – I	PP	70	0	0	0	0.6	0	0.25	0.5	4
82 – I	PP	70	0	0	0	0.9	0	0.25	0.5	4
83 – I	PP	70	0	0	0	0	3.0	0.25	0.5	4
84 – I	PP	70	0	0	0	0	4.5	0.25	0.5	4
85 – I	PP	70	0	0	0	0.6	0	0.5	0.5	4
86 – I	PP	70	0	0	0	0.9	0	0.5	0.5	4
87 – I	PP	70	0	0	0	0	3.0	0.5	0.5	4
88 – I	PP	70	0	0	0	0	4.5	0.5	0.5	4

Specimens were cut from the flat plates to allow for flexural testing and accelerated weathering. All formulations were subjected to accelerated weathering. Only selected formulations were tested in flexure. For formulations subjected to accelerated weathering only two specimens were cut per plate. This resulted in two specimens for controls (unweathered) and two specimens for accelerated weathering. For specimen formulations subjected to flexural testing, four specimens were cut from each plate resulting in four specimens to be used as control and four for flexural testing after exposure.

All specimens were 25mm x 64 mm x 3 mm (1 in. x 2.5 in. x 1/8 in) in size. Due to the high viscosity of the plastic composites, many molds were thicker than specified by American Society for Testing and Materials (ASTM) D 790 and required specimen thickness to be reduced by table sawing the compression face to the required thickness.

3.2.3 Testing

Every formulation was exposed to accelerated UV weathering. Following exposure specimen chromaticity was evaluated. Selected specimens were then tested in flexure.

The testing performed was in accordance with standard tests. The International Conference of Building Officials (ICBO) publishes acceptance Criteria for Special Roofing Systems (AC07) providing guidelines for testing these systems (ICBO 1997). The requirements in this standard apply to curved or flat tiles manufactured from plastic materials. ICBO outlines several tests that provided a relative measure of the performance of fiber-thermoplastic formulations intended for use as roofing tiles.

3.2.3.1 Accelerated Weathering

To evaluate weatherability, the ICBO standard references the use of an accelerated aging device (described in detail in ASTM Test Method G 26-96). A weatherometer is an accelerated weathering device used to simulate the effects of sunlight (UV) and rain on a test surface in a controlled environment. The weatherometer chamber (Atlas 65-WT) used in this study was located at the USDA Forest Products Laboratory (FPL), and meets the requirements of ASTM G26-96. A twin enclosed Xenon-arc lamp weatherometer chamber was used as outlined in the standard. Two water-cooled borosilicate filters were used to adjust the spectral output of the lamp to better correlate with natural exposure conditions, providing direct daylight simulation. The specimen drum inside the weatherometer chamber operated at 1 rpm and was set to provide 102 minutes of light followed by 18 minutes of light and water spray (a standard exposure cycle). The total exposure time was 1500 hrs. The length of exposure was chosen by TGRT to provide a preliminary indication of specimen response to accelerated weathering. Black panel temperature was maintained at 62°C (144°F). The temperature of the water was between 10.5 °C and 21.5 °C (60°F ± 9°F) and its pH was between 6.0 and 8.0. Specimens were wired to screens without stress and backing as shown in Figure 3.1.

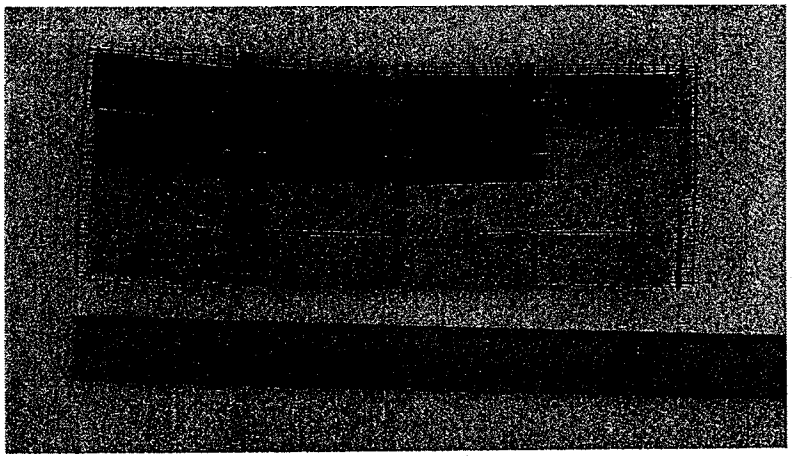

Figure 3.1 Specimens Attached to Screens Prior to Accelerated Weathering

3.2.3.2 Color Fade Measurement

The color intensity of the exposed and unexposed (control) specimens was measured using a tristimulus color analyzer (Minolta CR-200 Chroma Meter) as shown in Figure 3.2). Absolute chromaticity measurements were taken using three parameters recognized

by the CIE (International Commission on Illumination); L^*, a^*, and b^*. L^* is the lightness factor (amount of reflected light) and a^* and b^* are the chromaticity coordinates (chroma and hue, respectively). Three randomly selected locations were measured and averaged. Using the chromaticity coordinates, the total color difference (ΔE) was calculated according to equation 7 (Appendix 1). ΔE is the square root of the sum of the squares of the difference in chromaticity coordinates (Appendix 1). This factor provides a quantitative measure of the total color change between control and exposed specimens.

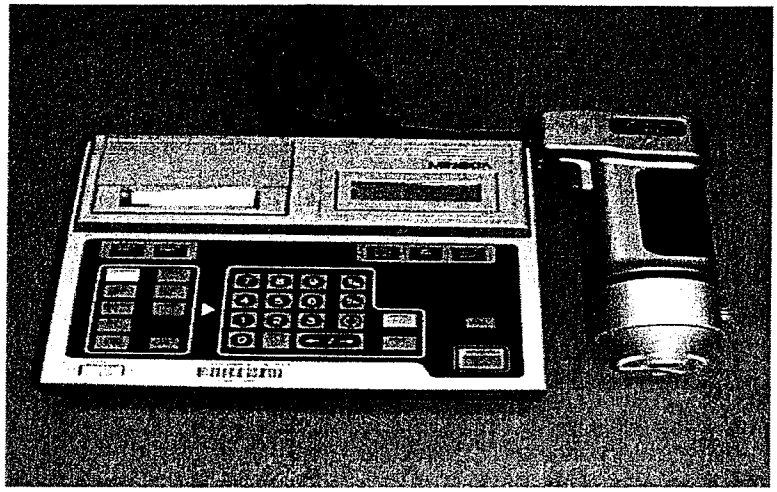

Figure 3.2 Minolta CR-200 Chroma Meter

In addition to color measurements, each specimen was visually evaluated for cracking, checking, crazing, erosion, or chalking at the end of the 1,500-hour exposure period. Due to the translucent nature of the unfilled thermoplastics tested in this study, all unfilled thermoplastics were measured on a calibration plate of known chromaticity (provided with the Minolta Chroma Meter).

3.2.3.3 Flexural Testing

Evaluation of specimen flexural properties was performed using ASTM D790-90, Standard Test Methods for Flexural Properties of Unreinforced and Reinforced Plastics and Electrical Insulating Materials. All flexural strength and stiffness testing was performed at the USDA Forest Service, Forest Products Laboratory (FPL) Engineering Mechanics Lab (EML). The specimens described above were tested according to Test Method I, a three-point loading system utilizing center loading on a simply supported beam (Figure 3.3). A 222 ± 2.0 N (50 ± 0.25 lbs) pound load cell was used. The support span was 51.2 mm (2.0 in.), corresponding to L/d of 16, and a rate of strain of 0.10 mm/mm/min (0.53 in/in/min) was maintained. Specimens were conditioned according to the standard at 23 ° C (73.4 ° F) and 50% relative humidity until no change in mass was recorded prior to testing. All Specimens tested in flexure were oriented with the exposed surface (surface nearest the light source) on the tension side. The specimen was deflected until rupture occurred in the outer fibers or until the maximum fiber strain of 5% was reached, whichever occurred first. Five percent strain in the outer fibers was determined

by relating the deflection at midspan to the support span and depth of beam. The deflection needed for 5% strain was calculated from equation 2 in ASTM D790-90 and is shown in Appendix 2. This level of strain was chosen as recommended by ASTM D790-90.

Translational deflection was measured by the use of a linear variable differential transformer (LVDT) located at the base of the support head and recorded relative displacement between the loading head and supports, from which the strain in the outer fibers was calculated.

Procedure A, which is designed for materials that undergo relatively small deflections was used until large deflections were observed at which point Procedure B was implemented. Because large deflections were observed for all tested specimens prior to failure, all presented results are from procedure B. Procedure B differs from Procedure A by an increased rate of crosshead motion, which is calculated from equation 1 in ASTM D790 and is shown in Appendix 2. The crosshead speed calculated for these specimens was 13.7 mm/min (0.53 in/min). As discussed in Chapter 2 the mechanical properties and failure characteristics of thermoplastics are dependant upon on the rate of strain. An increased rate of crosshead motion leads to increased modulus and can force failure in the outermost tension fibers. Load was applied to the specimen at the specified crosshead speed and simultaneous load-center point deflection data was recorded.

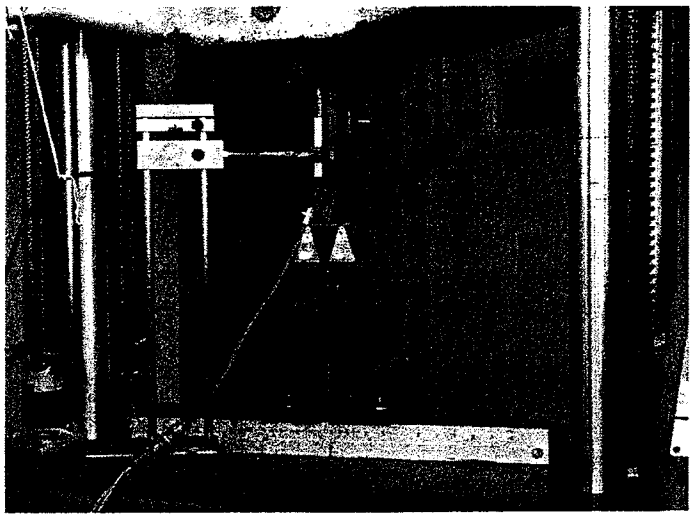

Figure 3.3 Phase I - Three-Point Bending Setup

Flexural strength was calculated either one of two ways depending on the mechanical behavior of each specimen. For specimens that did not fracture at the outer fiber before 5% strain was reached, the flexural strength is equal to the maximum fiber stress at 5% strain (yield stress). For specimens that fractured before 5% strain was reached, the flexural strength is equal to the modulus of rupture (MOR). MOR was calculated according to ASTM D 790-90. MOR is equal to the maximum stress in the outer fiber at failure assuming linear elastic behavior. For a simply supported beam loaded at the midpoint, the maximum stress is calculated from equation 3 in ASTM D790 and is shown

in Appendix 2. The flexural strength was calculated using the gross cross section for both methods.

Modulus of Elasticity (MOE) was calculated using the gross cross section. Due to the nonlinear stress-strain behavior of natural fiber-plastics composites, a modified method for determining MOE was used to determine the tangent modulus of elasticity (Murphy 1992). A single function four-parameter hyperbolic and a linear function were fit to the actual load-displacement (P - δ) curve resulting in a theoretical fitted curve that was then used to determine initial MOE. The advantage of using this method is that it provides a closed form solution to the nonlinear load deflection curve from which the slope at any location can be easily found. The equations used are given in Appendix 3. The parameters for this equation were estimated using standard nonlinear least-squares techniques and typically resulted in fits to the original test data of $R^2 > 0.90$.

3.3 Results and Discussion

Durability performance was evaluated by measuring specimen resistance to weathering. Resistance was determined by measuring changes to chromaticity, mechanical properties, and physical properties. Data was plotted and compared to indicate relative trends in performance. Due to the small sample sizes for the research presented in this chapter, a statistical analysis was not performed.

3.3.1 Effects of Accelerated Weathering on Color Fade

All exposed specimens experienced some color change after 1500 hours of accelerated weathering. Figure 3.4 shows color loss as a result of accelerated weathering on the fibers of a typical wood fiber composite. Figure 3.4 shows that there was significant whitening of some specimens after 1500 hours of exposure (Total Color Difference, $\Delta E = 34.7$).

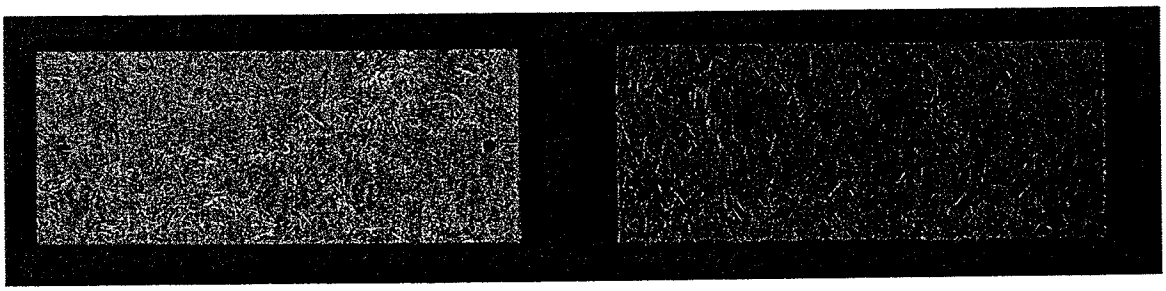

Figure 3.4 HDPE Test Specimens with 50% Wood Flour Left, Weathered Specimen (1500 hours); Right, Unweathered Specimen

Specimens were grouped according to the following divisions based upon composition and independent treatment for color fade analysis:

1. Effect of UV Stabilizer
2. Effect of Fungicide
3. Effect of Wood Flour Content
4. Effect of Alternative Fiber Content
5. Effect of Colorant

3.3.1.1 Effect of UV Stabilizer

A UV stabilizer was added at three different levels to determine its effectiveness in reducing the effects of color fade due to accelerated UV exposure. The effects of UV stabilizer on color fade were investigated for unfilled thermoplastics and formulations containing wood flour. For formulations containing no fiber reinforcement, UV stabilizer was only added in conjunction with 0.5% fungicide. After exposure unfilled HDPE specimens with no added UV stabilizer with and without 0.5% fungicide began to craze. Crazing of the surface of a typical HDPE specimen is shown in Figure 3.5.

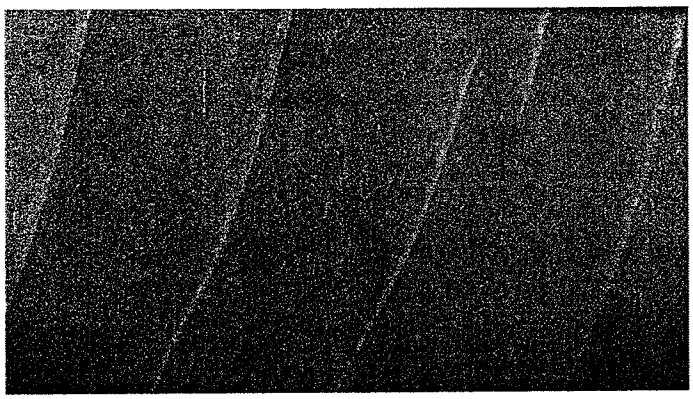

Figure 3.5 Surface Crazing of HDPE Specimen after 1500 Hours of Accelerated Weathering

The described surface crazing can be detected without magnification. After exposure, PP specimens without UV stabilizer, with and without 0.5% fungicide also began to craze, however a layer of fine talc like material appeared on the specimen surface. This talc like material was easily removed with mild abrasion. The talc like material increased the reflectance of the material effectively reducing the transparency and increasing the ΔE. The addition of 0.25% UV stabilizer eliminated surface crazing of unfilled HDPE and PP specimens.

Table 3.2 shows the effects of UV stabilizer on the average total color difference of unfilled thermoplastics with 0.5% fungicide after 1500 hours of accelerated weathering. The addition of UV stabilizer did reduce ΔE for unfilled PP composites by 63%. The large ΔE for Formulation 46 - I can be attributed to the increased reflectance due to the

layer of talky material. Table 3.2 also shows that the variability in properties is not consistent and is generally high. The high variability could be attributed to the intrinsic variability in the recycled materials.

Table 3.2 Effect of UV Stabilizer and Accelerated Weathering on Unfilled HDPE and PP resin with 0.5% Fungicide
Values reported are: Average Value of ΔE^* (% Coefficient of Variation)

Resin Type	UV Stabilizer (%)	Specimens Tested	Total Color Difference
HDPE	0	8	5.6 (8.6)
	0.25	8	6.1 (10.0)
	0.5	8	6.3 (15.7)
PP	0	8	15.5 (9.2)
	0.25	8	5.8 (25.1)
	0.5	8	6.3 (11.1)

Figure 3.6 - 3.8 show the effects of UV stabilizer and accelerated weathering on the average total color difference of 50% and 70% wood flour composites with different levels of added fungicide. Figure 3.6 – 3.8 show that UV stabilizer was ineffective for reducing ΔE on 50% and 70% wood flour composites. It is shown that for all four formulations, ΔE remained relatively unchanged regardless of the concentration of added UV stabilizer. The most significant reduction to the total color difference was 8% for HDPE composites with 50% wood flour and 0.5% fungicide when 0.25% UV stabilizer was added, though the total color difference did increase 5% when 0.5% UV stabilizer was added.

No HDPE specimens containing 50% wood flour were tested with 0.5% UV stabilizer and 2.0% fungicide. The effects of the addition of UV stabilizer were not investigated for formulations containing alternative fibers or added colorant in this study. In all cases the PP based formulations and those containing 70% wood flour experienced a greater change in color than HDPE based formulations and those with 50% wood flour.

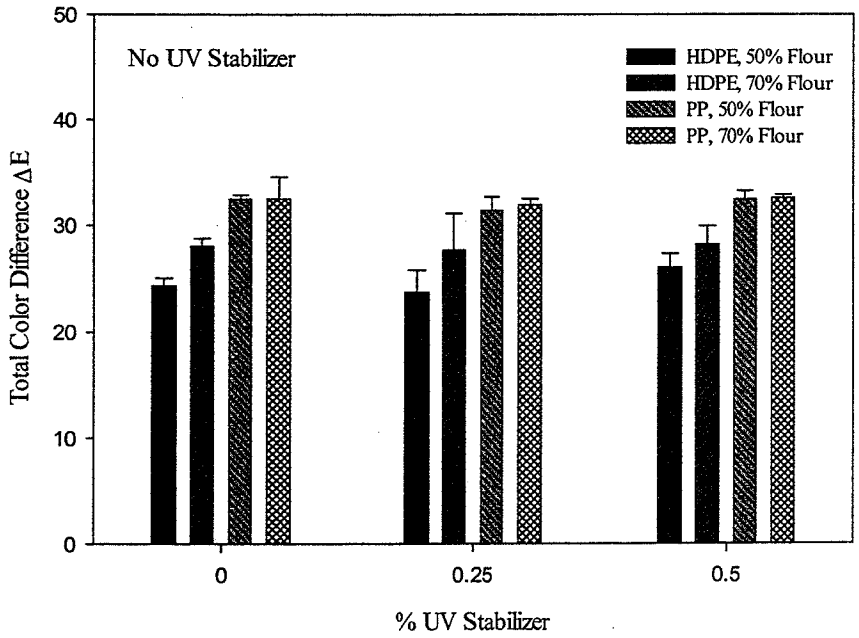

Figure 3.6 Effects of UV Stabilizer and Accelerated Weathering on the Total Color Difference of 50% and 70% Wood Flour Composites with No Added Fungicide (Mean values with error bars equal to one standard deviation)

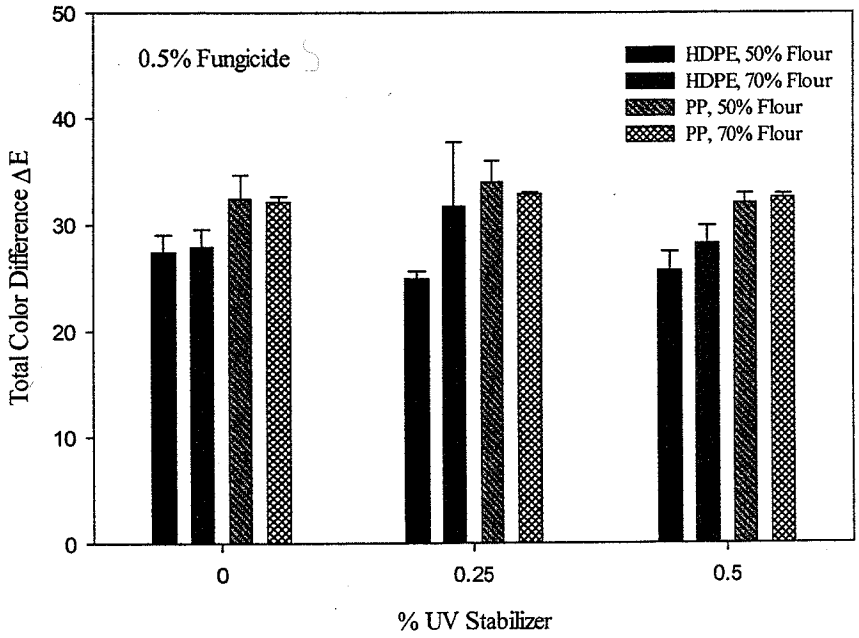

Figure 3.7 Effects of UV Stabilizer and Accelerated Weathering on the Total Color Difference of 50% and 70% Wood Flour Composites with 0.5% Fungicide (Mean values with error bars equal to one standard deviation)

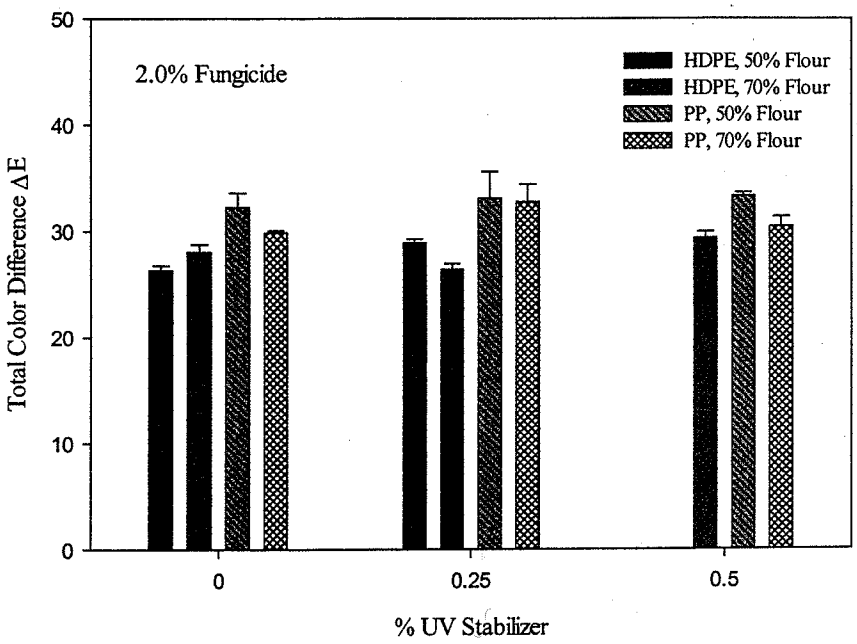

Figure 3.8 Effects of UV Stabilizer and Accelerated Weathering on the Total Color Difference of 50% and 70% Wood Flour Composites with 2% Fungicide (Mean values with error bars equal to one standard deviation)

3.3.1.2 Effect of Fungicide

A fungicide was added at three different levels to determine its effect on color fade due to accelerated UV exposure. The effects of fungicide on color fade were investigated for unfilled thermoplastics and formulations containing wood flour. The addition of 0.5% fungicide to pure PP resin increased the occurrence of surface crazing. The addition of fungicide to HDPE resin had no effect on the surface crazing present after exposure. Table 3.3 shows the effects of fungicide and accelerated weathering on the average total color difference of unfilled thermoplastics. The addition of 0.5% fungicide to PP resin did reduce ΔE by 23%.

Table 3.3 Effects of Fungicide and Accelerated Weathering on Unreinforced HDPE and PP resin
Values reported are: Average Value of ΔE (% Coefficient of Variation)

Resin Type	% Fungicide	Specimen Tested	Total Color Difference
HDPE	0	8	6.2 (18.7)
	0.5	8	5.7 (8.6)
PP	0	8	20.4 (16.2)
	0.5	8	15.6 (9.2)

Figure 3.9 – 3.11 shows the effects of added fungicide and accelerated weathering on the average total color difference of 50% and 70% wood flour composites with different levels of added UV stabilizer. Figure 3.6 – 3.8 show that the addition of increased concentration of fungicide did not result in increasing ΔE for 50% and 70% wood flour composites. It is shown that for all four formulations, ΔE remained relatively unchanged regardless of the concentration of added fungicide. The addition of 2% fungicide did increase the total color difference 18% for HDPE composites with 50% wood flour and 0.25% UV stabilizer. The addition of 0.5% fungicide did increase the total color difference 13% for HDPE composites with 70% wood flour and 0.25% UV stabilizer, however the total color difference was reduced by 5% when 2% fungicide was added. No HDPE composites with 50% wood flour, 2.0% fungicide and 0.5% UV stabilizer were tested.

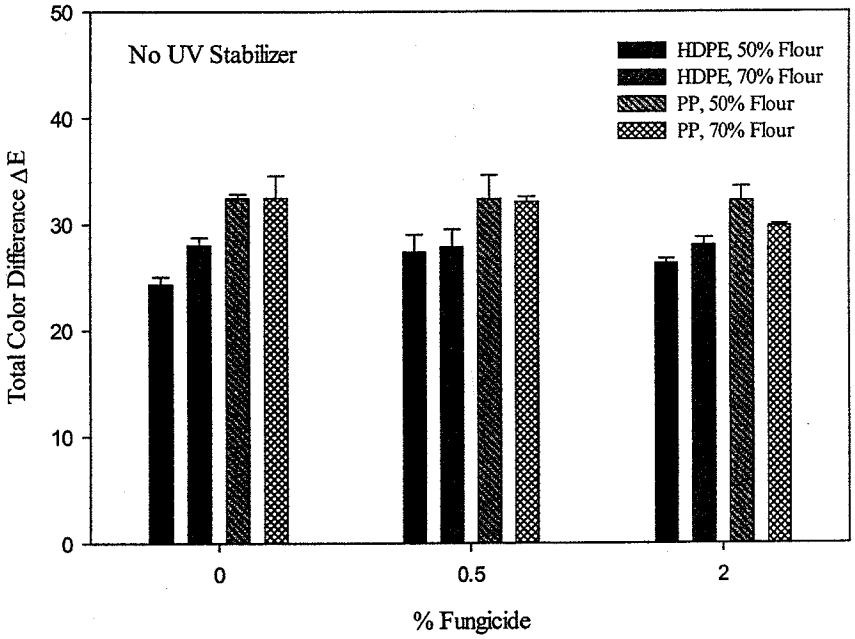

Figure 3.9 Effects of Fungicide and Accelerated Weathering on the Total Color Difference of 50% and 70% Wood Flour Composites
(Mean values with error bars equal to one standard deviation)

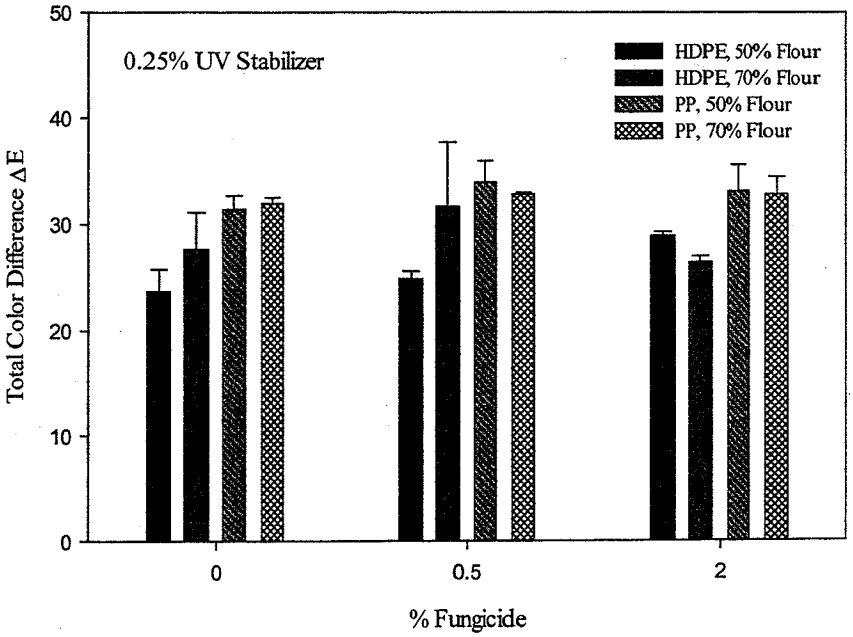

Figure 3.10 Effects of Fungicide and Accelerated Weathering on the Total Color Difference of 50% and 70% Wood Flour Composites with 0.25% UV Stabilizer (Mean values with error bars equal to one standard deviation)

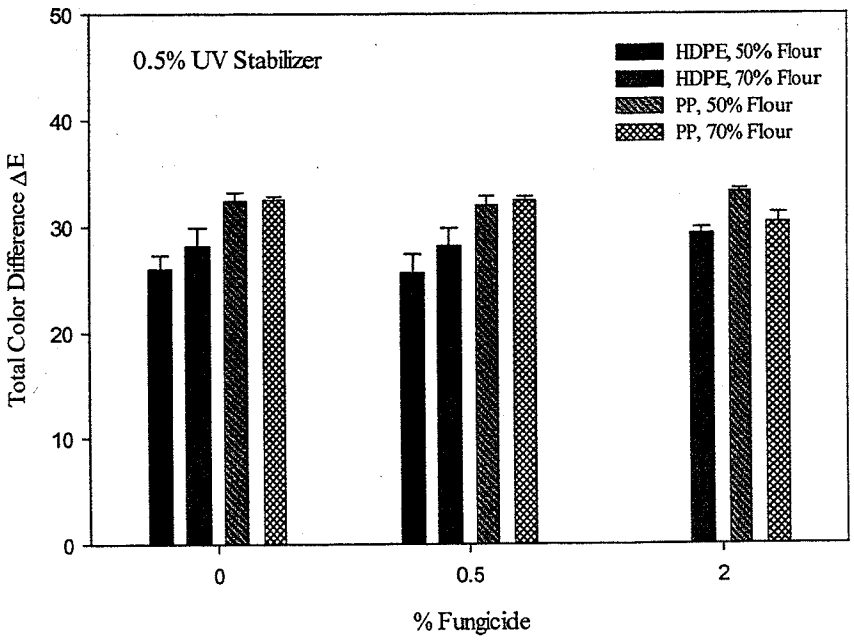

Figure 3.11 Effect of Fungicide and Accelerated Weathering on the Total Color Difference of 50% and 70% Wood Flour Composites with 0.5% UV Stabilizer (Mean values with error bars equal to one standard deviation)

3.3.1.3 Effect of Wood Flour Content

Wood flour was added at two different levels 50% and 70%. Figures 3.12 – 3.15 show the effects of accelerated weathering on the average total color difference for composites with increasing percentage of wood flour. In every figure it is shown that ΔE increased with increasing concentration of wood flour for HDPE composites. In every figure ΔE increased between 0% and 50% wood flour for PP composites, though composites with 70% wood flour had a ΔE of at most 4% different from similar composites with 50% wood flour. The addition of 50% wood flour to HDPE with 0.5% fungicide increased the total color difference 470%. The greatest increase in ΔE for PP composites was nearly 580% between 0% and 50% wood flour when 0.25% UV Stabilizer and 0.5% Fungicide were added.

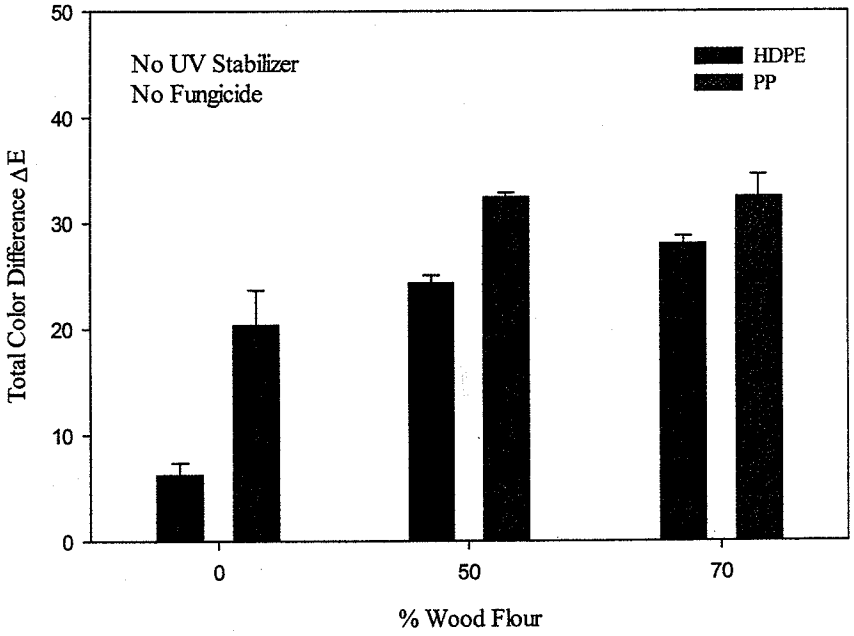

Figure 3.12 Effect of Wood Flour Content and Accelerated Weathering on the Total Color Difference of Thermoplastic Composites
(Mean values with error bars equal to one standard deviation)

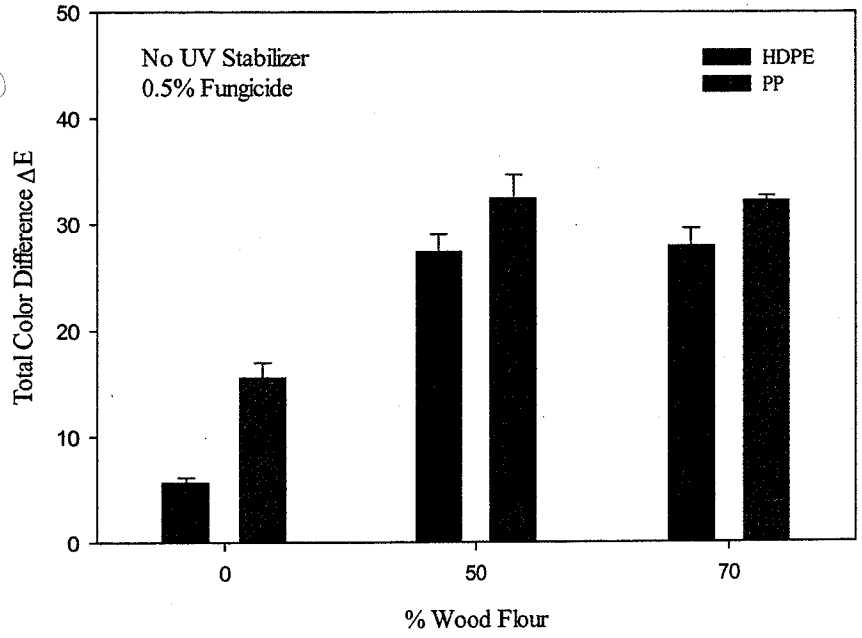

Figure 3.13 Effect of Wood Flour Content and Accelerated Weathering on the Total Color Difference of Thermoplastic Composites with 0.5% Fungicide (Mean values with error bars equal to one standard deviation)

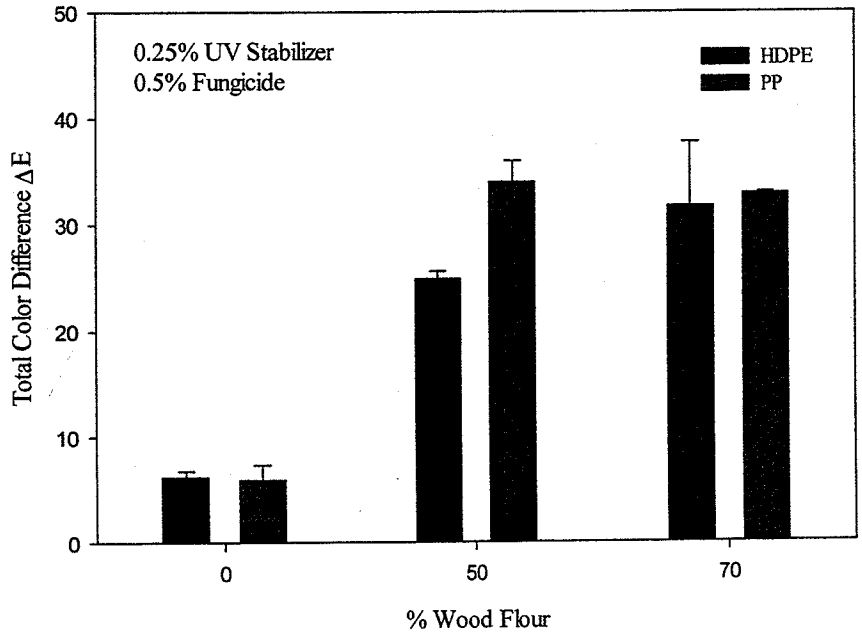

Figure 3.14 Effect of Wood Flour Content and Accelerated Weathering on the Total Color Difference of Thermoplastic Composites with 0.25% UV Stabilizer and 0.5% Fungicide (Mean values with error bars equal to one standard deviation)

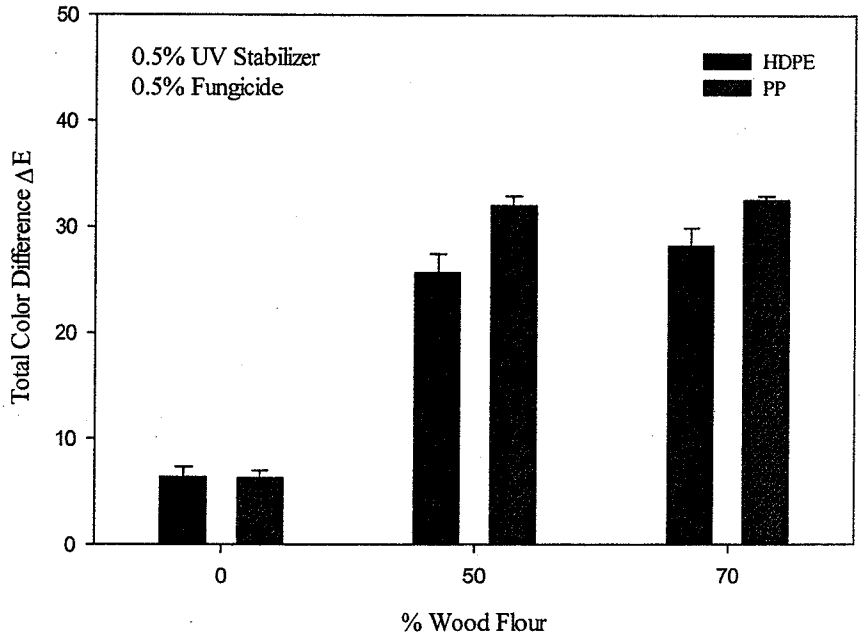

Figure 3.15 Effect of Wood Flour Content and Accelerated Weathering on the Total Color Difference of Thermoplastic Composites with 0.5% UV Stabilizer and 0.5% Fungicide (Mean values with error bars equal to one standard deviation)

3.3.1.4 Effect of Fiber Type and Content

Three different alternative fibers were investigated in this study, coir, sisal, and jute. These fibers were added at two different levels, 50% and 70%. All specimens that contained alternative fibers contained 0.25% UV stabilizer and 0.5% fungicide. No alternative fiber specimens were tested with 0.5% UV stabilizer, 2% fungicide, or added colorants.

Table 3.4 shows the results of accelerated weathering and alternative fiber content on the average total color difference. Table 3.4 shows that all of the specimens filled with fiber faded significantly after exposure regardless of fiber content and the addition of 0.25% UV stabilizer. The total color difference of composites with 50% lignocellulosic fiber was greater than similar unfilled composites. The increase in total color difference for specimens with 50% lignocellulosic can be explained by the fact that specimens were no longer translucent. The total color difference of 70% HDPE and PP wood composites and HDPE coir composites was greater than similar composites with 50% lignocellulosic. The total color difference of 50% jute and sisal HDPE composites and all PP composites except those filled with wood flour was greater than similar composites with 70% lignocellulosic. The total color difference of PP wood composites varied by at most 3%.

Table 3.4 Effect of Alternative Fibers and Accelerated Weathering on Total Color Difference for Thermoplastic Composites with 0.25% UV Stabilizer and 0.5% Fungicide

Values reported are: Average Value of ΔE (% Coefficient of Variation)

Resin Type	Fiber Type	% Fiber	Specimens Tested	Total Color Difference
HDPE	None	0	8	6.1 (10.0)
	Wood	50	8	24.9 (2.9)
		70	8	31.6 (19.1)
	Coir	50	8	33.8 (8.5)
		70	8	34.9 (5.4)
	Jute	50	8	31.2 (3.0)
		70	8	28.3 (2.1)
	Sisal	50	8	22.9 (2.3)
		70	8	24.3 (9.7)
PP	None	0	8	5.9 (25.1)
	Wood	50	8	33.9 (6.0)
		70	8	32.8 (0.5)
	Coir	50	8	43.3 (2.6)
		70	8	38.3 (4.1)
	Jute	50	8	37.3 (1.4)
		70	8	28.8 (5.9)
	Sisal	50	8	32.4 (3.2)
		70	8	29.3 (3.5)

3.3.1.5 Effect of Colorant

Two colorants were evaluated in this study, red (iron oxide) and black (manganese ferrite). For all specimens when colorant was added, 0.5% fungicide and either 0.25% or 0.5% stabilizer was also added. Figure 3.16 shows that red colorant effectively reduces color fade associated with accelerated weathering. There is only slight lightening of the fibers after 1500 hours of exposure (ΔE = 6.3).

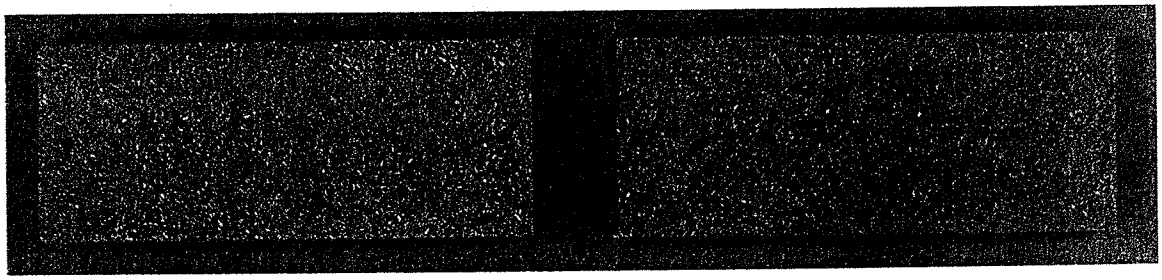

Figure 3.16 Test Specimens with Red Colorant Added Left, Weathered (1500 hours); Right Unweathered Specimen

Tables 3.5 – 3.8 show the effects of added red and black colorant and accelerated weathering to the average total color difference of 50% and 70% wood flour composites with 0.25% and 0.5% UV Stabilizer and 0.5% Fungicide. In all formulations the addition of red and black colorants reduced ΔE. The total color change was reduced 70% to 85% for HDPE composites. The total color change was reduced 50% to 70% for PP composites. For all formulations tested, the addition of black colorant was more effective in reducing these changes than red colorant. The black colorant may be more effective because it was added at higher percentages than red colorant.

It is interesting to note that the variability in properties for these composites is generally greater than composites containing alternative fibers.

Table 3.5 Effects of Colorants and Accelerated Weathering on the Total Color Difference for 50% Wood Flour Thermoplastic Composites with 0.25% UV Stabilizer, and 0.5% Fungicide

Values reported are: Average Value of ΔE (% Coefficient of Variation)

Resin Type	Colorant Added	% Colorant	Specimens Tested	Total Color Difference
HDPE	None	0	4	24.9 (2.9)
	Red	0.5	8	7.6 (13.8)
		0.75	8	6.3 (11.1)
	Black	2.7	8	4.1 (18.6)
		4.0	8	3.2 (12.3)
PP	None	0	4	33.9 (6.0)
	Red	0.5	8	17.5 (15.8)
		0.75	8	17.4 (3.9)
	Black	2.7	8	15.0 (3.3)
		4.0	8	10.8 (11.5)

Table 3.6 Effects of Colorants and Accelerated Weathering on the Total Color Difference for 70% Wood Flour Thermoplastic Composites with 0.25% UV Stabilizer, and 0.5% Fungicide

Values reported are: Average Value of ΔE (% Coefficient of Variation)

Resin Type	Colorant Added	% Colorant	Specimens Tested	Total Color Difference
HDPE	None	0	4	31.6 (19.1)
	Red	0.6	4	6.2 (16.2)
		0.9	4	5.0 (6.0)
	Black	3.0	4	5.7 (13.7)
		4.5	4	4.6 (23.8)
PP	None	0	4	32.8 (0.5)
	Red	0.6	4	13.3 (16.8)
		0.9	4	13.8 (15.3)
	Black	3.0	4	11.3 (2.4)
		4.5	4	12.4 (8.4)

Table 3.7 Effects of Colorants and Accelerated Weathering on the Total Color Difference for 50% Wood Flour Thermoplastic Composites with 0.5% UV Stabilizer, and 0.5% Fungicide

Values reported are: Average Value of ΔE (% Coefficient of Variation)

Resin Type	Colorant Added	% Colorant	Specimens Tested	Total Color Difference
HDPE	None	0	4	25.7 (6.9)
	Red	0.5	4	6.7 (12.9)
		0.75	4	7.1 (21.2)
	Black	2.7	4	6.1 (47.9)
		4.0	4	4.9 (30.6)
PP	None	0	4	31.9 (2.9)
	Red	0.5	4	15.0 (1.6)
		0.75	4	13.5 (0.4)
	Black	2.7	4	13.0 (22.9)
		4.0	4	11.5 (19.9)

Table 3.8 Effects of Colorants and Accelerated Weathering on the Total Color Difference for 70% Wood Flour Thermoplastic Composites with 0.5% UV Stabilizer, and 0.5% Fungicide
Values reported are: Average Value of ΔE (% Coefficient of Variation)

Resin Type	Colorant Added	% Colorant	Specimens Tested	Total Color Difference
HDPE	None	0	4	28.2 (6.1)
	Red	0.6	4	6.9 (9.7)
		0.9	4	6.4 (1.2)
	Black	3.0	4	5.0 (0.4)
		4.5	4	4.3 (3.4)
PP	None	0	4	32.5 (1.2)
	Red	0.6	4	13.0 (0.6)
		0.9	4	11.3 (1.8)
	Black	3.0	4	12.9 (4.0)
		4.5	4	10.8 (10.9)

3.3.2 Effects of Accelerated Weathering on Flexural Properties

Forty NFTC formulations were selected and subjected to flexural testing. Flexural tests were performed on both unexposed specimens and those exposed to 1500 hours of accelerated weathering. A total of eight specimens per formulation were tested in flexure, four of which were held as controls. Data on the flexural properties of the NFTC specimens were analyzed to indicate trends in strength and stiffness performance. Specimens were grouped according to the following divisions based upon composition and treatment for analysis:

1. Effect of UV Stabilizer
2. Effect of Fungicide
3. Effect of Wood Flour Content
4. Effect of Alternative Fiber Content
5. Effect of Colorant

Figure 3.17 shows typical load deflection plots and fitted theoretical hyperbolic functions used to calculate flexural modulus. The variation of load-deflection data points from the theoretical curve appeared minimal, the fitted function is not visually discernable from the actual data. The average standard error of estimate, SEE, for all specimens tested in flexure was 2.62 N (0.59 lb) for the control specimens and 1.73 N (0.39 lb) for the exposed specimens. The larger SEE observed in the unexposed specimens, is directly related to the more linear load-deflection behavior exhibited by those specimens.

All of the specimens fractured in the outer fibers beneath the loading head before reaching the 5% strain limit, except the specimens that contained no fiber (a few specimens that contained no fiber did fracture after exposure). For those specimens that

did not fail, the flexural strength was calculated as the yield stress corresponding to 5% strain in the outer fibers.

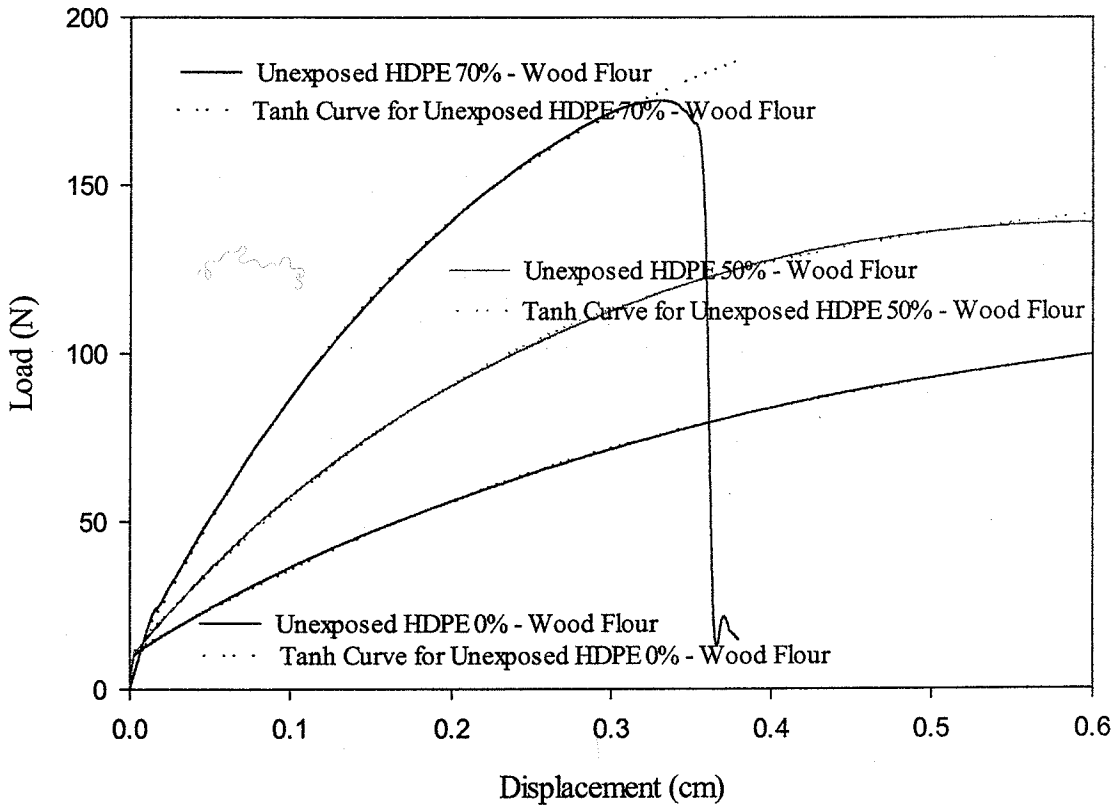

Figure 3.17 Load Deflection Curves For Unexposed and Exposed 0%, 50%, 70% Wood Flour Composites of HDPE and PP and Fitted Tanh Functions

3.3.2.1 Effect of UV Stabilizer

The effect of added UV stabilizer and accelerated weathering on flexural properties was investigated for unreinforced thermoplastics and to thermoplastics containing 50% wood flour. Figure 3.18 and Figure 3.19 show the effects of UV stabilizer and accelerated weathering for unreinforced thermoplastics with 0.5% fungicide on average flexural strength and modulus respectively.

Figure 3.18 shows that at all three concentrations of added UV stabilizer, the unexposed strength of HDPE composites varied by less than 1%. It is shown that as the concentration of added UV stabilizer increased, the flexural strength of unexposed PP composites increased 4%. This graph also shows that the UV stabilizer was more effective in reducing the loss in strength in HDPE composites than in PP composites of the same formulation. When 0.5% UV stabilizer was added, the loss in flexural strength due to exposure was less than 1% for HDPE but 33% for PP.

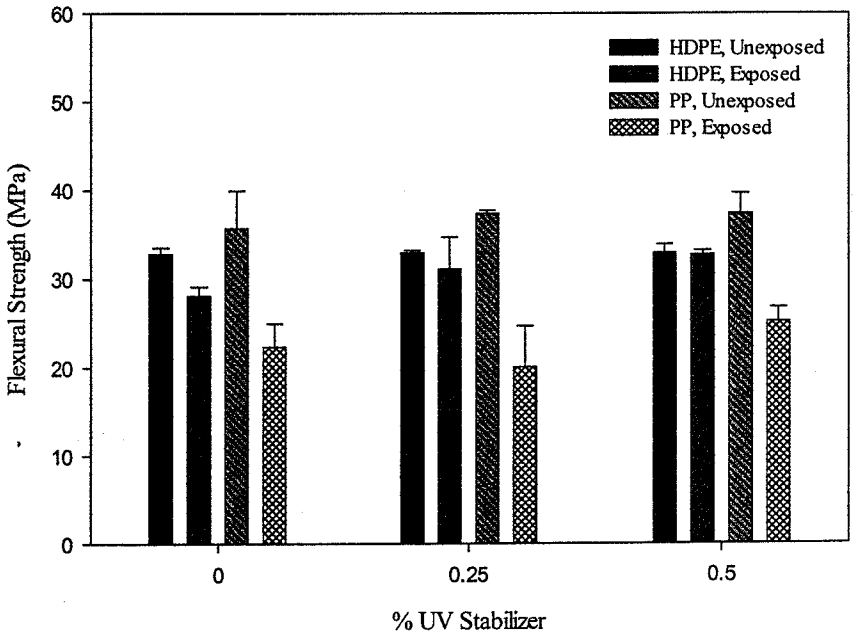

Figure 3.18 Effect of UV Stabilizer and Accelerated Weathering on the Flexural Strength of Unreinforced Thermoplastics with 0.5% Fungicide
(Mean values with error bars equal to one standard deviation)

Figure 3.19 shows that the unexposed modulus of unreinforced HDPE specimens varied by less than 3% regardless of the concentration of UV stabilizer. The modulus of exposed unreinforced HDPE was at most 5% different than unexposed specimens of the same formulation regardless of the concentration of UV stabilizer. The unexposed modulus of unreinforced PP specimens was consistently 15% greater than unexposed HDPE specimens of the same formulation. The flexural modulus for unreinforced PP composites with no added UV stabilizer decreased by 61% after exposure. The addition of UV stabilizer to unreinforced PP specimens was effective in reducing the effects of exposure to less than 1%.

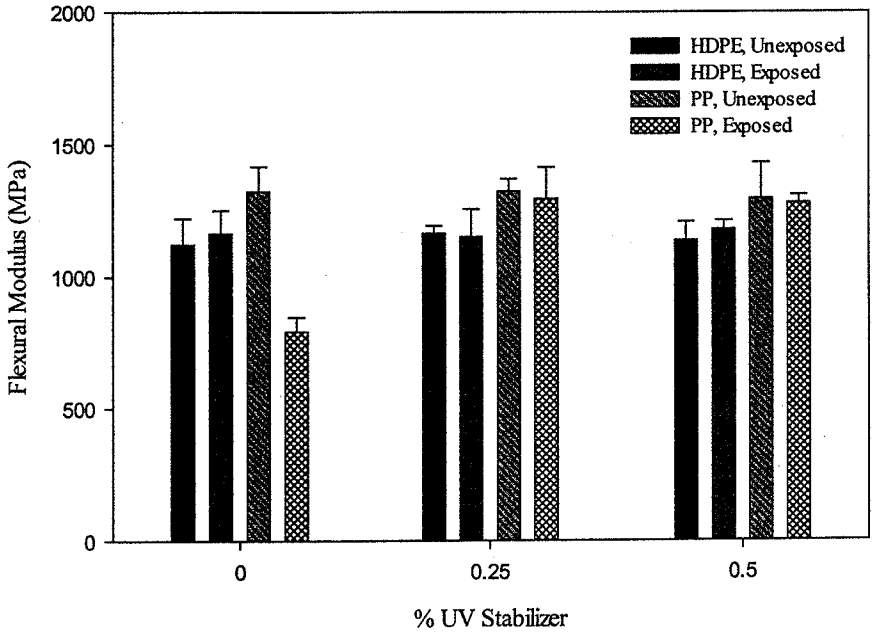

Figure 3.19 Effect of UV Stabilizer and Accelerated Weathering on the Flexural Modulus of Unreinforced Thermoplastics with 0.5% Fungicide
(Mean values with error bars equal to one standard deviation)

Figure 3.20 and 3.21 show the effects of added UV stabilizer and accelerated weathering on the average flexural strength and modulus for 50% wood flour-thermoplastic composites.

Figure 3.20 shows that the addition of 0.25% UV stabilizer to 50% wood flour-HDPE composites reduced unexposed flexural strength 22%. The addition of UV stabilizer to 50% wood flour-PP composites reduced unexposed flexural strength 11% and 21% when 0.25% and 0.5% UV stabilizer were added respectively. The loss in flexural strength due to exposure was reduced 3% when 0.5% UV stabilizer was added for HDPE composites. The loss in flexural strength was reduced 8% when 0.5% UV stabilizer was added to PP composites.

Figure 3.21 shows the unexposed modulus of HDPE composites decreased 11% with the addition of 0.25% UV stabilizer. The loss in modulus due to exposure was between 26% and 30% regardless of the concentration of UV stabilizer for HDPE composites. The unexposed modulus of PP composites was 15% less than composites with no UV stabilizer. The loss in flexural modulus of 50% wood flour-PP composites was reduced 10% when 0.5% UV stabilizer was added.

The reduction in flexural properties for unexposed wood flour composites due to the addition of UV stabilizer could indicate that the UV stabilizer is reducing the interfacial bond between the fiber and matrix.

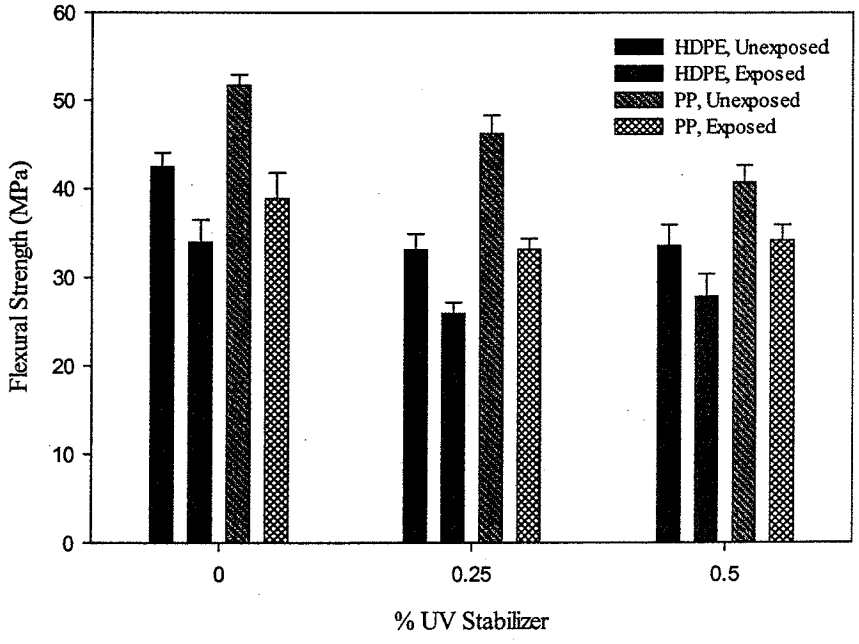

Figure 3.20 Effect of UV Stabilizer and Accelerated Weathering on Flexural Strength for 50% Wood Flour-Thermoplastic Composites
(Mean values with error bars equal to one standard deviation)

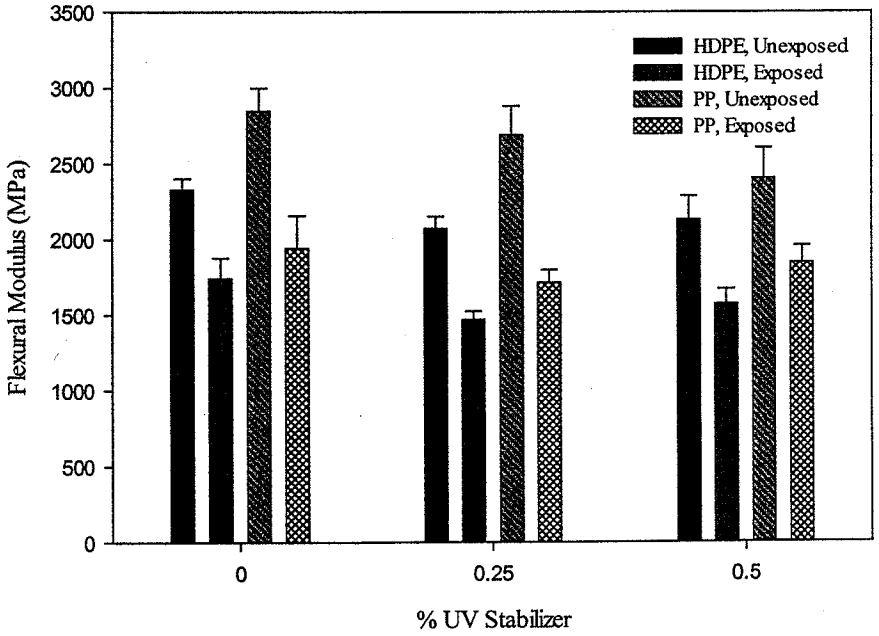

Figure 3.21 Effect of UV Stabilizer and Accelerated Weathering on Flexural Modulus for 50% Wood Flour-Thermoplastic Composites
(Mean values with error bars equal to one standard deviation)

3.3.2.3 Effect of Fungicide

The effects of added fungicide and accelerated weathering were investigated for 50% wood flour-thermoplastic composites in flexure. Figures 3.22 and 3.23 show the effects of fungicide and accelerated weathering on the average flexural strength and modulus of 50% wood flour – thermoplastic composites with no UV stabilizer.

Figure 3.22 shows that the unexposed strength of HDPE composites with 0.5% fungicide is 13% greater than HDPE composites without fungicide. It is shown that the unexposed strength of PP composites with 2.0% fungicide was 14% less than composites without fungicide. The exposed strength of HDPE composites with 2.0% fungicide was 5% less than composites with no added fungicide. The strength of exposed PP composites was between 23% and 25% of the unexposed strength regardless of the concentration of added fungicide. The addition of 0.5% fungicide did increase the loss in strength 11% for HDPE composites with 50% wood flour.

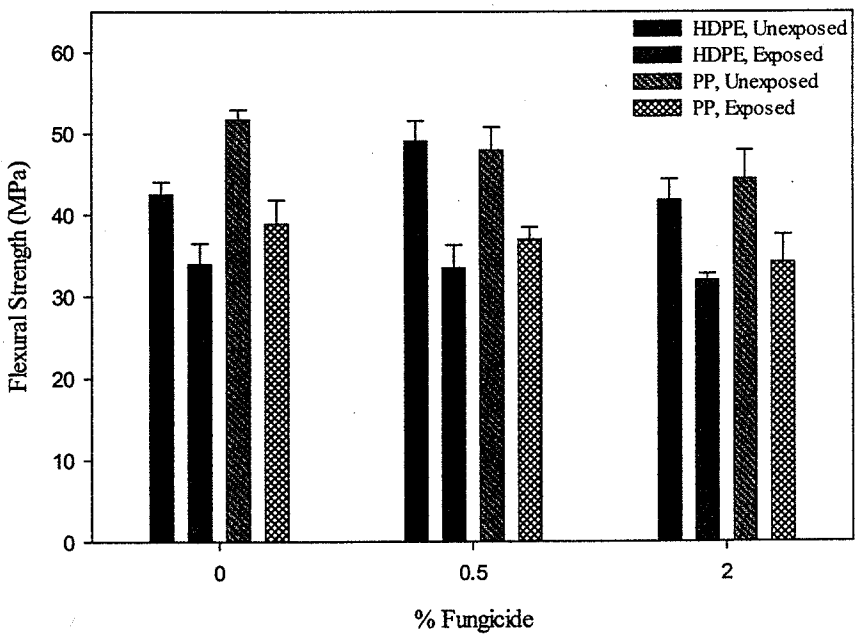

Figure 3.22 Effect of Fungicide and Accelerated Weathering on Flexural Strength for 50% Wood Flour – Thermoplastic Composites
(Mean values with error bars equal to one standard deviation)

Figure 3.23 shows that HDPE composites with 0.5% fungicide were stiffer than composites without fungicide and those with 2.0% fungicide. The unexposed modulus of PP composites with 2.0% fungicide was 14% less than composites without fungicide. The exposed modulus for HDPE composites was between 73% and 68% of similar unexposed specimens regardless of the concentration of added fungicide. The exposed modulus for PP composites was between 72% and 68% of similar unexposed specimens. The exposed modulus for HDPE composites varied by at most 7% depending on the

concentration of added fungicide. The exposed modulus for PP composites varied by at most 3% depending on the concentration of added fungicide.

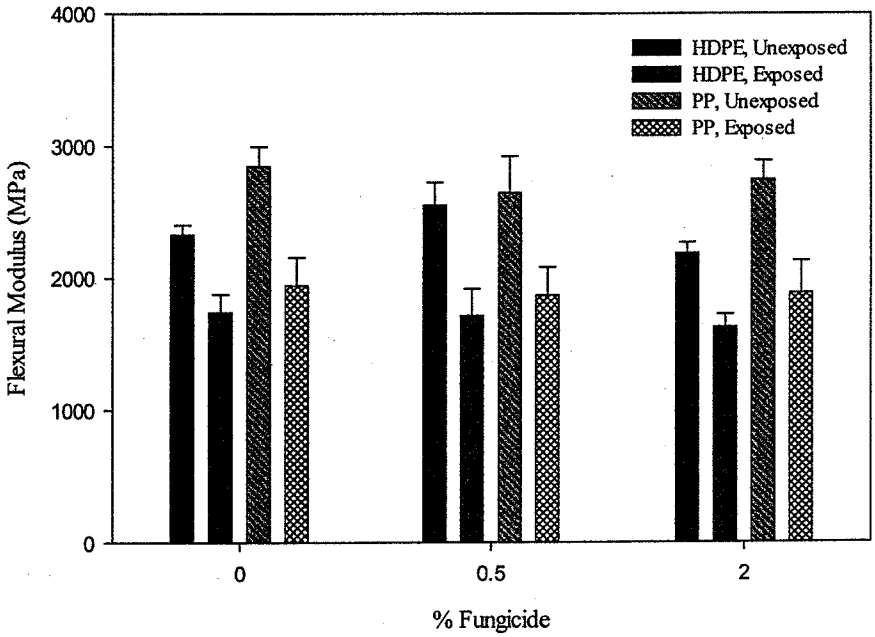

Figure 3.23 Effect of Fungicide and Accelerated Weathering on Flexural Modulus for 50% Wood Flour-Thermoplastic Composites
(Mean values with error bars equal to one standard deviation)

3.3.2.3 Effect of Wood Flour Content

The effects of wood flour content and accelerated weathering on flexural properties were investigated. Figures 3.24 and 3.25 show the effects of wood flour content and accelerated weathering on the average flexural strength and modulus of thermoplastic composites with no added UV stabilizer or fungicide.

Figure 3.24 shows that both HDPE and PP composites with 50% wood flour were stronger than similar composites with no added flour regardless of exposure. The unexposed strength of HDPE with 50% wood flour was 29% greater than unfilled HDPE. The unexposed strength of PP composites with 50% wood flour was 40% greater than unfilled PP. It is shown that the flexural strength of unexposed wood flour-PP composites was greater than unexposed wood flour-HDPE composites with the same fiber concentration. For both HDPE and PP wood flour composites, the unexposed and exposed flexural strength was greater when 50% flour was added than when 70% flour was added. After exposure the strength of 50% wood flour HDPE composites was 80% of the unexposed strength while the exposed strength of 70% wood flour HDPE composites was only 71% compared to unexposed composites of the same formulation.

Figure 3.25 shows that unexposed HDPE and PP composites containing 70% wood flour were stiffer than similar composites with 50% wood flour. It is shown that unexposed

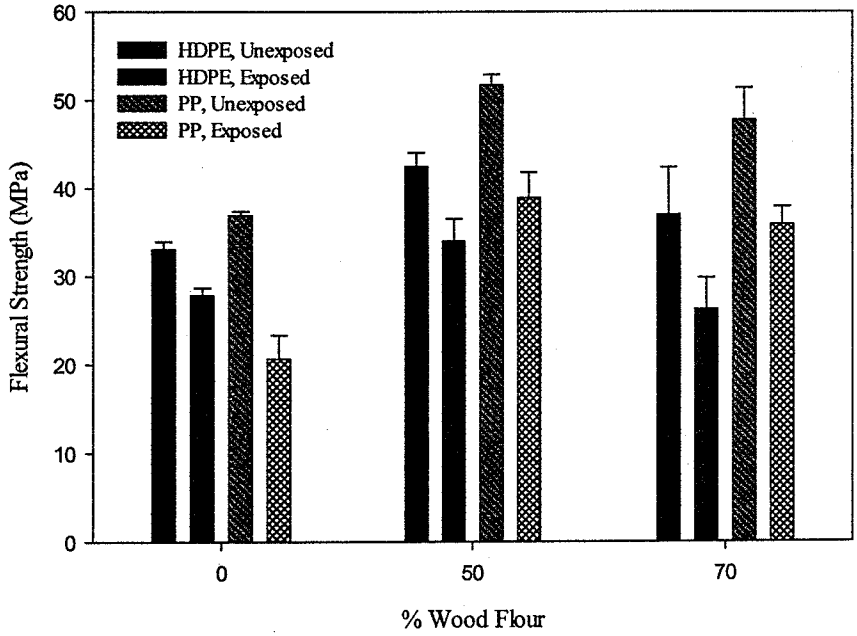

Figure 3.24 Effect of Wood Flour Content and Accelerated Weathering on Flexural Strength for Thermoplastic Composites with No Added UV Stabilizer and Fungicide (Mean values with error bars equal to one standard deviation)

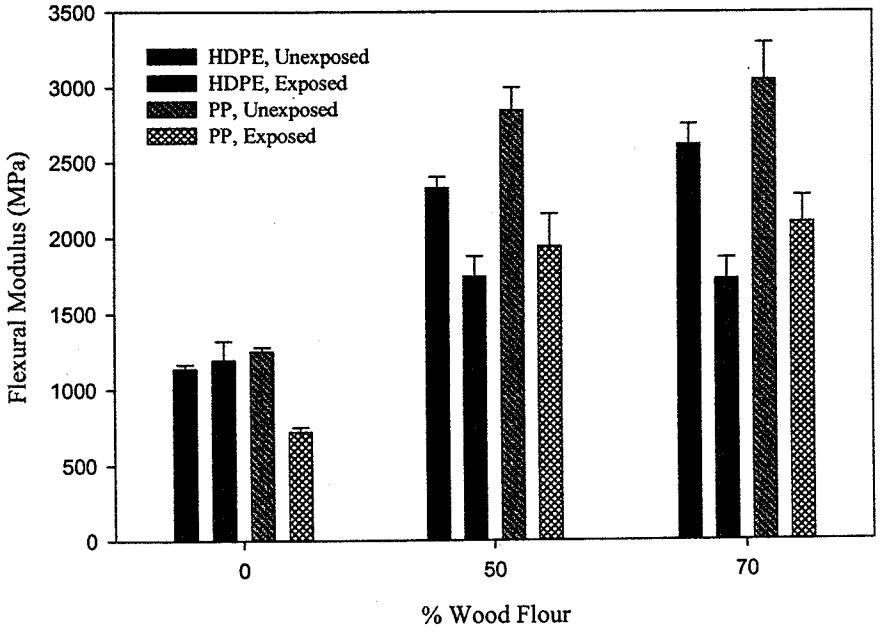

Figure 3.25 Effect of Wood Flour Content and Accelerated Weathering on Flexural Modulus for Thermoplastic Composites with No Added UV Stabilizer and Fungicide (Mean values with error bars equal to one standard deviation)

50% and 70% wood flour-PP composites were stiffer than similar unexposed HDPE composites. After exposure the modulus of 50% and 70% wood flour-HDPE composites was reduced 27% and 35% respectively. The modulus of 50% and 70% wood flour-PP composites was reduced 32% and 30% respectively.

3.3.2.4 Effect of Fiber Type and Content

Thermoplastic composites with coir, jute, and sisal fibers tested in flexure contained both 0.25% UV stabilizer and 0.5% fungicide. Table 3.9 shows the effect of fiber type,

Table 3.9 Effect of Fiber Type, Content, and Accelerated Weathering on Flexural Properties for Thermoplastic Composites with 0.25% UV Stabilizer and 0.5% Fungicide

Values reported: Average (% Coefficient of Variation)

Resin Type	Fiber Composition	Flexural Modulus (MPa)		% Change	Flexural Strength (MPa)		% Change
		0 Hours	1500 Hours		0 Hours	1500 Hours	
HDPE	0%	1150 (6.3)	1150 (9.1)	0.0	32.9 (0.8)	31.0 (11.6)	5.8
	50% Coir	1960 (6.1)	1090 (2.7)	44.4	32.3 (12.4)	23.5 (11.4)	27.2
	70% Coir	1960 (6.2)	750 (20.4)	61.7	24.2 (18.8)	12.9 (47.7)	46.7
	50% Jute	2820 (20.0)	1900 (18.9)	32.6	40.2 (15.2)	33.2 (15.7)	17.4
	70% Jute	2990 (14.0)	1380 (18.9)	53.8	24.9 (17.6)	16.3 (9.8)	34.5
	50% Sisal	2360 (4.5)	1090 (3.1)	53.8	30.0 (8.4)	19.1 (6.2)	36.3
	70% Sisal	2930 (6.3)	632 (16.8)	78.4	25.6 (20.6)	8.7 (26.0)	66.0
PP	0%	1323 (3.5)	1323 (9.3)	0.0	37.3 (1.0)	20.1 (23.1)	46.1
	50% Coir	2130 (2.6)	977 (5.7)	54.1	35.0 (11.0)	23.1 (14.5)	34.0
	70% Coir	2190 (9.2)	977 (8.3)	55.3	33.1 (6.8)	18.3 (2.4)	44.7
	50% Jute	2820 (7.3)	2010 (9.0)	28.7	44.2 (5.7)	33.8 (7.7)	23.5
	70% Jute	3390 (4.8)	1320 (12.8)	61.0	33.5 (17.9)	18.6 (11.2)	44.5
	50% Sisal	2820 (15.6)	1440 (18.1)	48.9	47.2 (18.5)	32.6 (8.8)	30.9
	70% Sisal	3390 (3.9)	748 (7.5)	77.9	37.4 (5.7)	13.9 (14.0)	62.8

content, and accelerated weathering on flexural modulus and strength. Table 3.9 shows that the unexposed modulus increased and strength decreased with increasing content of lignocellulosic for both HDPE and PP composites. Modulus and strength of all composites with a greater content of lignocellulosic were more severally affected by exposure than those composites with smaller content. The unexposed modulus for 50% and 70% coir fiber-HDPE composites is the same. The modulus for all other fiber composites is shown to increase with increasing fiber content. After accelerated weathering, the modulus of all fiber composites tested was reduced. The most significant reduction in modulus occurred in sisal fiber-HDPE and PP composites. It is shown that there is a 78% loss in modulus for both HDPE and PP composites with 70% sisal fiber. The smallest reduction in modulus occurred for 50% jute fiber composites of HDPE and PP. It is shown that there is a 33% and 29% loss in modulus for 50% jute fiber composites of HDPE and PP respectively. The unexposed modulus of PP composites with coir, jute, and sisal was greater than similar composites of HDPE. Table 3.9 shows that the unexposed strength decreased as the content of coir, jute, and sisal increased from 50% to 70%. The composite with the greatest reduction in unexposed strength when fiber content increased from 50% to 70% were jute fiber-HDPE and PP composites. Accelerated weathering reduced the flexural strength of 70% sisal fiber-HDPE and PP composites most severely. A 66% and 63% loss in strength due to exposure was recorded for these composites. Composites that were most severely affected by exposure were those filled with sisal fiber, and least affected were those filled with wood flour. This can likely be explained by the relative size of the lignocellulosic. Sisal fibers were much larger than wood flour and could result in more fibers at or near the surface that could be deteriorated. It is also shown that the variability in properties for these composites is inconsistent. The inconsistency could again be attributed to the variability in the recycled polymer and lignocellulosic used.

3.3.2.5 Effect of Colorant

The effect of red and black colorant and accelerated weathering on flexural properties of 50% wood flour thermoplastic composites with 0.25% UV stabilizer and 0.5% fungicide were investigated. No specimens were tested in flexure that contained 50% wood flour and 0.25% UV stabilizer and 0.5% fungicide. Table 3.10 shows the effects of colorants and accelerated weathering on 50% wood flour thermoplastic composites with 0.25% UV stabilizer and 0.5% fungicide. Table 3.10 shows that the strength and modulus of PP specimens containing red colorants was greater than PP specimens that containing black colorant regardless of exposure. Table 3.10 shows that for HDPE composites the loss in strength and modulus due to accelerated weathering was less severe in composites with black colorant than red colorant. The loss in modulus due to accelerated weathering for HDPE composites with 0.5% and 0.75% red colorant was 26% and 15% respectively. The reduction in modulus due to accelerated weathering for HDPE composites for 2.7% and 4.0% black colorant was 9% and 7% respectively. Table 3.10 shows that for HDPE composites the flexural strength increased with increasing content of colorant. It is shown that for PP composites the flexural strength decreased with increasing content of

colorant. Colorants were more effective in reducing changes in flexural properties for HDPE wood filled composites than similar PP composites.

The colorants used in this study have reduced the effects of accelerated weathering. The pigments could be effectively coating the fibers and protecting them from deterioration. The pigments could also be acting as UV absorbers effectively absorbing the UV light and re-emitting it as heat.

Table 3.10 Effect of Colorants and Accelerated Weathering on the Flexural Properties of HDPE & PP Specimens with 50% Wood Flour, 0.25% UV Stabilizer, 0.5% Fungicide

Values reported: Average (% Coefficient of Variation)

Resin Type	Colorant	% Colorant	Flexural Modulus (MPa)		% Change	Flexural Strength (MPa)		% Change
			0 Hours	1500 Hours		0 Hours	1500 Hours	
HDPE	Red	0.5	2430 (7.8)	1800 (4.0)	25.9	43.4 (7.6)	35.0 (7.3)	19.4
		0.75	2540 (3.4)	2160 (10.9)	14.9	45.6 (3.0)	39.4 (5.8)	13.6
	Black	2.7	2070 (12.2)	1880 (15.9)	9.2	38.4 (16.2)	36.5 (13.7)	4.9
		4.0	2570 (9.1)	2380 (6.4)	7.4	44.5 (15.1)	43.2 (7.1)	2.9
PP	Red	0.5	2790 (11.7)	2090 (16.8)	25.0	47.8 (9.3)	37.2 (13.0)	22.2
		0.75	2720 (7.6)	2130 (9.4)	21.7	46.3 (8.2)	38.3 (7.0)	17.3
	Black	2.7	2540 (7.9)	1920 (5.6)	24.4	43.5 (8.7)	34.9 (5.4)	19.8
		4.0	2340 (5.1)	1480 (1.9)	36.8	37.1 (6.0)	27.6 (4.4)	25.6

3.3.3 Effects of Accelerated Weathering on Dimensional Changes

All specimens were measured after conditioning to determine the effects of accelerated weathering on the dimensional changes. Measurements were made using a digital micrometer accurate to .01 mm (.001 in). Specimens showed minimal length and width dimensional change due to accelerated weathering. Some specimens did however exhibit thickness swelling (perpendicular to exposure) as great as 8%. Specimens which exhibited swelling either contained alternative fibers: Coir, Jute, Sisal, or contained 70% wood Flour. No significant distinction was made between thermoplastic types and swelling. A significant change in thickness could result in fastener pullout or surface ponding, which would be detrimental to roofing applications. At 70% wood flour content, some crumbling was noted around the specimen edges in HDPE after accelerated weathering.

After exposure, PP specimens containing alternative fibers displayed mild to severe surface fiber protrusion indicating that the bond between the thermoplastic and fiber had deteriorated. No such observations were noted for HDPE specimens.

The addition of 0.9% red or 4.5% black was effective in reducing crumbling associated with 70% wood flour for HDPE specimens.

3.4 Conclusions

In this chapter the durability of a variety of NFTC were exposed to accelerated weathering. Physical and mechanical properties were measured to determine the relative durability of these composites. Based on the results presented the following conclusion can be drawn:

1. The UV stabilizer was effective in reducing surface crazing for unreinforced HDPE and PP composites due to accelerated weathering. The UV stabilizer did reduce the effects of exposure on the flexural strength and modulus for unfilled HDPE with 0.5% fungicide to less than 1%. The UV stabilizer did reduce the effects of exposure on the flexural modulus of unfilled PP to less than 1%.
2. The UV stabilizer used in this study was not effective in reducing color change or loss in mechanical properties due to accelerated weathering for 50% and 70% wood flour composites. The UV stabilizer reduced the unexposed strength between 11% - 21% and modulus between 9% - 11% for wood filled HDPE and PP composites.
3. The addition of fungicide increased the occurrence of surface crazing for unreinforced PP specimens. The addition of fungicide does not appear to affect the color durability of wood flour composites.
4. Composites with 50% lignocellulosic by weight exhibited greater color change due to exposure than unfilled composites. The color change of PP composites with 70% wood flour was at most 3% different than similar composites with 50% wood flour. The color change for PP composites containing alternative fibers was greater for those that contained 50% fiber than those that contained 70% fiber. For most formulations, the color change for 70% wood flour HDPE composites was greater than those that contained 50% flour.
5. Strength and modulus of all composites with a greater content of lignocellulosic were more severally affected by exposure than those composites with lesser content except for PP composites filled with wood flour. The unexposed modulus increased with increasing content of wood flour for both HDPE and PP composites. Composites with 50% lignocellulosic were both stronger and stiffer than similar unfilled composites.
6. The use of colorants mitigated both changes to chromaticity and flexural properties in exposed specimens. The strength and modulus of PP specimens was greater than PP specimens containing black colorant regardless of the exposure. Colorants were more effective in reducing changes in flexural properties for HDPE wood filled composites than similar PP composites. Colorants were more

effective for reducing color change in HDPE composites than similar PP composites. Black Colorant was more effective than red colorant.

7. HDPE were generally less affected by accelerated weathering than similar PP composites.
8. The high variability in properties measured could be attributed to the intrinsic variability of the recycled materials used and or due to inconsistent batch mixing.

The conclusion drawn from Phase I are limited in that only a few replications were tested per formulation, the length of exposure was only 1500 hours and properties were only measured after the full exposure. In Phase II these limitation are addressed.

Chapter 4. Phase II. Effect of Length of Exposure on the Physical and Mechanical Properties of Natural Fiber Thermoplastic Composites

4.1 Introduction

In Phase I the effects of different concentrations of additives, lignocellulosic fillers, and accelerated weathering were determined for two thermoplastics. It was shown that accelerated laboratory weathering affected both the physical and mechanical properties of NFTC. Based on the performance of composites investigated in Phase I, four formulations were selected for further detailed study in Phase II. Because the HDPE composites were generally less affected by exposure than similar PP composites, only HDPE composites are evaluated in Phase II. Composites with 50% fiber were chosen because of higher flexural strength compared to 70% composites despite slightly lower flexural modulus values. The flexural properties of composites with 50% fiber were also less affected by accelerated weathering. Using an average variability of 8% for the results found in Phase I, the required sample size was determined for estimating the mean to within 5% specified confidence for Phase II according to ASTM D2915 (Appendix 4). To reduce variability and increase the confidence in the estimate of mean properties, a virgin polymer was chosen. In addition to static bending tests, impact tests were included in Phase II. How the mechanical properties changed throughout the exposure was not determined in Phase I; therefore it was decided for Phase II that sets of specimens be removed after increasing increments of exposure. A set of specimens was tested with the exposed surface oriented on the tension side, and a set of specimens was tested with the exposed surface oriented on the compression side to provide simulation of a variety of prospective service conditions.

The objective of the research presented in this chapter was to evaluate a limited number of formulations and the effects due to increments of accelerated weathering on physical and mechanical engineering properties.

4.2 Experimental

4.2.1 Materials

The materials used were high-density polyethylene (HDPE) and two natural fiber fillers, wood flour and kenaf fiber. The HDPE was Mobil 30-melt injection mold grade HMA018, and the wood flour was 425 μm (#40 mesh) maple flour (American Wood Fibers, Sheboygan, WI). Manufacturers plastic specifications are given in Appendix 5. The kenaf fiber was purchased from the recycled fiber market. In an attempt to control fiber length, we utilized only the fibers passing through a 6.35-mm (1/4-inch) screen and stopped by a 1.59-mm (1/16-inch) screen. Additives used in some formulations included a hindered amine UV stabilizer (TINUVIN 783 FDL; HALS), an antioxidant process stabilizer (B225 IRGANOX), and a compatibilizer (maleic anhydride grafted polyethylene, MAPE). The hindered amine was added at 0.4%, the antioxidant was

added 0.2%, and the compatibilizer was added at 2.0% by weight. The additives used in Phase II were the same as in Phase I.

4.2.2 Specimen Preparation

Four formulations were compounded by TGRT using proprietary compounding equipment (Table 4.1). Formulation 1 consisted of pure HDPE (no additives). Formulation 2 consisted of HDPE with antioxidant, HALS and MAPE additives. Formulation 3 contained 50% wood flour by weight and Formulation 4, 50% kenaf fiber by weight.

Table 4.1 Phase II Test Matrix

Formulation	Polymer	Additives			Filler	
	HDPE	HALS	Antioxidant	MAPE	Wood Flour	Kenaf
1 - HDPE	X					
2 - Additives	X	X	X	X		
3 - Wood	X	X	X	X	X	
4 - Kenaf	X	X	X	X		X

After compounding, the formulations were granulated and passed through a 6.35-mm (1/4-inch) screen and dried at 82°C (180°F) for 24 h prior to injection molding (Figure 4.1). Injection molding (Figure 4.2) was performed at the Forest Products Laboratory (FPL) using a 33-metric ton reciprocating-screw injection molder (Vista Sentry VSX-33, Cincinnati Milacron). Static bending specimens were molded in accordance with ASTM D790, which recommends specimen dimensions of 127 by 12.7 by 3.2 mm (5 by 1/2 by 1/8 inch). Impact testing specimens were 63.5 by 12.7 by 3.2 mm (2.5 by ½ by 1/8 inch). Injection molding cycle times are given in Appendix 6. Injection pressures and speeds were varied for the different formulations and are given in Appendix 7.

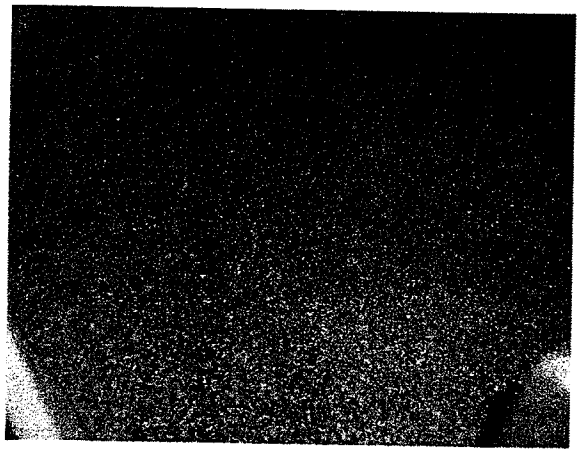

Figure 4.1 Granulated Polymer and Fiber after Compounding

Figure 4.2 30-Metric Ton Reciprocating-Screw Injection Molder

4.2.3.3 Flexural Testing

4.2.3.3.1 Static Bending Testing

Static bending tests were performed at the FPL Engineering Mechanics Laboratory, using a 2-KN (450-lb) Instron 5540 testing machine and a three-point bending setup (Figure 4.4). Specimens were tested in according to the procedure described in Chapter 3. A total of 1080 specimens were tested. Thirty specimens per formulation were held as controls and two sets of 15 specimens were tested at the end of every 500 hours of exposure. One set of 15 specimens was tested with the exposed surface oriented on the tension side. The other set of 15 specimens was tested with the exposed surface on the compression side. Flexural modulus was calculated using the same method as described in Phase I; however, the calculation of flexural strength was different than in Phase I. Linear elastic bending theory was again used; however, for specimens that did not fracture (typical of ductile plastics) the strain at yield was defined differently. In Phase I for specimens that did not fail before 5% strain was reached, the stress at 5% strain was reported as the yield stress. In Phase II tension tests were performed, and it was determined that full yielding occurred at about 3% strain. For this reason, in Phase II a 3% strain level was chosen to determine the yield stress. The stress strain diagrams for tension and 3-point bending tests are given in Appendix 9. In calculations of both flexural strength and modulus the gross cross section is used.

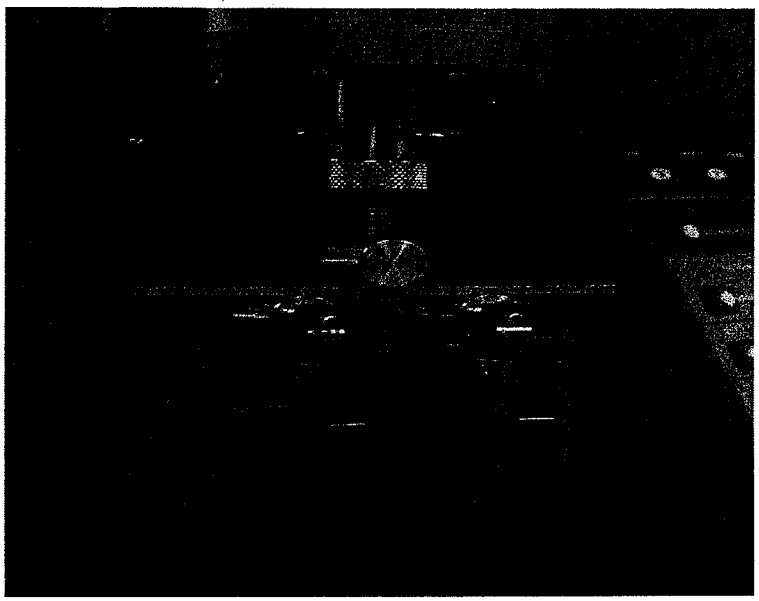

Figure 4.4 Phase II Three-Point Bending Setup (Instron 5540)

4.2.3.3.2 Impact Testing

Impact tests were performed on both unweathered (control) and weathered specimens at the FPL Composites Laboratory, using an Instron Dynatup 8250 drop weight impact testing (gravity driven) machine using a three-point bending setup (Figure 4.5). A total of

200 unnotched specimens were tested. Ten specimens per formulation were held as controls and two sets of 5 specimens were tested at the end of every 500 hours of exposure. One set of 5 specimens was tested with the exposed surface on the tension side. The other set of 5 specimens was tested with the exposed surface on the compression side. The maximum exposure of specimens tested in impact was 2000 hours. The support span was 51.2 mm (2.0 in.), corresponding to an L/d of 16. The impact velocity averaged 1.1 m/s, and the mass of the impacter was 5.2 kg (11.5 lbs) Specimens were conditioned for at least 48 h at 20°C (68°F) and 50% relative humidity (RH) prior to testing or until no change in mass was recorded. Continuous load and deflection data were recorded.

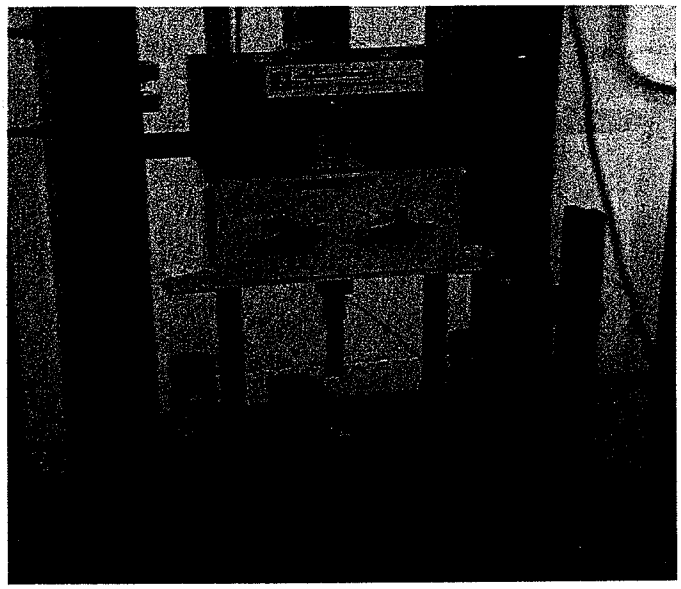

Figure 4.5 Impact Bending Setup (Instron 8250)

4.3 Results and Discussion

4.3.1 Effects of Accelerated Weathering on Color Fade

It was observed that the gated end of the specimens experienced smaller changes in color than the non-gated ends for injection molded parts. A possible explanation for this is that as the mold cavity is filled, the polymer begins to cool as it touches the cavity wall. The longer cooling times could result in a higher degree of crystallinity and could also result in a greater volume of polymer at the surface that could in turn protect the underlying fibers. Another possible explanation is that the higher crystallinity results in greater molecular orientation that could result in more scattering of UV light and less absorption.

The effect of accelerated weathering on specimen chromaticity was determined on both the side facing towards (front) and away from (back) the light source. Table 4.2 shows the effects of accelerated weathering on the average total color difference for all four

Table 4.2 Effect of Accelerated Weathering on Composite Chromaticity
Values reported: Average (% Coefficient of Variation)

Formulation	Orientation of Measured Surface	Total color difference (ΔE) at various exposure times			
		1000 h	2000 h	3000 h	4000 h
1 - HDPE	Front	1.6 (14.4)	2.6 (21.7)	1.9 (39.0)	4.2 (8.0)
	Back	1.8 (26.1)	2.4 (17.6)	1.8 (19.3)	4.1 (4.5)
2 - Additives	Front	4.4 (11.8)	5.0 (19.5)	5.5 (8.8)	5.8 (14.0)
	Back	4.2 (6.5)	5.1 (9.5)	4.7 (16.6)	7.3 (40.8)
3 – Wood	Front	24.4 (10.3)	31.3 (5.3)	32.2 (18.6)	37.8 (3.8)
	Back	6.1 (8.7)	8.0 (13.1)	9.7 (37.3)	15.7 (20.2)
4 – Kenaf	Front	46.0 (2.7)	50.6 (3.6)	51.5 (2.5)	53.6 (3.2)
	Back	21.9 (7.1)	22.5 (8.1)	23.2 (22.9)	28.5 (18.1)

formulations. Table 4.2 shows that all composite specimens showed a change in color due to accelerated weathering. It is shown that both the front and back of the specimens exhibited a change in chromaticity. It is shown that the fiber filled composites experienced the greatest change in color while Formulation 4 – kenaf experienced the greatest change in chromaticity of the four formulations. It is also shown that the most change in color for the fiber filled composites occurred during the first 1000 hours of exposure. Formulation 3 – wood and Formulation 4 – kenaf had 65% and 86% of the total color change occur during the first 1000 hours. Table 4.2 shows that for Formulation 1 – HDPE there does not appear to be a difference in chromaticity response for either the front or back surface. It is also shown that for Formulation 2 – HDPE the back of the specimen underwent a greater color change than the surface facing the lamp. For Formulation 3 – wood, the front of the specimen was 2.4 times more affected than the back of the specimen. The front of Formulation 4 – kenaf was 1.9 times more affected than the back. This suggests that there could be significant reflection of light inside the weatherometer.

If the walls were assumed to reflect the light perfectly (no loss in energy), the extra distance that the light must travel would be sufficient to reduce the magnitude of the incident light significantly. Using the inverse square law (Eq. 4.1) that states the intensity per unit area, E, varies in inverse proportion to the square of the distance, d, the reduction in irradiance can be estimated.

$$E = 1/d^2 \qquad (4.1)$$

Letting the energy that reaches the front of the specimen equal to the energy that is reflected to the back of the specimen (Eq. 4.2) and solving for the intensity of light that reaches the back of the specimen (Eq. 4.3)

$$E_1 d_1^2 = E_2 d_2^2 \qquad (4.2)$$

$$E_2 = \frac{E_1 d_1^2}{d_2^2} \tag{4.3}$$

Substituting in the irradiance, E_1, and distance, d_1, to the front of the specimen and the shortest distance the reflected light would travel to reach the back of the specimen, d_2, the irradiance reaching the back of the specimen would be 0.13 W/m^2.

$$E_2 = \frac{\left(0.35\ {}^{W}/_{m^2}\right)(0.46\ m)^2}{(0.76\ m)^2} \tag{4.4}$$

$$E_2 = 0.13\ {}^{W}/_{m^2} \tag{4.5}$$

If the color change was solely dependant upon the intensity of the UV light, it would be expected that the surface facing the lamp would experience at least a 64% greater change in color than the surface facing away from the lamp. For both fiber filled composites, the reduction in color change between the front and back was 42% and 53% for Formulation 3 – wood and Formulation 4 – kenaf respectively; that might indicate that other degradation mechanisms are occurring in the weathering chamber other than photooxidation.

For both unfilled composites the change in chromaticity due to accelerated weathering was less dependant upon orientation in the weathering chamber than the fiber filled composites. This suggests the degradation mechanisms of the filled composites were more dependant upon the irradiance than those in the unfilled polymers or that the change in chromaticity was better able to indicate photooxidative changes in the fiber filled composites than unreinforced composites.

Figures 4.6 – 4.9 show the effects of accelerated weathering on the total color difference of both the front and back surfaces for Formulations 1-4 respectively. Figures 4.6 – 4.9 show the mean values error bars equal to one standard deviation. It is shown that the variability in ΔE was high for all four formulations. It is shown that for all formulations except for Formulation 3 – wood, the total color difference was less after 2500 hours of exposure than specimens exposed for 2000 hours (Eq. 4.6). Equation 4.6 is only valid for the front surface for Formulation 3 – wood and not the back surface of that formulation.

$$\Delta E_{2000} > \Delta E_{2500} \tag{4.6}$$

The reduction in color change at 2500 hours of exposure can be explained by how sets of specimens were staggered during exposure (Appendix 8). Specimens that were exposed for 2000 hours were started at the beginning of the first bulb and were not exposed to the second bulb. Specimens exposed for 2500 hours were started after 1500 hours on the first bulb and were exposed to the entire second bulb. This would imply that accelerated weathering had more of an effect on changes to chromaticity during the first bulb (hours

0-2000) than the second (hours 2000 – 4000) by at least 500 hours (Eq. 4.7) even though the irradiance was maintained at 0.35 W/m^2 at 340 nm for the duration of both bulbs.

$$\Delta E_{Hours\ 0-2000} > \Delta E_{Hours\ 2000-4000} + \Delta E_{Hours\ 1500-2000} \qquad (4.7)$$

It was observed that specimens exposed for the final 1000 hours of the first bulb appeared to be less severely affected by accelerated weathering than specimens exposed to the first 1000 hours (Eq. 4.8).

$$\Delta E_{Hours\ 0-1000} > \Delta E_{Hours\ 1000-2000} \qquad (4.8)$$

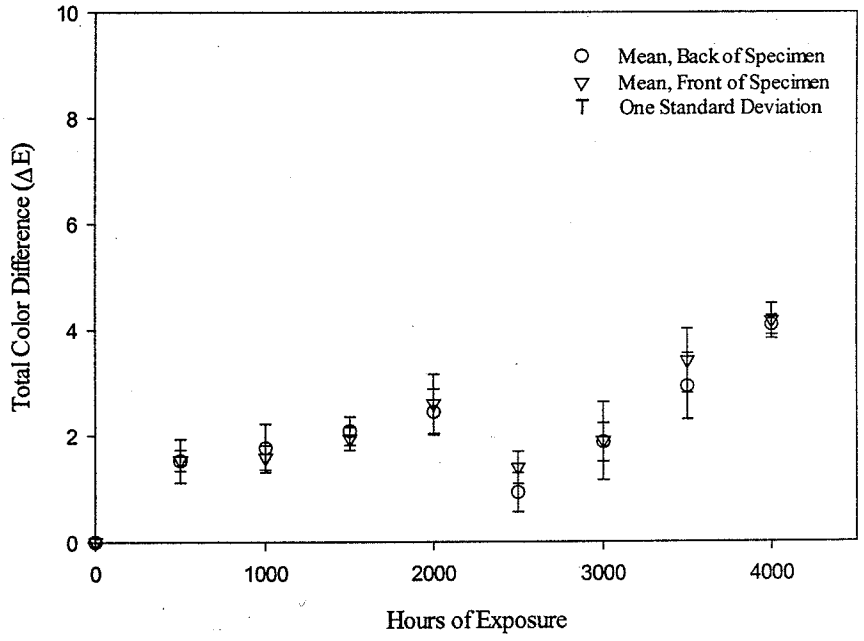

Figure 4.6 Effect of Accelerated Weathering on the Total Color Difference of Formulation 1 – HDPE

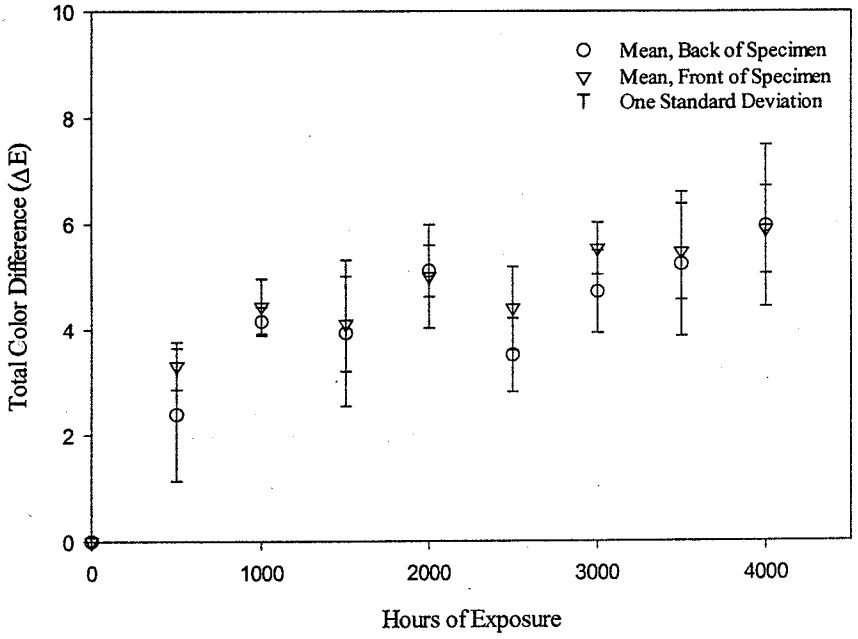

Figure 4.7 Effect of Accelerated Weathering on the Total Color Difference of Formulation 2 – Additives

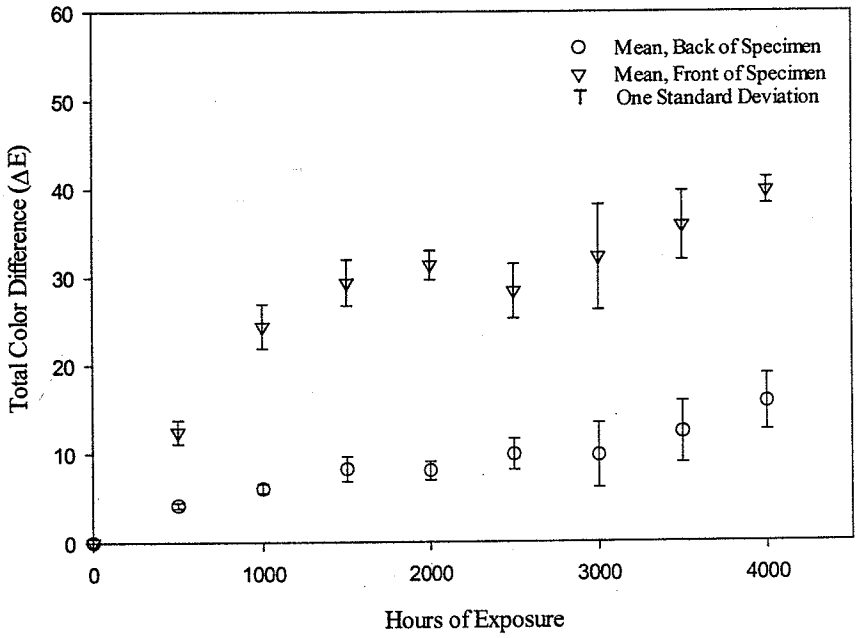

Figure 4.8 Effect of Accelerated Weathering on the Total Color Difference of Formulation 3 – Wood

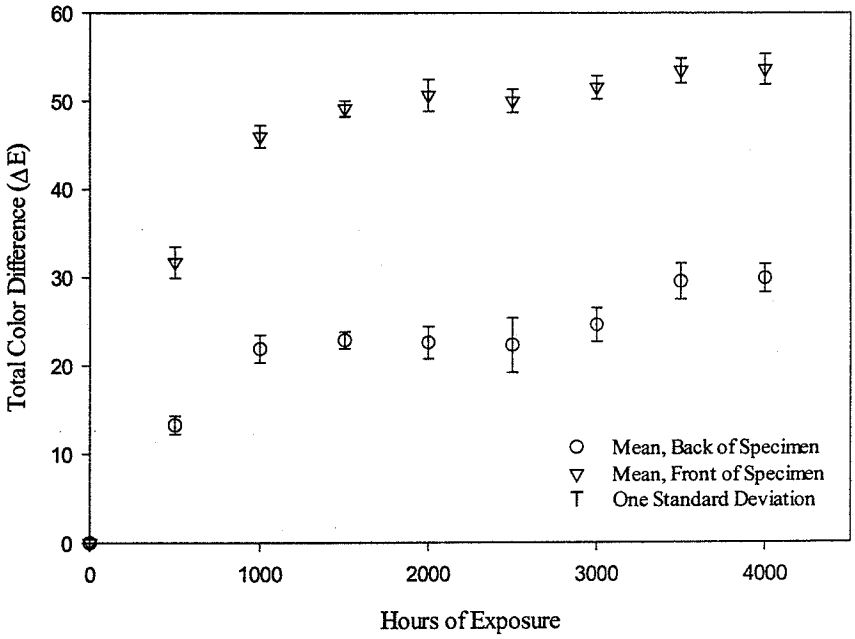

Figure 4.9 Effect of Accelerated Weathering on the Total Color Difference of Formulation 4 – Kenaf

To verify this observation, the chromaticity was determined for specimens that were placed in the weatherometer during the final 1000 hours. Ten specimens, five of Formulation 3 – wood, and five of Formulation 4 – kenaf exposed for the final 500 and ten specimens exposed the final 1000 hours of bulb 1 were selected and measured. The results are shown in Figure 4.10. Figure 4.10 shows that the average total color difference of specimens exposed for the final 1000 hours of bulb 1 was less than specimens exposed for the first 1000 hours. It is shown that for Formulation 3 – wood, specimens exposed for the final 500 hours only, were 23% less affected than specimens exposed for only the first 500 hours. Formulation 4 - kenaf specimens exposed for the final 500 hours were 28% less affected than those specimens exposed for the first 500 hours. After 1000 hours of exposure the difference in color change is reduced to 17% and 21% respectively for Formulation 3 – wood, and Formulation 4 – kenaf. A possible explanation for these differences could lie in the composites' sensitivity to the wavelength distribution of energy. The wavelengths that are most damaging to polyolefins and lignocellulosic materials are those less than 300 nm (Davis 1983, Hon 2001). The spectral power distribution of energy may have shifted away from the more damaging wavelengths even though the irradiance at one single wavelength remained constant. This spectral shift would complicate correlating accelerated weathering to outdoor exposure. To account for the apparent shift in the spectral power distribution, the entire spectral output would need to be known and the wattage would need to be adjusted so that more critical wavelengths could be consistently maintained.

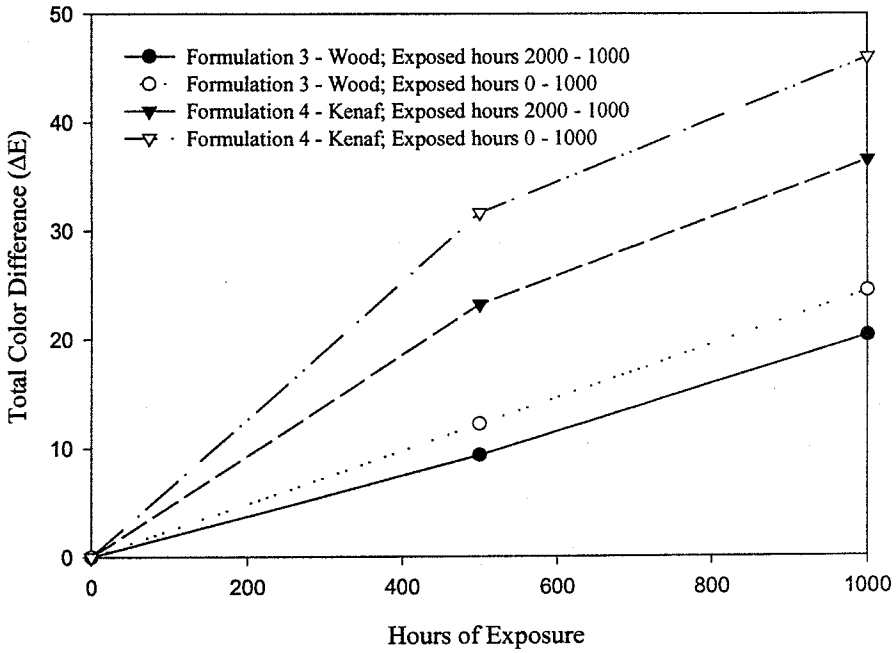

Figure 4.10 Comparison of The Mean Total Color Difference Between Specimens Exposed for the First and Last 1000 hours of Bulb 1

4.3.2 Effects of Accelerated Weathering on Flexural Properties

4.3.2.1 Load Deflection Curves

The effects of accelerated weathering on the flexural properties of NFTC were determined through physical testing. The mechanical properties were calculated using load-deflection data obtained during flexural testing. Figures 4.11 through 4.14 show typical load deflection response of all four formulations tested after specific increments of exposure. The typical curves represent the load – deflection curve of a specimen that at any increment of exposure the maximum load for that specimen was nearest to the mean of the specimen set. Figure 4.11 shows that with increasing exposure the strain at failure decreased for Formulation 1 – HDPE. Figure 4.12 shows that Formulation 2 – additives experienced little change in load deflection characteristics due to accelerated weathering. For both fiber filled composites, Formulation 3 - wood and 4 – kenaf, there was an increase in strain and decrease in stress at failure with increased exposure. The increase in strain at failure could imply that there has been a reduction in the interfacial bond between the fiber and matrix due to exposure. A loss in interfacial bond could result in the fiber slipping in the matrix allowing for greater strain.

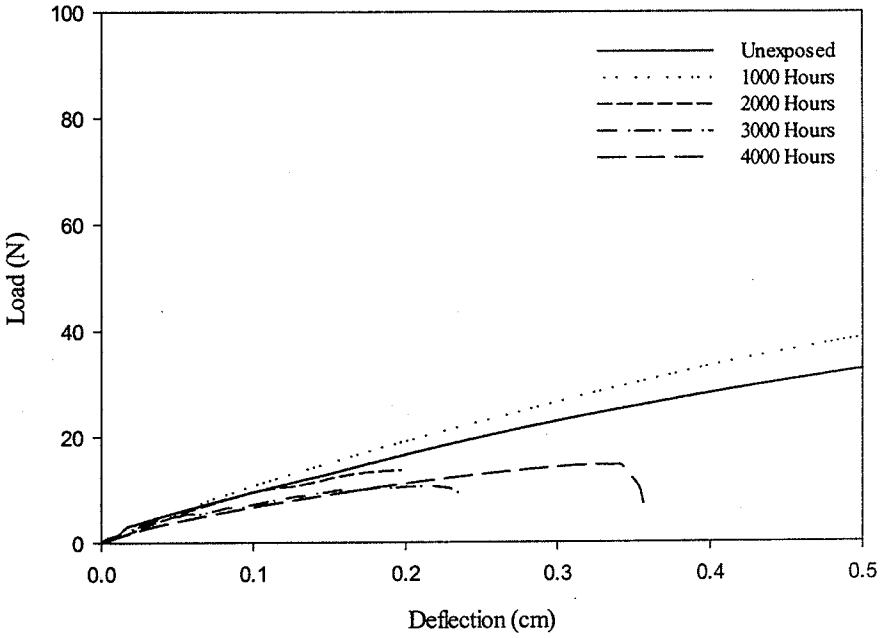

Figure 4.11 Typical Load Deflection Curves for Formulation 1 – HDPE

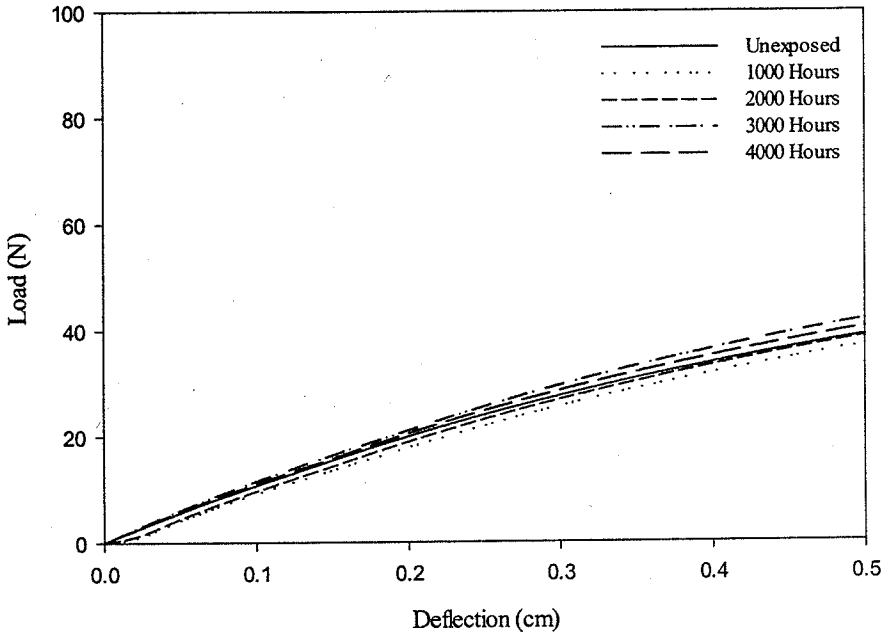

Figure 4.12 Typical Load Deflection Curves for Formulation 2 - Additives

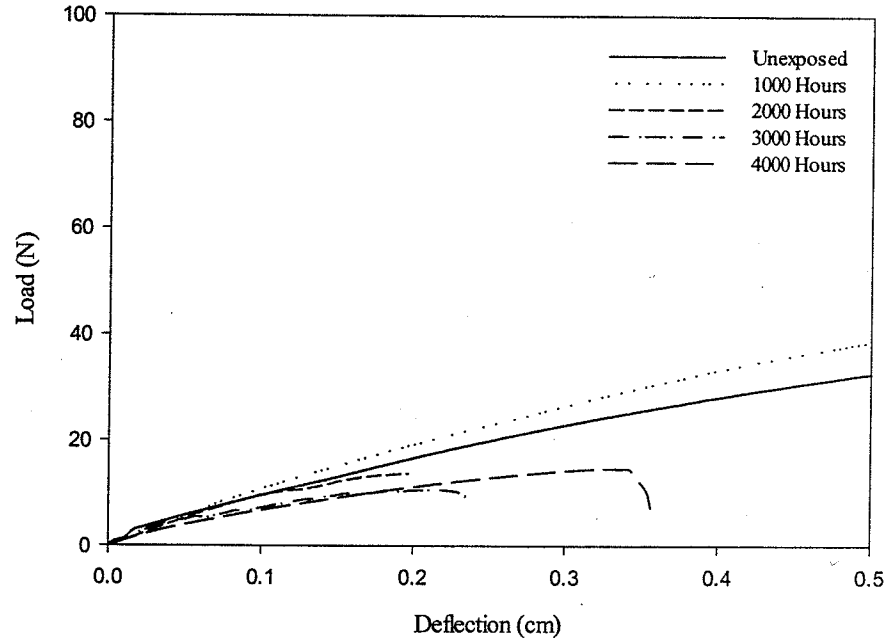

Figure 4.11 Typical Load Deflection Curves for Formulation 1 – HDPE

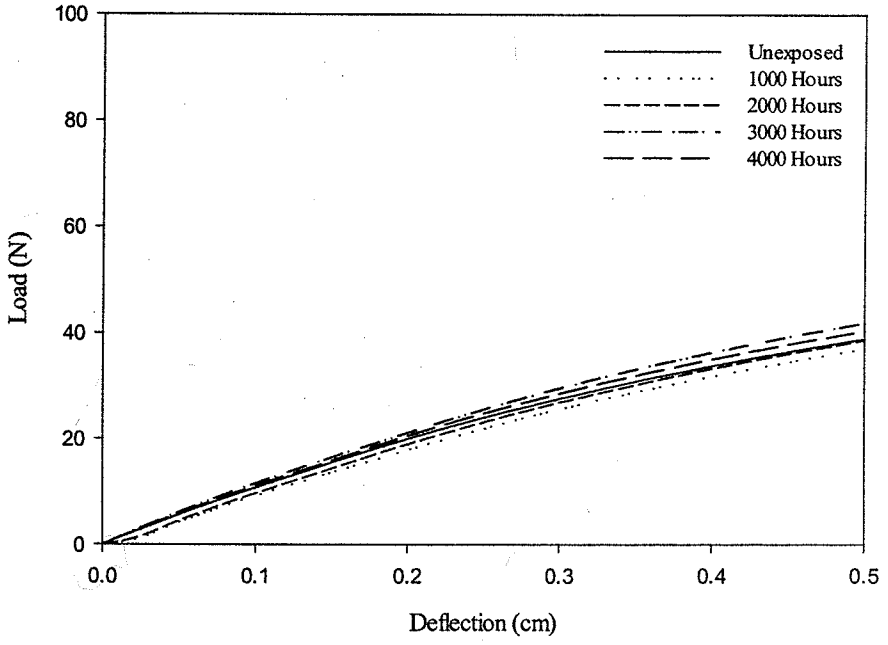

Figure 4.12 Typical Load Deflection Curves for Formulation 2 - Additives

4.3.2.2 Orientation of the Degraded Layer

To determine if the orientation of the degraded layer (the surface nearest to the light source) affects the flexural properties of NFTC, a statistical analysis was performed. A one – way analysis of variance was performed for all formulations for both flexural modulus and strength. Table 4.3 and 4.4 show the effects of accelerated weathering on the flexural modulus and strength. If there was no statistically significant difference between the means at 95% confidence of those specimens tested with the degraded layer on the compression side and those tested with the degraded layer on the tension side in flexure. Only one number appears in the table at that exposure. This number is the mean of 30 specimens, fifteen of which were oriented with the degraded layer on the compression side and fifteen oriented with the degraded layer on the tension side. If two numbers appear in the table at any exposure for any one formulation, it indicates that there was a statistically significant difference and the number reported is the mean of 15 specimens.

4.3.2.3 Flexural Modulus

To provide an indication of changes induced by accelerated weathering, flexural modulus was calculated. Table 4.3 shows the effect of weathering on composite flexural modulus.

Table 4.3—Effect of Accelerated Weathering on Composite Flexural Modulus
Values Reported: Averages (% Coefficient of Variation)

Formulation	Flexural Modulus (MPa) at various exposure times				
	0 h	1000 h	2000 h	3000 h	4000 h
1 - HDPE – Exposed Surface on Compression Side	668 (4.2)	944 (4.4)	1140 (5.9)	522 (55.9)	567 (7.8)
1 - HDPE– Exposed Surface on Tension Side		989 (3.8)	1060 (6.3)	735 (8.8)	497 (8.6)
2 - Additives– Exposed Surface on Compression Side	817 (2.7)	751 (2.2)	790 (1.9)	703 (3.5)	702 (3.5)
2 - Additives– Exposed Surface on Tension			762 (2.5)		686 (1.6)
3 - Wood	3,950(1.7)	2800 (2.5)	2,630 (3.0)	2040 (2.9)	1770 (4.9)
4 – Kenaf – Exposed Surface on Compression Side	5,950 (6.7)	3600 (5.8)	3,390 (3.3)	2550 (4.7)	2280 (5.3)
4 – Kenaf – Exposed Surface on Tension			3462 (5.4)		

The flexural modulus for both fiber filled composites (Formulation 3 and 4) was greater than that of both unreinforced thermoplastics (Formulation 1 and 2). The flexural modulus of Formulation 4 – kenaf was greater than all other formulations regardless of the length of exposure. It is shown that the flexural modulus of Formulation 1 – HDPE is 74% of published values for this particular resin (Appendix 5). The variability in unexposed properties was low and probably can be attributed to the use of a virgin polymer. The flexural modulus for all four formulations decreased after 4000 hours of exposure. Accelerated weathering was most severe on Formulation 4 – kenaf. This reduction might be explained by the breakdown of the fiber or particle (flour) and/or the fiber–plastic bond and will be addressed in Chapter 5.

The flexural modulus for Formulation 1 – HDPE increased 70% after 2000 hours of exposure. This could indicate that up until 2000 hours Formulation 1 – HDPE was undergoing cross linking, resulting in greater modulus. The flexural modulus of Formulation 1 – HDPE was greater than Formulations 2 – additives after 1000 and 2000 hours of exposure but was less than Formulation 2 – additives at exposures greater than 2000 hours. After 2000 hours the modulus dropped significantly to 74% and 85% of the unexposed modulus when the exposed surface was oriented on the tension and compression side, respectively. After 2000 hours Formulation 1 – HDPE was potentially going through chain scission resulting in lowered modulus. The orientation of the exposed surface for Formulation 1 – HDPE did significantly affect the flexural modulus at all lengths of exposure. For Formulation 1 – HDPE specimens tested with the exposed surface on the tension side, the loss in modulus was more severe.

The flexural modulus for Formulation 2 – Additives decreased between 0 – 1000 hours and 2000 and 4000 hours but increased between 1000 and 2000 hours of exposure. After 4000 hours the modulus was 84% of the unexposed modulus and could indicate that the some of the UV stabilizer was consumed. Formulation 2 – Additives after 4000 hours of accelerated weathering was as stiff as unexposed Formulation 1 – HDPE. The orientation of the exposed surface was significant at 2000 and 4000 hours of exposure.

The flexural modulus for Formulation 3 – Wood decreased with increasing exposure. The modulus decreased the most between 0 – 1000 hours of exposure. After 4000 hours of exposure the modulus was only 45% of the unexposed modulus. The orientation of the exposed surface did not significantly affect the flexural modulus at all lengths of exposure.

The flexural modulus for Formulation 4 – kenaf decreased with increasing exposure. The modulus decreased the most between 0 – 1000 hours of exposure. After 4000 hours of exposure the modulus was only 38% of the unexposed modulus. The orientation of the exposed surface was only significant at 2000 hours of exposure.

Figures 4.15 – 4.19 show the effects of accelerated weathering on the flexural modulus for Formulations 1-4. Figures 4.15 – 4.19 show the mean value with error bars equal to one standard deviation. Figure 4.15 shows the effects of accelerated weathering on the flexural modulus of Formulation 1 – HDPE tested with the exposed surface on the

compression side. After 2000 hours of exposure, the variability in modulus increased significantly then decreased for 3500 and 4000 hours of exposure. This could be explained by the occurrence of surface crazing. Crazing began to appear after 1000 hours of exposure, and the concentration of these cracks increased with increasing exposure. Crazing induced a slight camber in Formulation 1 – HDPE specimens. If the crazing was not evenly distributed, the curvature of the specimen would not be constant. If a specimen were then loaded and allowed to deflect, crazing induced curvature would influence the deflected shape resulting in a variety of deflected shapes dependant upon the location of the crazes and the induced curvature. After 3500 hours of exposure the surface crazing was severe and occurred along the entire surface of the specimen. This regularity allowed for a more symmetric camber and would reduce the variability in the deflected shape.

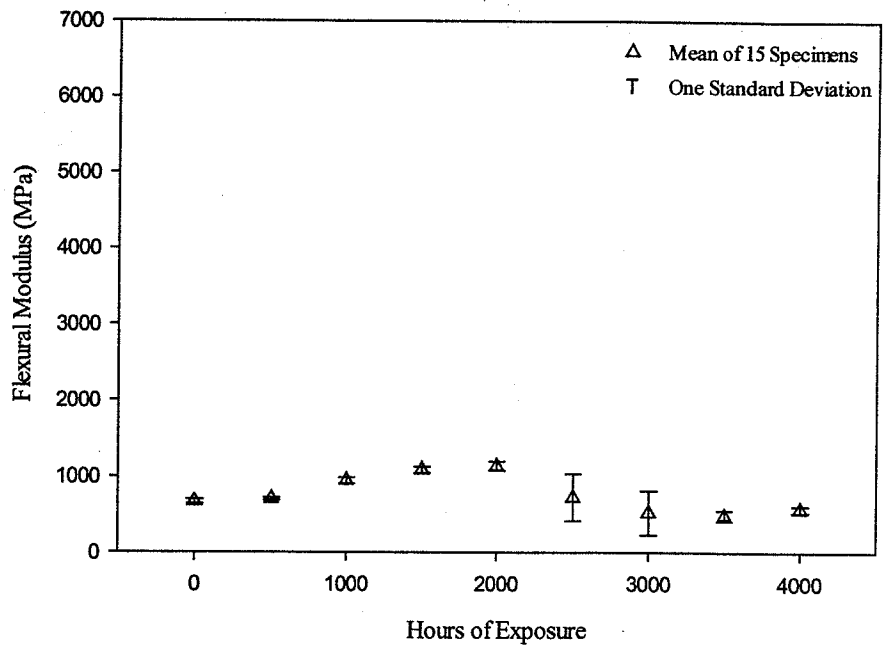

Figure 4.15 Effect of Accelerated Weathering on the Flexural Modulus of Formulation 1 – HDPE Tested With Exposed Surface on Compression Side

Figure 4.16 shows the effects of accelerated weathering on the flexural modulus of Formulation 1 – HDPE tested with the exposed surface on the tension side. Unlike Figure 4.15 the variability in modulus is not as great. Figure 4.17 shows that the variability is very low, and the modulus remains relatively unchanged for the 4000 hours of exposure. This probably indicates that the UV stabilizer and antioxidant were effective in reducing the change in modulus observed for Formulation 1 – HDPE. Figure 4.18 and 4.19 show that after the initial reduction, the modulus seems to remain relatively constant from 1500 hours to 3000 hours. After 3000 hours the modulus again appeared to decrease.

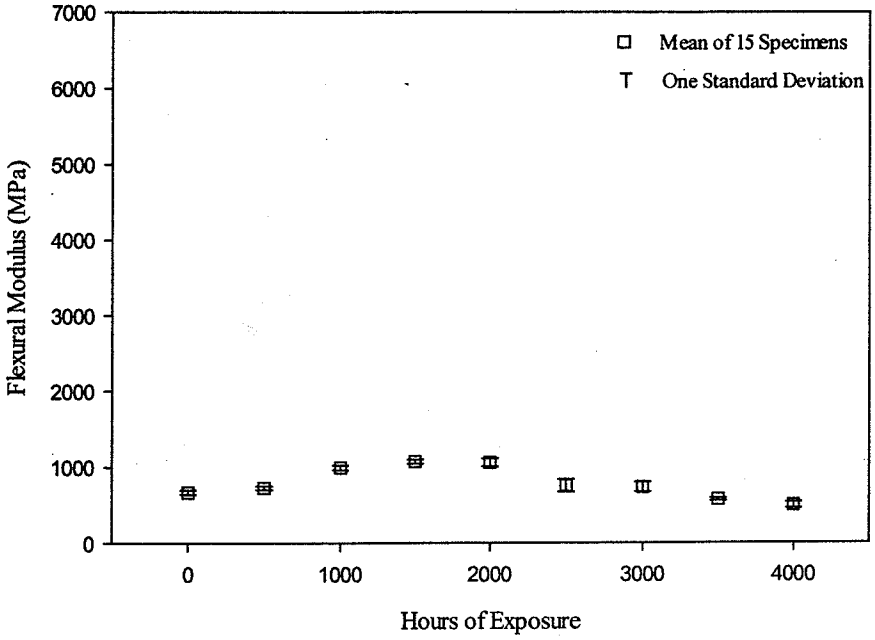

Figure 4.16 Effect of Accelerated Weathering on the Flexural Modulus of Formulation 1 – HDPE Tested With Exposed Surface on Tension Side

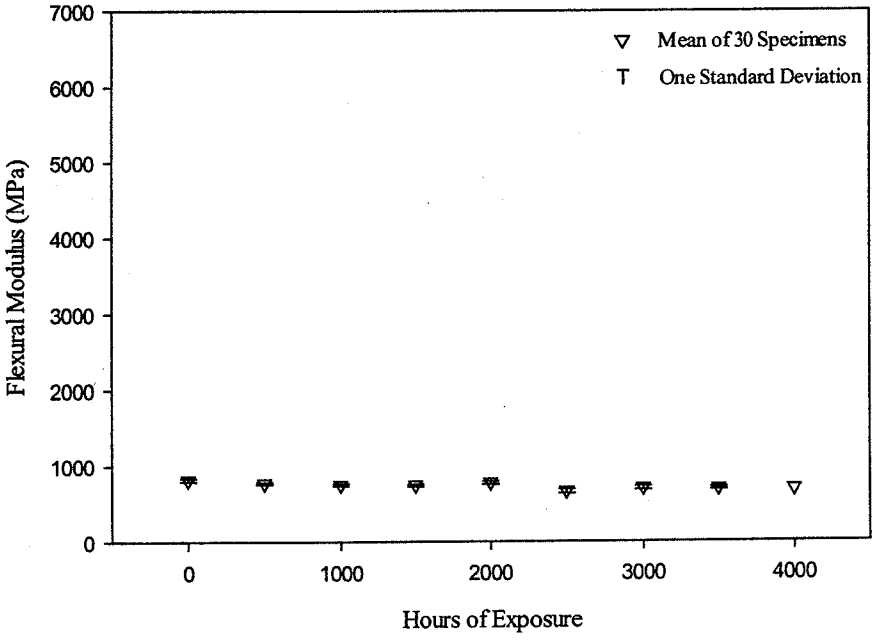

Figure 4.17 Effect of Accelerated Weathering on the Flexural Modulus of Formulation 2 –Additives

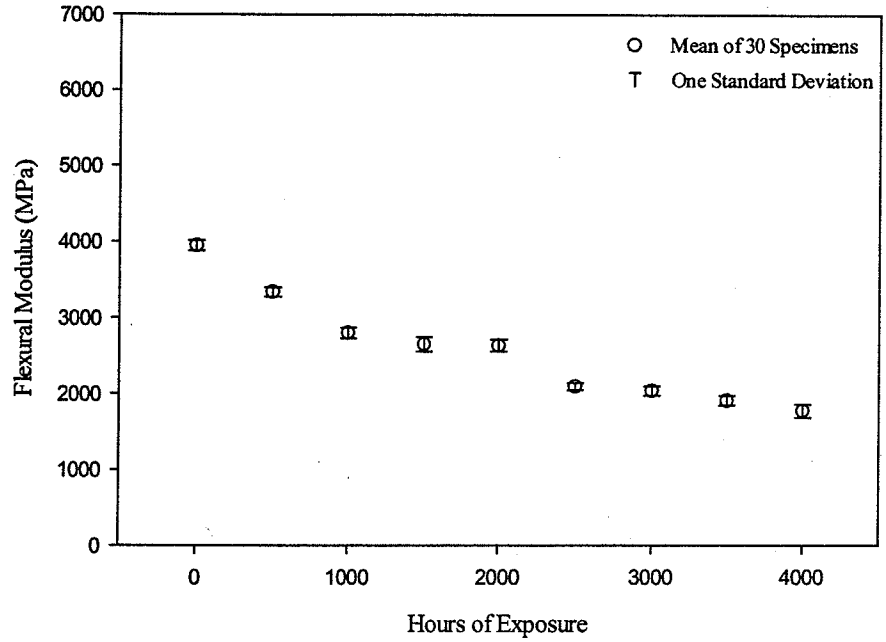

Figure 4.18 Effect of Accelerated Weathering on the Flexural Modulus of Formulation 3 – Wood

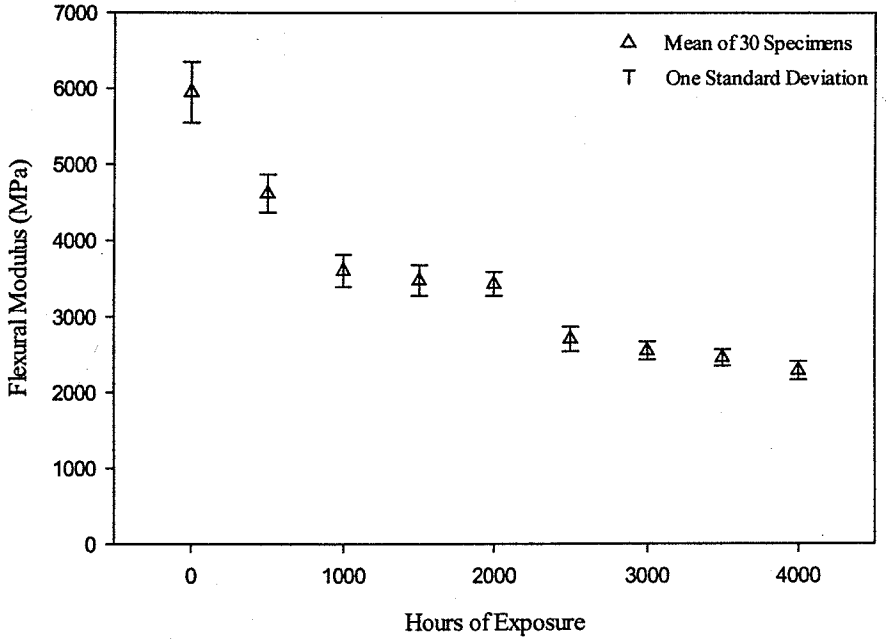

Figure 4.19 Effect of Accelerated Weathering on the Flexural Modulus of Formulation 4 – Kenaf

4.3.2.4 Flexural Strength

Modulus of rupture (MOR) was calculated for each specimen that fractured. Formulation 1- HDPE specimens exposed for 500 h or less and all Formulation 2 – additives specimens regardless of length of exposure did not fracture until the deflection became excessive. In these cases, the flexural yield stress was calculated using stress corresponding to 3% strain. At 1000 h of exposure, Formulation 1 – HDPE specimens tested with the exposed surface on the compression side did not fracture before 3% strain (full yielding) was reached; however, Formulation 1 – HDPE specimens tested with the exposed surface on the tension side did fracture. All Formulation 1 - HDPE specimens fractured at exposures greater than 1000 h.

Accelerated weathering had a similar effect on strength and modulus. Table 4.4 shows the effect of accelerated weathering on average composite flexural strength. Table 4.4 shows that the flexural strength of both fiber filled composites (Formulation 3 - wood and 4 - kenaf) was significantly greater than both unreinforced thermoplastics (Formulation 1- HDPE and 2 - additives) regardless of the length of exposure. Formulation 4 – kenaf had the greatest flexural strength, and Formulation 1- HDPE had the smallest flexural strength of all formulations. Formulation – 2 additives, is largely unaffected by the exposure conditions, though there was an increase in flexural strength at 3000 hours. It is shown that the flexural strength for both Formulation – 3 wood and Formulation – 4 kenaf, decreased with increasing exposure.

The flexural strength for Formulation 1 – HDPE increased 13% after 1000 hours when the degraded layer was oriented on the compression side. The flexural strength decreased with increasing exposure for all other lengths of exposure and orientations. After 4000 hours the flexural strength was 78% and 58% of the unexposed strength for specimens oriented with the exposed surface on the tension and compression side respectively. The orientation of the degraded layer was significant at all lengths of exposure for Formulation 1 – HDPE. At 2000 hours of exposure and greater, the strength was greater for those specimens oriented with the exposed surface on the tension side.

The flexural strength for Formulation 2 – Additives increased 5% after 4000 hours of exposure. The orientation of the exposed surface was significant at 2000 and 3000 hours of exposure.

The flexural strength for Formulation 3 – Wood decreased with increasing exposure for all specimens with the exposed surface on the tension side. The strength increased 3% between 3000 and 4000 hours when the exposed surface was oriented on the compression side. After 4000 hours of exposure, the strength was 71% and 67% of the unexposed strength when the exposed surface was oriented on the compression and tension side respectively. The most significant (17%) loss in strength occurred between 0 – 1000 hours of exposure. The orientation of the exposed surface was only significant after 3000 hours of exposure.

The flexural strength for Formulation 4 – kenaf decreased with increasing exposure. The most significant loss (22%) in strength occurred during the first 1000 hours. After 4000 hours the strength was 62% and 65% of the unexposed strength when the exposed surface was oriented on the tension and compression side respectively. The orientation of the exposed surface was only significant at 4000 hours of exposure.

Table 4.4 Effect of Accelerated Weathering on Composite Flexural Strength
Values Reported: Average (%Coefficient of Variation)

Formulation	Flexural Strength (MPa) at Various Exposure Times				
	0 h	1000 h	2000 h	3000 h	4000 h
1 – HDPE – Exposed Surface on Compression Side	14.0 (4.7)	15.8 (6.8)	9.4 (16.5)	5.6 (6.5)	8.1 (6.1)
1 – HDPE – Exposed Surface on Tension Side		13.0 (11.0)	10.2 (6.1)	11.4 (4.0)	10.9 (8.9)
2 - Additives – Exposed Surface on Compression Side	16.5 (1.3)	16.0 (1.4)	16.6 (1.2)	17.9 (1.9)	17.3 (1.4)
2 - Additives – Exposed Surface on Tension Side			16.4 (1.8)	18.5 (1.2)	
3 - 50% Wood – Exposed Surface on Compression Side	36.9 (2.4)	30.8 (2.4)	29.7 (3.0)	25.3 (3.6)	26.2 (4.0)
3 - 50% Wood – Exposed Surface on Tension Side				28.4 (2.6)	24.8 (7.4)
4 - 50% Kenaf – Exposed Surface on Compression Side	48.2 (4.8)	37.6 (5.0)	36.5 (3.6)	31.6 (3.6)	31.5 (4.6)
4 - 50% Kenaf – Exposed Surface on Tension Side					30.1 (4.4)

Table 4.4 shows that the variability in unexposed properties is generally low and can probably be attributed to the virgin polymer. Additionally the variability for Formulation 2 – additives is very low. This may be attributed to the use of an antioxidant that probably limited degradation associated with processing. Table 4.4 shows that the coefficient of variation for Formulation 3 – wood increased with increasing exposure

though no changes in types of failures were observed. Significantly higher variability was observed in flexural strength for Formulation 1 - HDPE for exposures greater than 1000 h. Observations of the weathered specimens and the corresponding failure types offer an explanation for this variability. Nearly all the weathered Formulation 1 specimens began to exhibit surface crazing at irregular intervals across the surface at 1000 h of exposure. This crazing propagated surface cracks perpendicular to the mold filling flow (perpendicular to the specimen length). At 1000 h of exposure, these cracks were located sporadically and lowered the strength of only some specimens. Other specimens were not affected. This had the overall effect of increasing variability in the strength results. As exposure time increased, more cracks formed in more specimens. This lowered not only strength but also variability at the longer exposure levels (1500 and 2000 h). Again high variability is observed for formulation 1 at 3000 hours of exposure. This high variability can was again attributed to the occurrence of surface crazing. At 3000 hours of exposure the crazing on the specimen surface began to propagate through the thickness of the polymer and began to appear on the backside of the composite. These crazes were sporadically located along the length of the specimen on the backside. After 3500 hours of exposure, the crazing became regular along the backside resulting in more consistent failures for Formulation 1 - HDPE.

Figures 4.20 – 4.24 show the effects of accelerated weathering on the flexural strength of Formulations 1 – 4. Figures 4.20 – 4.24 show the mean values with error bars equal to one standard deviation. Figure 4.20 shows the effect of accelerated weathering on the flexural strength of Formulation 1 – HDPE oriented with the exposed surface on the compression side in bending. Shown is an increase in strength with increasing exposure up to 1000 hours. The variability in strength was greatest at 1000 hours of exposure. At lengths of exposure greater than 1000 hours, the flexural strength decreases.

Figure 4.21 shows the effect of accelerated weathering on the flexural strength of Formulation 1 – HDPE oriented with the exposed surface on the tension side in bending. There was a slight increase in strength at 500 hours of exposure. After 500 hours of exposure the flexural strength was less than that of the exposed specimens. The flexural strength does appear to be somewhat constant at 1000 hours and greater even though a significant number of surface cracks were visible.

Figure 4.22 shows the effect of accelerated weathering on the flexural strength of Formulation 2 – additives. Yield stress for Formulation 2 – additives is relatively constant with exposure. It is noted that a slight decrease in yield stress is observed at 2500 hours of exposure. This decrease in yield stress could be related to the decrease in color change also observed at this length of exposure. It can be concluded that the UV stabilizer and antioxidant used in Formulation 2 – additives was effective in reducing loss in strength for 4000 hours of accelerated weathering

Figure 4.23 shows the effect of accelerated weathering on the flexural strength of Formulation 3 – wood. It is shown that the flexural strength decreased with increasing exposure. It is shown that the greatest loss in strength occurred during the first 1000 hours.

Figure 4.24 shows the effect of accelerated weathering on the flexural strength of Formulation 4 – kenaf. It is shown that the flexural strength decreased with increasing exposure. It is shown that the greatest loss in strength occurred during the first 1000 hours of exposure.

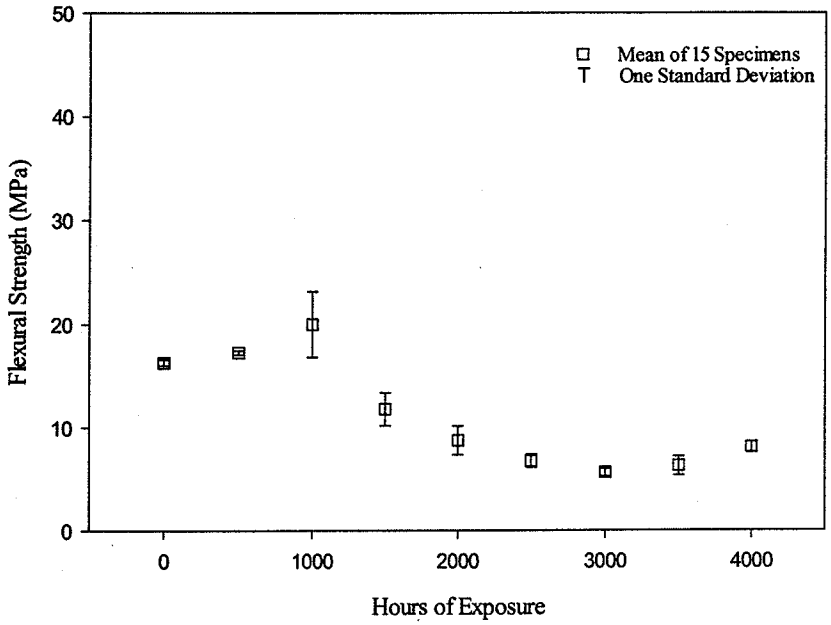

Figure 4.20 Effect of Accelerated Weathering on the Flexural Strength of Formulation 1 – HDPE Tested with Exposed Surface on Compression Side

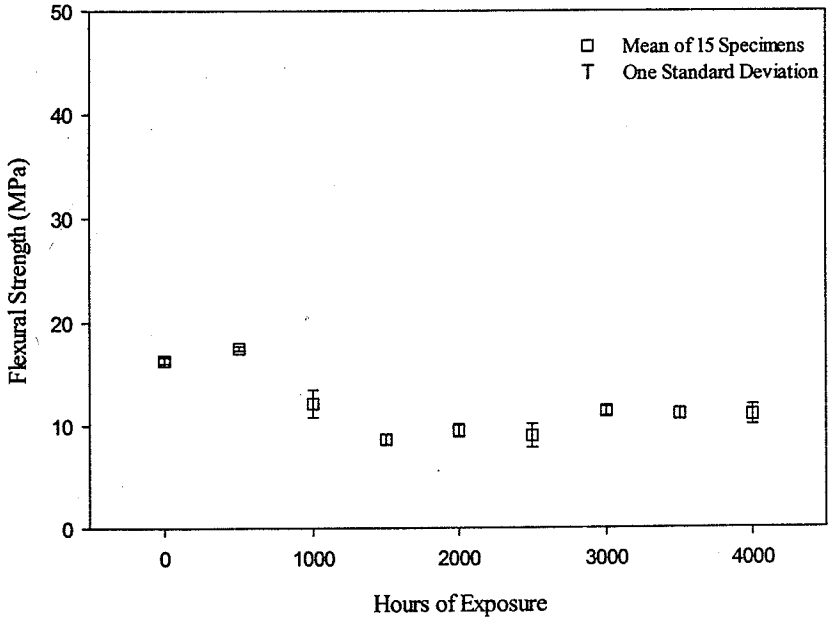

Figure 4.21 Effect of Accelerated Weathering on the Flexural Strength of Formulation 1 – HDPE Tested with Exposed Surface on Tension Side

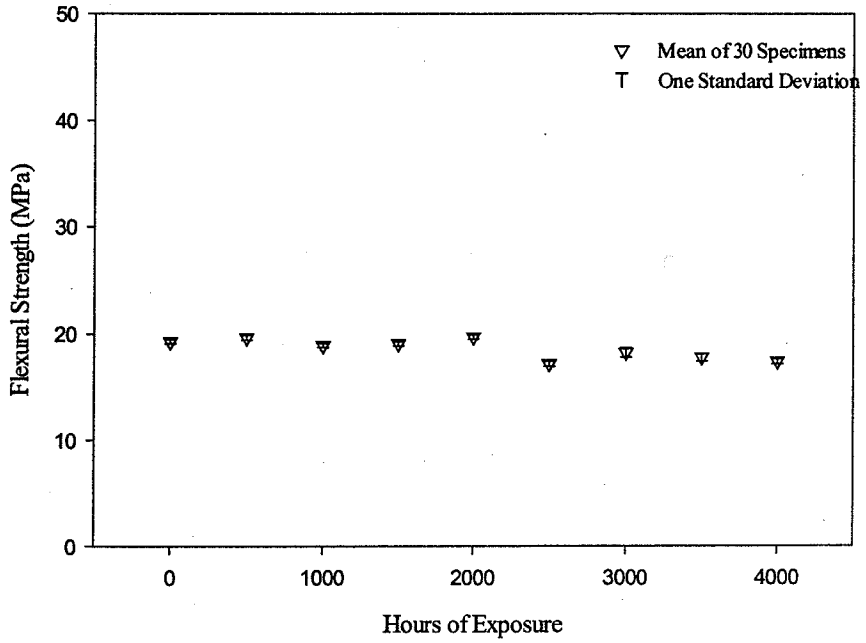

Figure 4.22 Effect of Accelerated Weathering on Maximum Fiber Stress for Formulation 2 – Additives

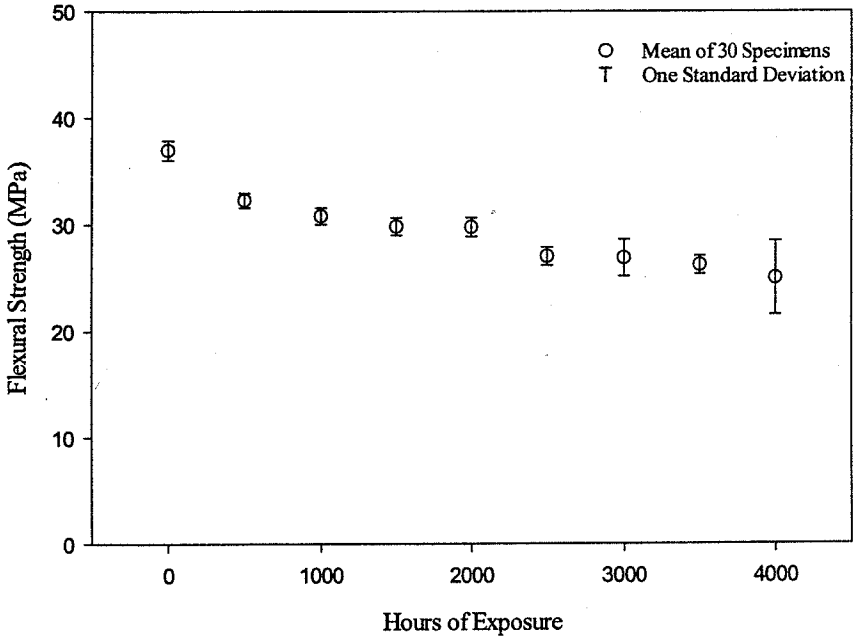

Figure 4.23 Effect of Accelerated Weathering on Maximum Fiber Stress for Formulation 3 – Wood

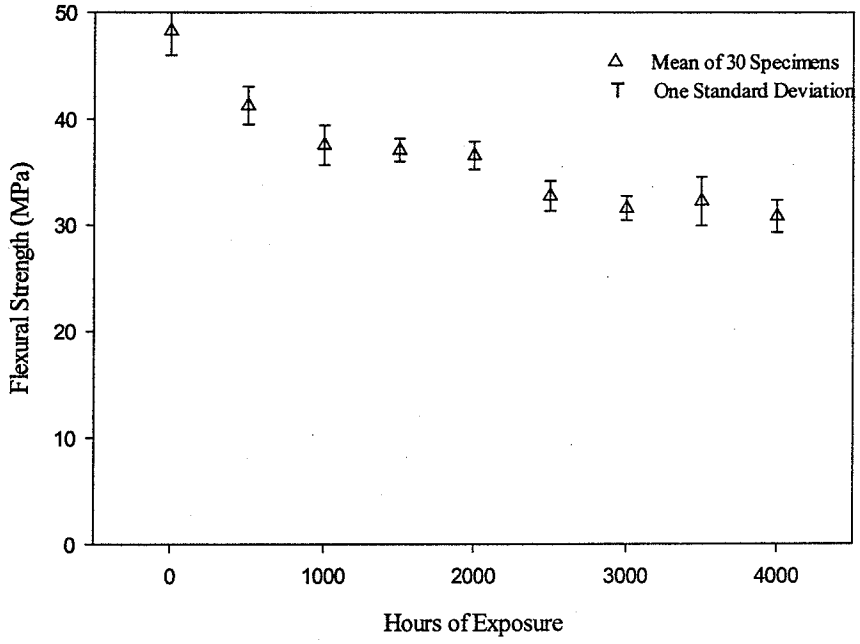

Figure 4.24 Effect of Accelerated Weathering on Maximum Fiber Stress for Formulation 4 – Kenaf

4.3.2.5 Impact Properties

The impact properties were determined to evaluate the effects of impact loading on weathered composites. All unexposed Formulation 1 – HDPE specimens and those exposed for 500 hours failed to fracture before being pushed through the supports. After 500 hours of exposure, all Formulation 1 – HPDE specimens fractured. All Formulation 2 – additives specimens failed to fracture regardless of the length of exposure and eventually were pushed through the supports. All Formulation 3 – wood and 4 – kenaf fractured regardless of the length of exposure. The load deflection plots for all four formulations contained small oscillations, especially at the beginning of the load deflection trace. Oscillatory behavior is due to the specimen and impact tester vibrating due to initial impact. These oscillations dampened out for all formulations except for Formulation 1 – HPDE exposed for 1000 hours and greater. As a consequence of the large dynamic effects for Formulation 1, typical impact values of energy are not reported and maximum loads are reported in Table 4.5

Table 4.5 shows the effects of accelerated weathering on the average composite impact strength. The data in Table 4.5 are the mean values of 10 specimens for all formulations except Formulation 1 – HDPE. The mean values for Formulation 1 are those of 5 specimens. It is shown that the impact strength of Formulation 2 – additives is the greatest of all four formulations and actually increased 4% after exposure. The impact strength of both fiber filled composites (Formulation 3 and 4) is greater than that of Formulation 1 – HDPE. The impact strength of all formulations except Formulation 2 –

additives decreased with increasing exposure. The impact strength for Formulation 1 – HDPE was 51% and 60% of unexposed specimens when the exposed surface was oriented on the tension and compression side respectively. It is shown that for Formulation 3 – wood and Formulation 4 – kenaf the impact strength after 2000 hours is 75% and 70% respectively of the unexposed specimens of the same formulation.

Table 4.5 Effect of Accelerated Weathering on Composite Impact Strength
Values Reported: Average (% Coefficient of Variation)

Formulation	Mean Impact Strength (MPa) at Various Exposure Times				
	0 h	500 h	1000 h	1500 h	2000 h
1 - HDPE– Exposed Surface on Tension Side	30.7 (1.8)	29.7 (1.5)	26.0 (16.8)	18.0 (11.4)	16.0 (16.5)
1 – HDPE: Exposed Surface on Compression Side		31.2 (3.0)	32.9 (4.5)	20.8 (12.4)	18.5 (2.4)
2 - Additives	82.5 (6.5)	84.0 (6.2)	85.9 (8.2)	86.1 (8.8)	86.4 (8.4)
3 - 50% Wood	55.4 (3.7)	49.6 (2.3)	47.0 (2.2)	43.7 (4.1)	41.8 (4.3)
4 - 50% Kenaf	67.5 (3.3)	57.6 (6.9)	52.1 (8.4)	51.0 (4.5)	47.2 (2.1)

Impact tests are useful in determining materials toughness, or the energy per unit area necessary for fracture. Figures 4.25 – 4.27 show the effect of accelerated weathering on the energy to maximum load for Formulation 2 – additives, Formulation 3 – wood, and Formulation 4 – kenaf. A plot is not presented for Formulation 1 – HDPE. Formulation 1 – HDPE was not included due to the large dynamic effects observed after 1000 hours of exposure, resulting in a coefficient of variation greater than 100%. The data in Figures 4.25 - 4.27 is that of ten samples, five of which were tested with the exposed surface on the tension side and five of which were tested with the exposed surface on the compression side. Figures 4.25 – 4.27 show the mean values with error bars equal to one standard deviation. It is shown that the energy to max load is not dramatically reduced due to 2000 hours of accelerated weathering for all three formulations presented. This can be explained by discussing the load deflection curves for these formulations. The energy to maximum load is the area under the load deflection curves up till the maximum load. For Formulation 2 – additives, the maximum load increased with increasing exposure but the deflection was reduced. For Formulation 3 – wood and 4 – kenaf the maximum load was reduced with increasing exposure but the deflection was increased similar to the load deflection curves for the static bending tests. For Formulation 3 – wood and 4 – kenaf tested in impact a decrease in strength is a better indication of the influence of weathering than the energy to maximum load.

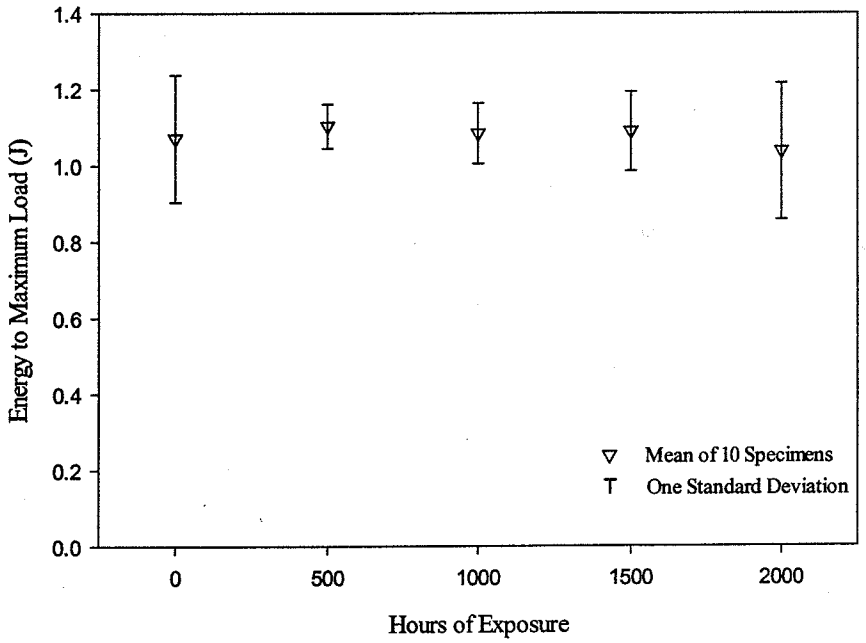

Figure 4.25 Effect of Accelerated Weathering on the Energy to Maximum Load for Formulation 2 - Additives

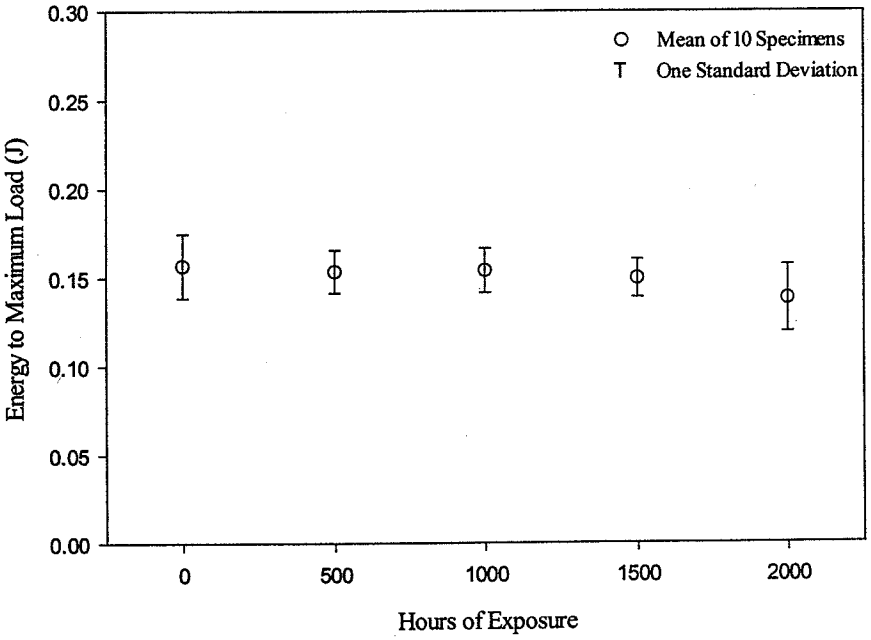

Figure 4.26 Effect of Accelerated Weathering on the Energy to Maximum Load for Formulation 3 – Wood

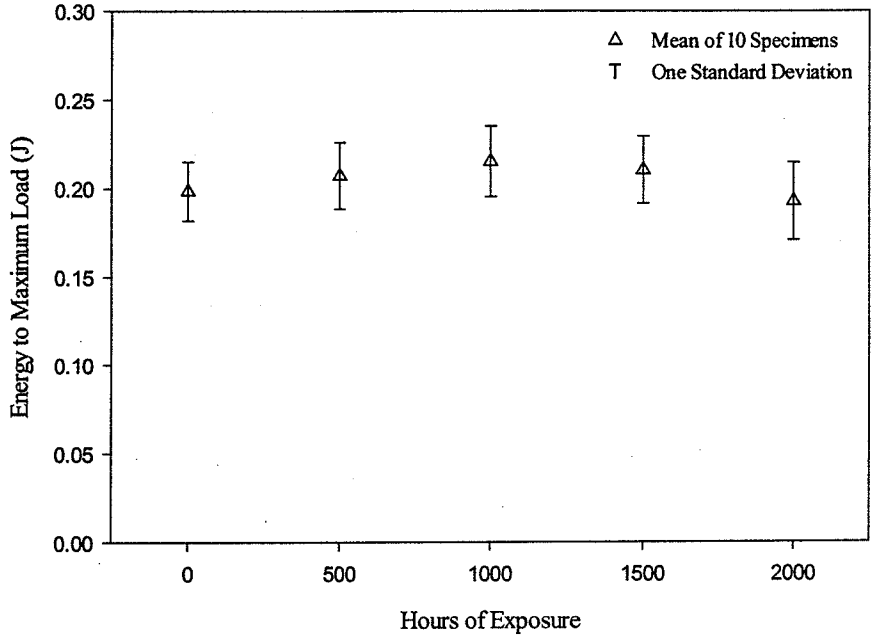

Figure 4.27 Effect of Accelerated Weathering on the Energy to Maximum Load for Formulation 4 – Kenaf

4.4 Conclusions

In this chapter the changes in physical and mechanical properties due to increments of accelerated weathering were presented. The orientation of the degraded in layer in flexure was also investigated. Based on the results the following conclusions have been drawn:

1. Specimen color change was not uniform across the surface of the specimen. The end closest to the gate exhibited less color change than the non-gated end. A possible explanation is that as the mold cavity fills, the polymer begins to cool as it touches the cavity wall. The longer cooling times result in a higher degree of crystallinity and could result in a greater volume of polymer at the surface that could protect the underlying fibers. The higher degree of crystallinity could also result in more scattering of UV light and less absorption needed to initiate photodegradation.
2. The effects of accelerated weathering that can be monitored are not constant with exposure. It was found that specimens had a greater color change in the first 1000 hours of the light than in the second and this could indicate a shift in the spectral power distribution.
3. Both sides of all composites experienced a change in chromaticity due to accelerated weathering. The back surface was found to degrade more than could be attributed to perfect reflection in the chamber and could indicate that

other degradation mechanisms are occurring in the weatherometer besides photodegradation.

4. The flexural modulus for Formulation 1 – HDPE increased 70% after 2000 hours of exposure. The increase in modulus could likely be attributed to the increase in crystallinity associated with photodegradation. After 2000 hours the modulus dropped significantly to 74% and 85% of the unexposed modulus when the exposed surface was oriented on the tension and compression side respectively. The loss in modulus may be explained by chain scission. The orientation of the exposed surface for Formulation 1 – HDPE did significantly affect the flexural modulus at all lengths of exposure.
5. The flexural modulus for Formulation 2 – Additives decreased between 0 – 1000 hours and 2000 and 4000 hours but increased between 1000 and 2000 hours of exposure. After 4000 hours the modulus was 84% of the unexposed modulus. The orientation of the exposed surface was significant at 2000 and 4000 hours of exposure.
6. The flexural modulus for Formulation 3 – Wood decreased with increasing exposure. The modulus decreased the most between 0 – 1000 hours of exposure. After 4000 hours of exposure the modulus was only 45% of the unexposed modulus. The orientation of the exposed surface did not significantly affect the flexural modulus at all lengths of exposure.
7. The flexural modulus for Formulation 4 – kenaf decreased with increasing exposure. The modulus decreased the most between 0 – 1000 hours of exposure. After 4000 hours of exposure the modulus was only 38% of the unexposed modulus. The orientation of the exposed surface was only significant at 2000 hours of exposure.
8. The flexural strength for Formulation 1 – HDPE increased 13% after 1000 hours when the degraded layer was oriented on the compression side. The flexural strength decreased with increasing exposure for all other lengths of exposure and orientations. After 4000 hours the flexural strength was 78% and 58% of the unexposed strength for specimens oriented with the exposed surface on the tension and compression side respectively. The orientation of the degraded layer was significant at all lengths of exposure for Formulation 1 – HDPE. At 2000 hours of exposure and greater, the strength was greater for those specimens oriented with the exposed surface on the tension side.
9. The flexural strength for Formulation 2 – Additives increased 5% after 4000 hours of exposure. The orientation of the exposed surface was significant at 2000 and 3000 hours of exposure.
10. The flexural strength for Formulation 3 – Wood decreased with increasing exposure for all specimens with the exposed surface on the tension side. The strength increased 3% between 3000 and 4000 hours when the exposed surface was oriented on the compression side. After 4000 hours of exposure the strength was 71% and 67% of the unexposed strength when the exposed surface was oriented on the compression and tension side respectively. The most significant (17%) loss in strength occurred between 0 – 1000 hours of exposure. The orientation of the exposed surface was only significant after 3000 hours of exposure.

11. The flexural strength for Formulation 4 – kenaf decreased with increasing exposure. The most significant loss (22%) in strength occurred during the first 1000 hours. After 4000 hours the strength was 62% and 65% of the unexposed strength when the exposed surface was oriented on the tension and compression side respectively. The orientation of the exposed surface was only significant at 4000 hours of exposure.
12. The impact strength for Formulation 1 – HDPE was 51% and 60% of unexposed specimens when the exposed surface was oriented on the tension and compression side respectively.
13. The impact strength for Formulation 2 – Additives increased 4% due to accelerated weathering.
14. The impact strength decreased 25% for Formulation 3 – Wood and 30% for Formulation 4 – kenaf after 2000 hours of accelerated weathering.
15. For fiber filled composite formulations tested in impact, it was found that a decrease in strength is a better indication of the influence of weathering than the energy to maximum load.

Chapter 5. Phase III. Modeling and Characterization of the Degraded Layer of Natural Fiber Thermoplastic Composites

5.1 Introduction

There are many methods available for measuring the degradation of photo-oxidized polymers. Methods can be grouped according to the following divisions depending on the property of interest, mechanical properties, physical properties, solution properties, spectroscopic properties, electrical properties, thermal properties, and oxygen uptake.

Mechanical properties of polymers relate the materials performance to practical situations. Mechanical properties of interest include tensile, compressive, and flexural. From tests, values of modulus and strength can be calculated. For polymer and polymer based composite products intended for use in deleterious environments there is a need to develop a technique capable of modeling the effect of degradation on the residual engineering properties of the composites. Ultimately, such a model could be used to assess the service life of a NFTC product exposed to weathering.

The objective of Phase III was to investigate the correlations between changes to physical and mechanical properties due to accelerated weathering.

5.2 Surface Degradation

Electron micrographs of the surface of NFTC were taken at various intervals of exposure (Figures 5.1-5.2). It is seen that on the exposed surface the fiber is visible and there is little bond between the fiber and matrix. Without sufficient bond, stress cannot be transferred effectively. To evaluate that weathering was the cause of the formation of surface cracks and reduction in interfacial bond, three specimens per formulation

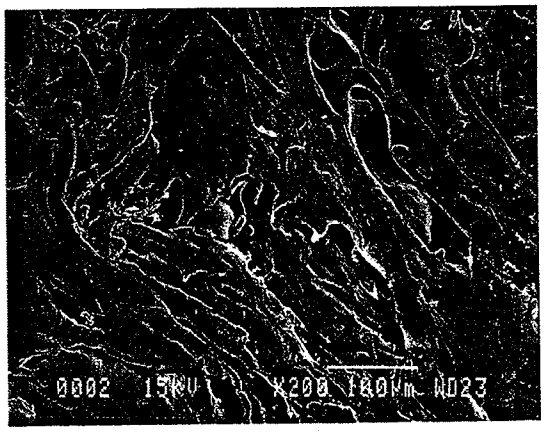

Figure 5.1 Electron Micrograph of Unexposed Wood Flour Composite Surface

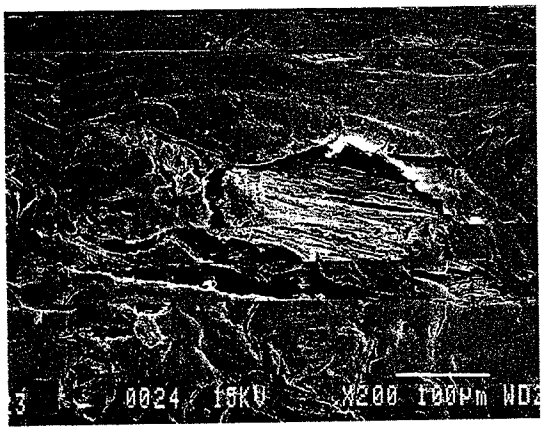

Figure 5.2 Electron Micrograph Wood Flour Composite Exposed for 2000 Hours

were monitored optically at two locations of interest for 2000 hours of exposure. The end of the specimen furthest from the injection mold gate was chosen for observation, because it had been observed to experience greater surface degradation.

Figures 5.3 and 5.4, and show the surface of a kenaf fiber composite unexposed and after 1000 hours of exposure respectively. It can be seen that the fiber matrix interface along the top and bottom edge of the large piece of pith wood deteriorated due to exposure.

Figure 5.3 Unexposed Surface of Kenaf Fiber Composite

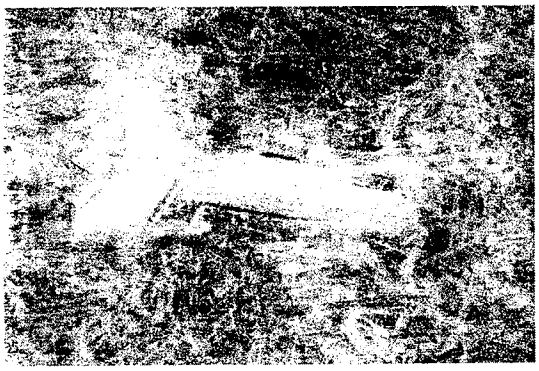

Figure 5.4 Surface of Kenaf Fiber Composite – 1000 Hours of Exposure

Figure 5.5 Unexposed Surface of Wood Fiber Composite

Figure 5.6 Surface of Wood Fiber Composite – 1000 Hours Exposure

For large kenaf fibers (pith) the degradation along the fiber matrix interface was more noticeable. Similarly in Figure 5.6 it is shown that the material adjacent to the larger fiber has been removed due to the accelerated weathering. Figures 5.3-5.6 also show that the surface of the specimens begin to whiten after exposure. This whitening appears to follow individual lignocellulosic fibers.

5.3 Visible Depth of Degradation

In an attempt to quantify the degradation of the weathered surface, the depth of degradation was measured using an optical microscope. Color fade measurements solely quantify the changes occurring on the surface making it difficult to examine any through thickness effects that could potentially affect mechanical properties. To monitor the effects of weathering a visible depth of degradation (corresponding to the whitened layer) was measured. This whitened layer was only visible after exposure on both fiber filled composites. Because of this, the results presented in the rest of Chapter 5 only pertain to Formulation 3 – wood and Formulation 4 – kenaf.

Figures 5.7 – 5.12 show the edge of Formulation 3 – wood and 4 – kenaf composites after 0, 2000, and 4000 hours of exposure respectively. It is seen that an identifiable whitened layer exists after accelerated weathering.

In evaluating the specimens, it was noted that the amount of whitening was not consistent in depth across the surface of the specimens. Generally the edge of the specimens whitened more significantly than the center of the specimens. This variation was particularly pronounced at the gated end of the specimen. To quantify this effect the visible depth of degradation was measured across the width of the specimen. Specimens were hand planned and the visible depth of degradation was measured after each pass of the plane.

Figure 5.13 shows the depth of degradation as a function of distance from the edge. It is shown that the depth of degradation is not consistent across the surface of the specimen. The greatest depth of degradation occurs at the edge of the specimen. For this reason, for all of the specimens where the visible depth of degradation was measured, at least 2.0 mm of material was removed from the edge to eliminate any edge effects.

The depth of degradation for both Formulation 3 – wood and 4 – kenaf is shown as a function of length of exposure in Figures 5.14 and 5.15, respectively. Figures 5.14 and 5.15 show the mean measured value and with error bars equaling one standard deviation. A least squares regression line using a two parameter exponential rise to maximum function was fit to the actual data and is also plotted. A rather large variation in measured depths of degradation is apparent. The coefficient of variation ranges from 18% to 30% for Formulation 3 – wood and 15 % - 25% for Formulations 4 - kenaf. The large variation could be a result of the non-uniform orientation of fiber particles.

Figure 5.7 Edge of Unexposed Specimen Formulation 3 - Wood

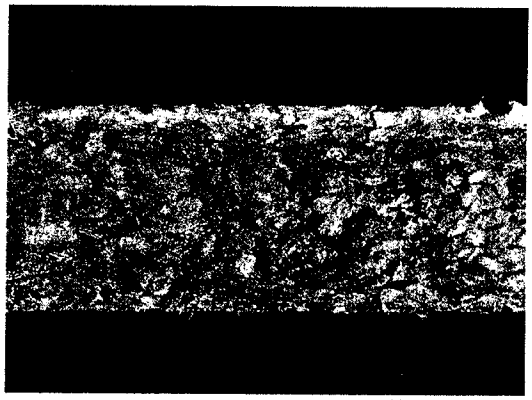

Figure 5.8 Edge of Formulation 3 – Wood 2000 Hours of Exposure

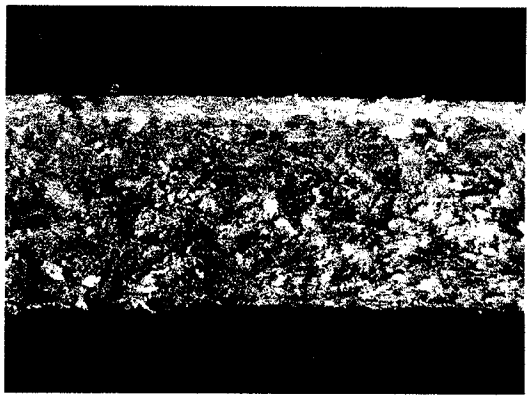

Figure 5.9 Edge of Formulation 3 – Wood 4000 Hours of Exposure

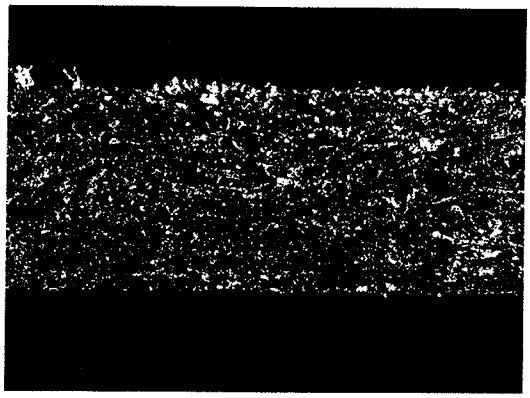

Figure 5.10 Edge of Unexposed Specimen Formulation 4 – Kenaf

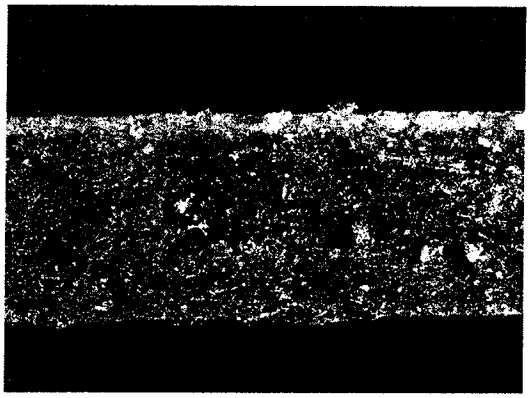

Figure 5.11 Edge of Formulation 4 – Kenaf 2000 Hours of Exposure

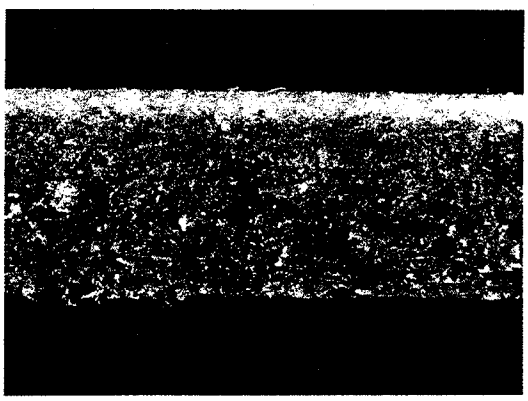

Figure 5.12 Edge of Formulation 4 – Kenaf 4000 Hours of Exposure

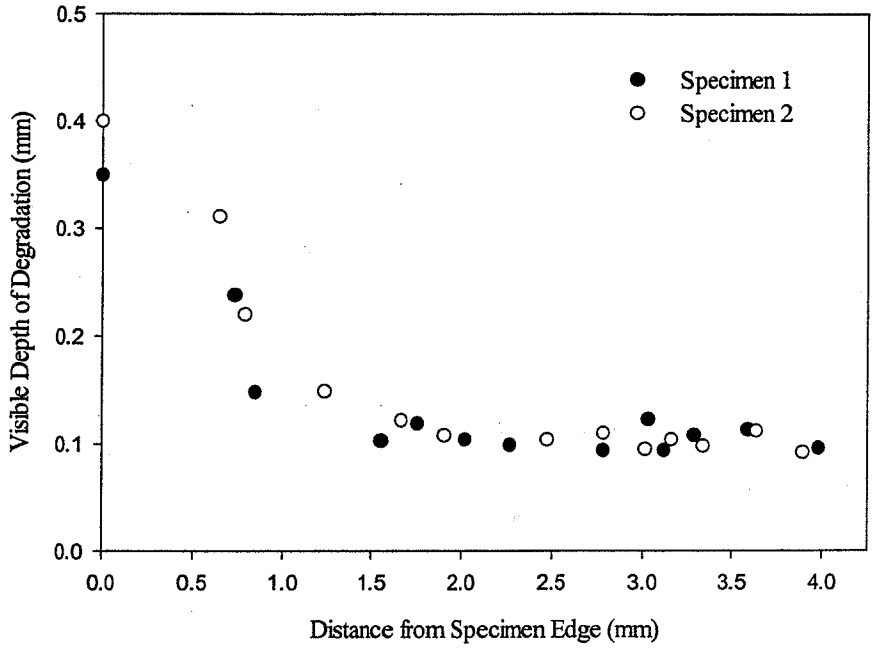

Figure 5.13 Depth of Degradation as a Function of Distance from Edge

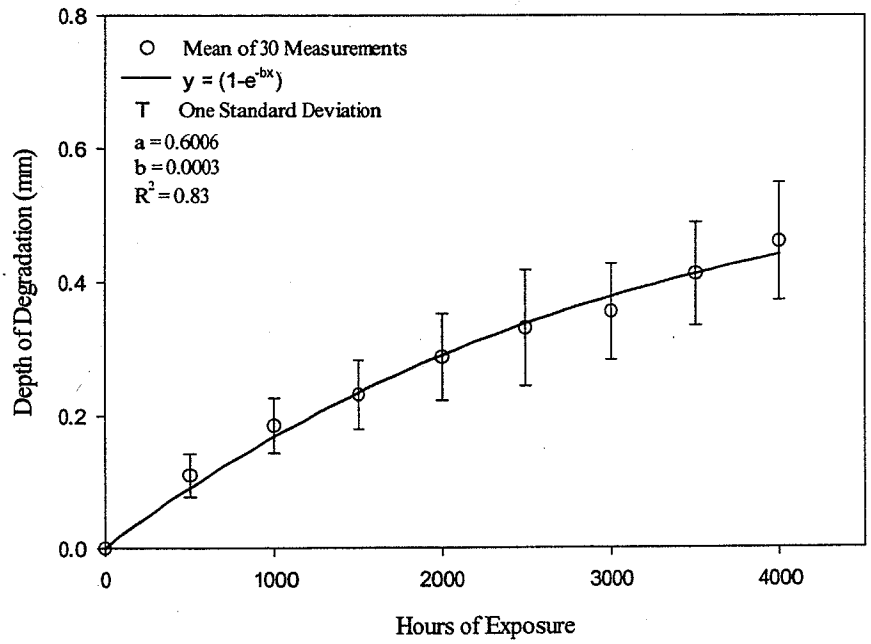

Figure 5.14 Effect of Accelerated Weathering on the Visible Depth of Degradation for Formulation 3 - Wood

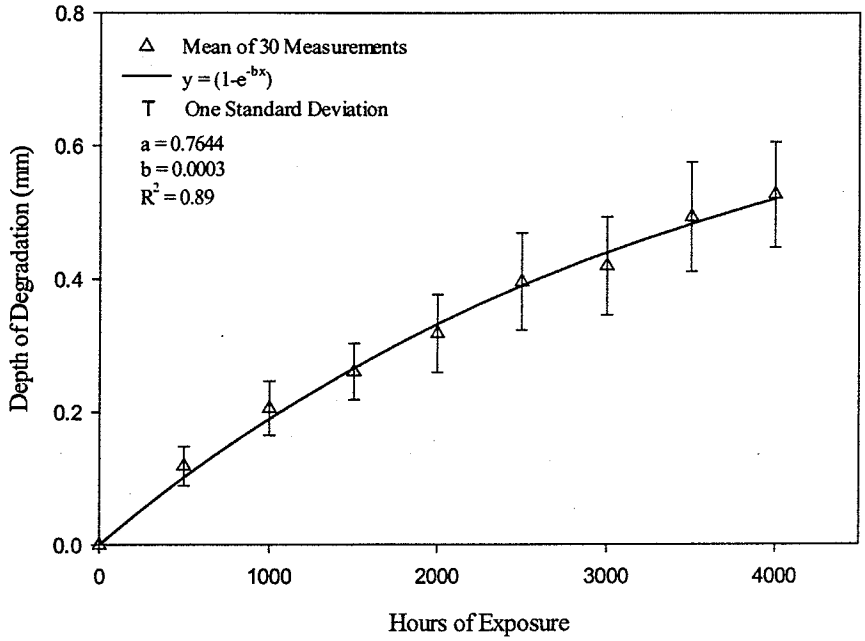

Figure 5.15 Effect of Accelerated Weathering on the Visible Depth of Degradation Measurements for Formulation 4 – Kenaf

5.4 Analysis of Phase III Results

A useful tool for the evaluation of NFTC could be developed if the changes in physical properties could be related to the changes in mechanical properties. The intention was to relate changes in chromaticity to changes in the visible depth of degradation and changes in mechanical properties. If a correlation existed it would then be possible to reasonably determine the mechanical properties of NFTC nondestructively. A variety of functions including polynomial, exponential, hyperbolic, and logarithmic were fit to the data. Least squares regression fits were made from specimen data of total color difference, visible depth of degradation, changes in flexural modulus (ΔMOE), and changes in flexural strength (ΔMOR) for both Formulation 3 – wood and 4 – kenaf (Appendix 10). It was found that a two parameter exponential function (Eq. 5.1) provided the best fits for these two formulations.

$$y = a\left(1 - e^{-bx}\right) \qquad (5.1)$$

5.4.1 Relation Between Color Fade and Depth of Degradation

Figures 5.16 and 5.17 show least squares regression curves for the total color difference in relation to the visible depth of degradation. Figures 5.16 and 5.17 show that there is a more linear increase to the visible depth of degradation than the total color difference for both Formulation 3 and 4.

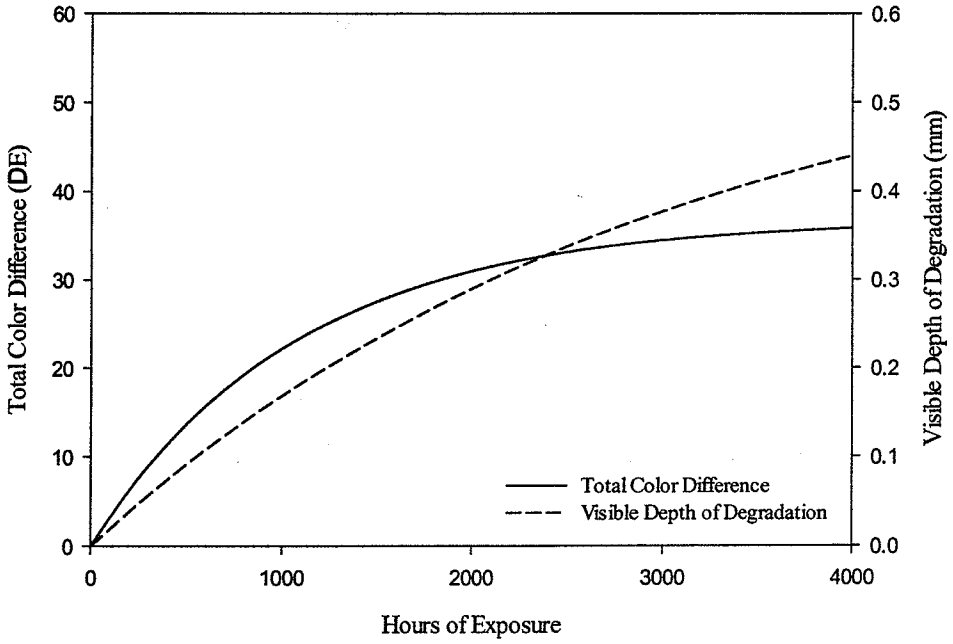

Figure 5.16 Effect of Accelerated Weathering on the Total Color Difference and Visible Depth of Degradation for Formulation 3 – Wood

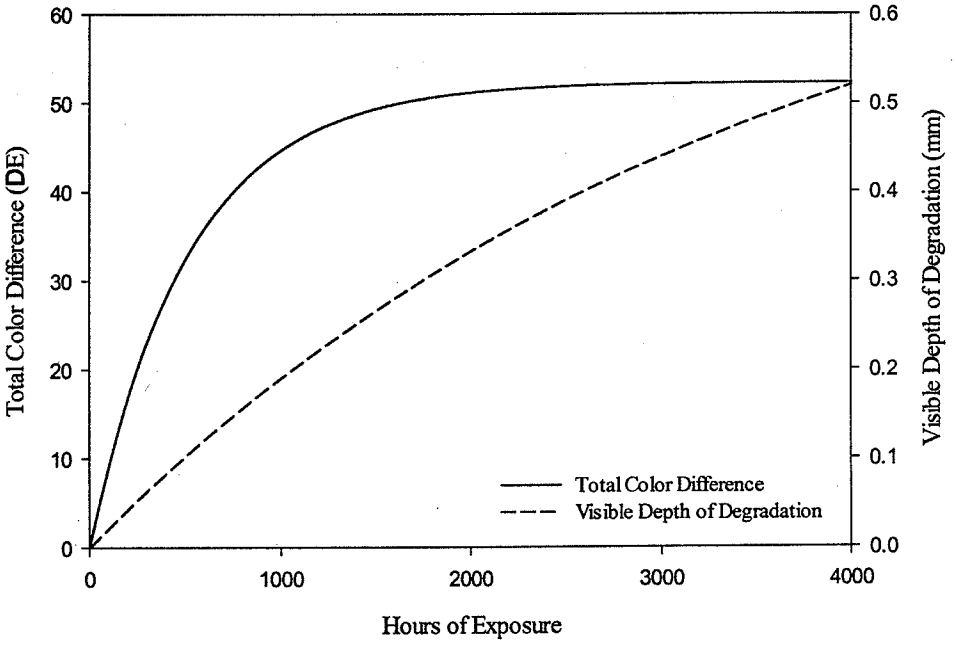

Figure 5.17 Effect of Accelerated Weathering on the Total Color Difference and Visible Depth of Degradation for Formulation 4 – Kenaf

5.4.2 Relation Between Color Fade and Flexural Properties

Figures 5.18 – 5.19 show the effects of accelerated weathering on the total color difference and ΔMOE for formulation 3 and 4 respectively. Figures 5.20 – 5.21 show the effects of accelerated weathering on the total color difference and ΔMOR for formulation 3 and 4 respectively. It is shown that the changes in chromaticity more closely follow the changes in mechanical properties for formulation 3: 50% wood than they do for formulation 4: kenaf

5.4.3 Relation Between Depth of Degradation and Flexural Properties

Figures 5.22 – 5.23 show the effects of accelerated weathering on the visible depth of degradation and ΔMOE for formulation 3 and 4 respectively. Figures 5.24 - 5.25 show the effects of accelerated weathering on the visible depth of degradation and ΔMOR for formulation 3 and 4 respectively. It is shown that the increase in visible depth of degradation is more linear than the changes in MOE and MOR. However it is also shown that the changes in properties are relatively similar.

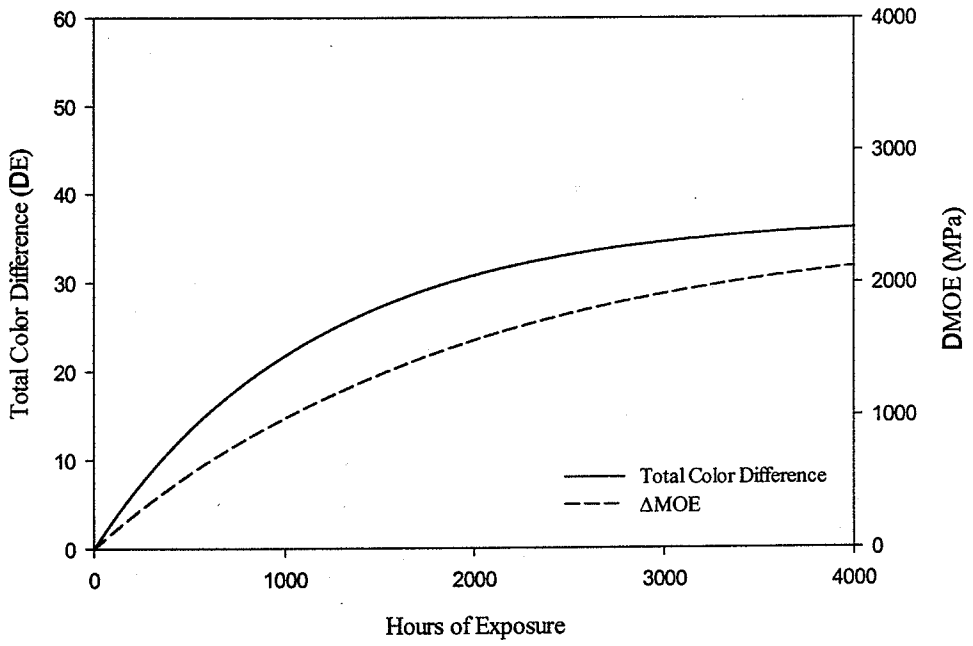

Figure 5.18 Effect of Accelerated Weathering on the Total Color Difference and Change in Flexural Modulus for Formulation 3 – Wood

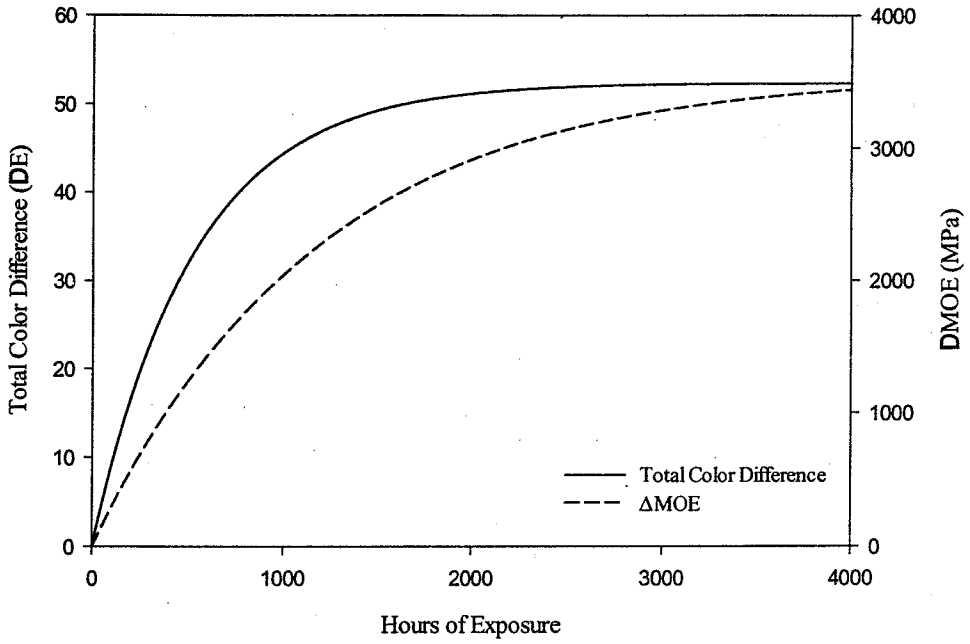

Figure 5.19 Effect of Accelerated Weathering on the Total Color Difference and Change in Flexural Modulus for Formulation 4 – Kenaf

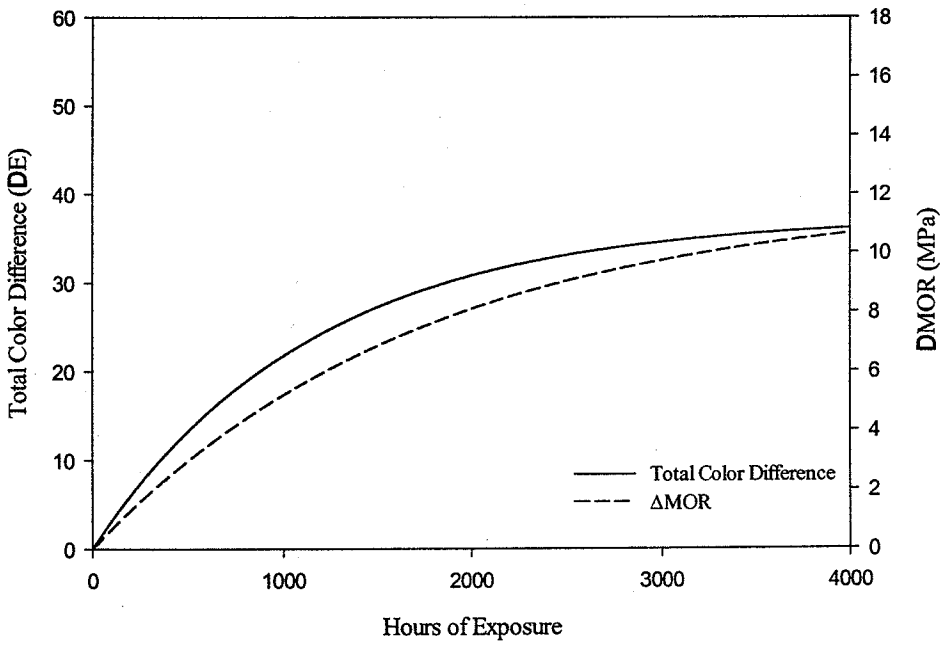

Figure 5.20 Effect of Accelerated Weathering on the Total Color Difference and Change in Flexural Strength for Formulation 3 – Wood

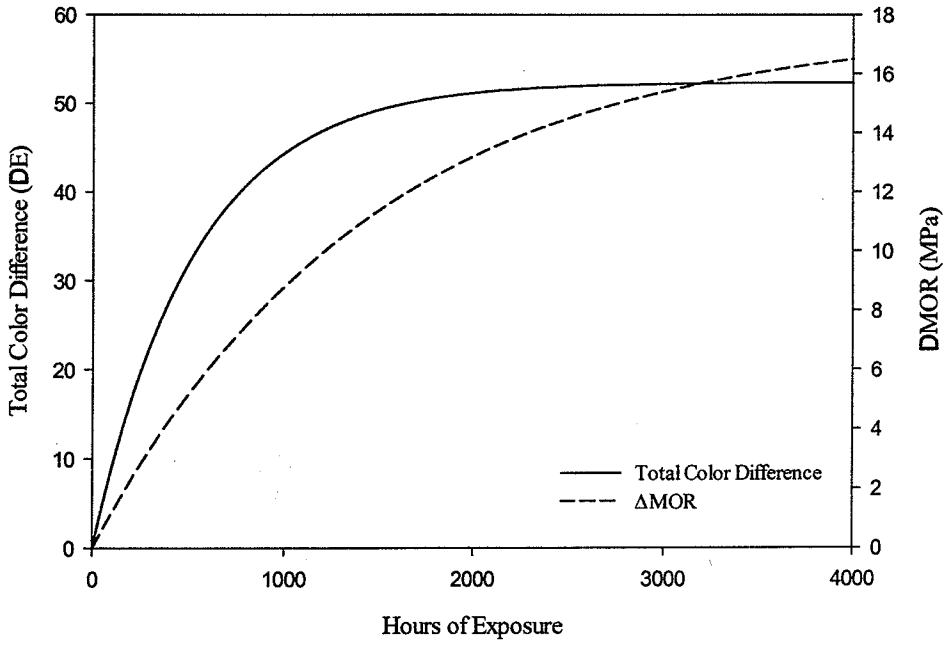

Figure 5.21 Effect of Accelerated Weathering on the Total Color Difference and Change in Flexural Strength for Formulation 4 – Kenaf

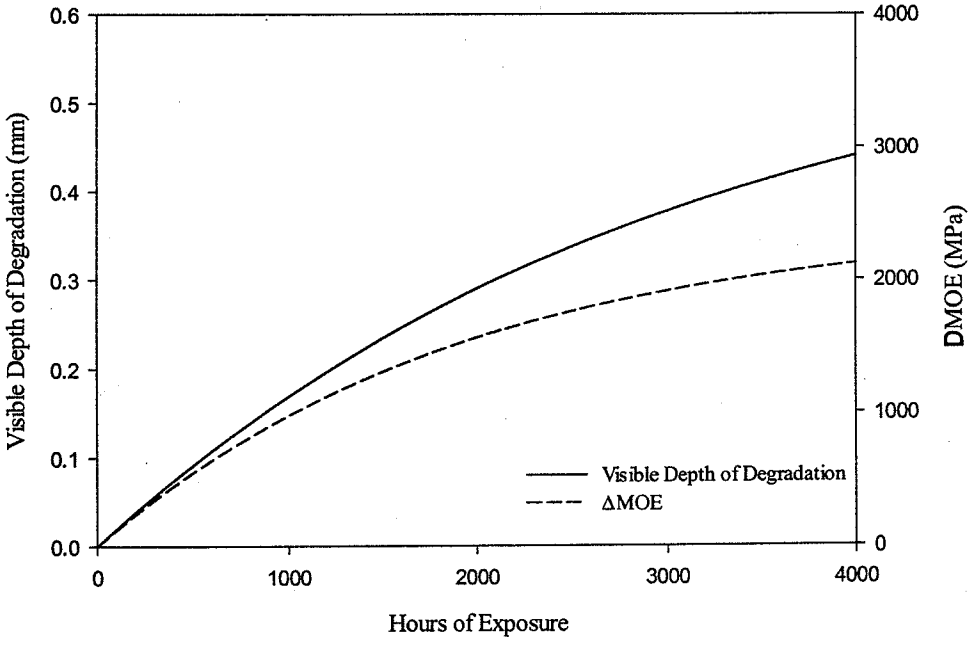

Figure 5.22 Effects of Accelerated Weathering on the Visible Depth of Degradation and Change in Flexural Modulus for Formulation 3 – Wood

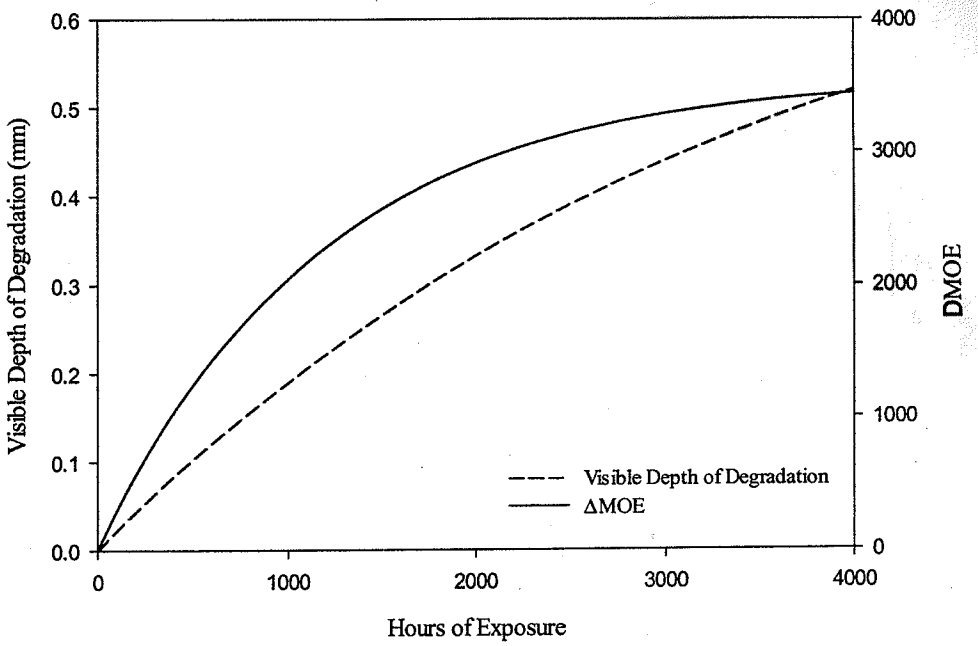

Figure 5.23 Effects of Accelerated Weathering on the Visible Depth of Degradation and Change in Flexural Modulus for Formulation 4 – Kenaf

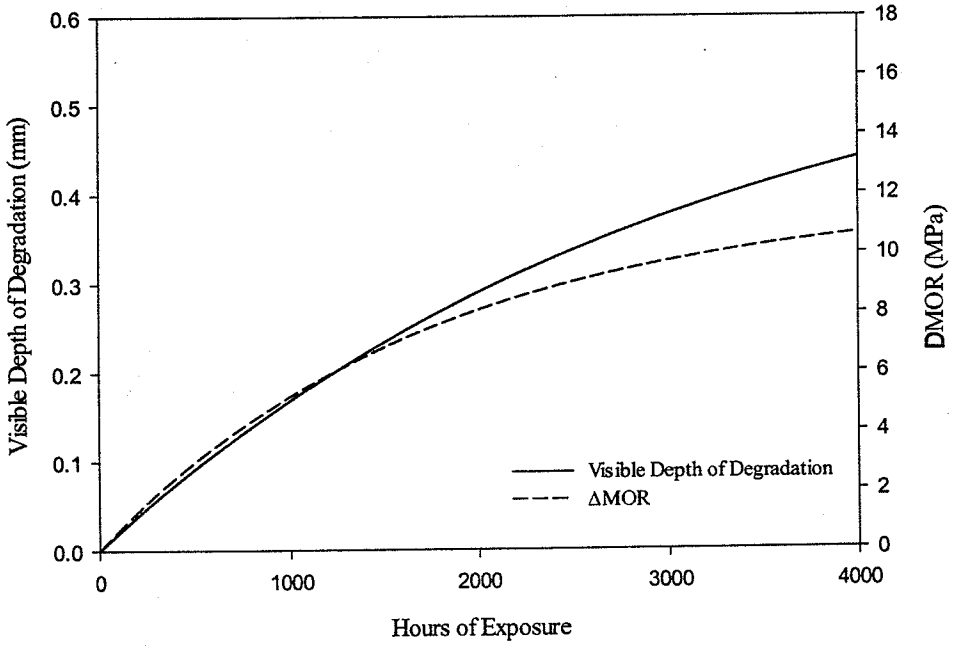

Figure 5.24 Effect of Accelerated Weathering on the Visible Depth of Degradation and Change in Flexural Strength for Formulation 3 – Wood

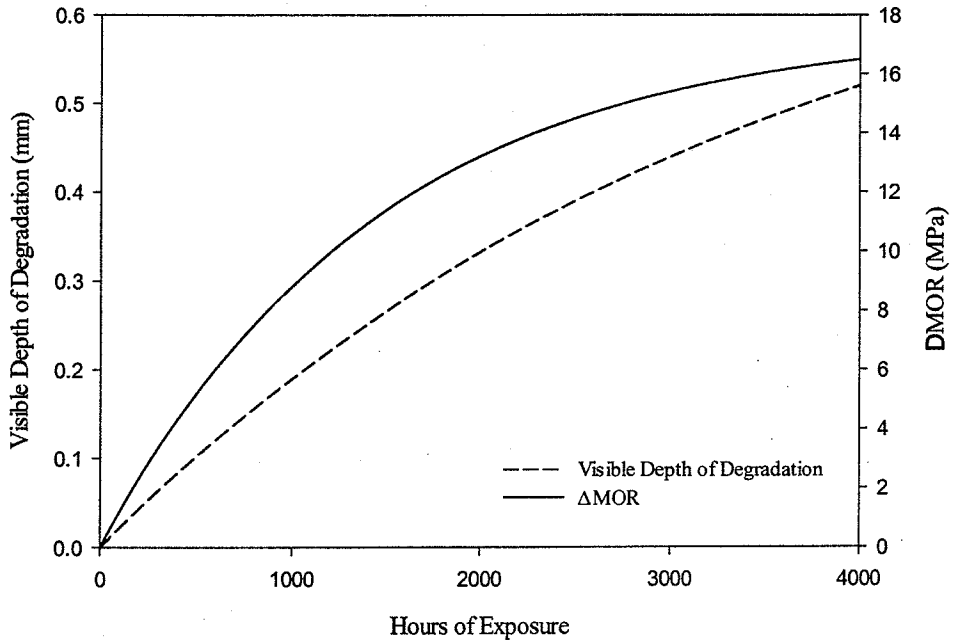

Figure 5.25 Effect of Accelerated Weathering on the Visible Depth of Degradation and Change in Flexural Strength for Formulation 4 – Kenaf

5.4.4 Effect of Depth of Degradation on the Effective Moment of Inertia

To relate the loss in flexural properties to the observed physical changes a simple two-layer model was developed to predict flexural modulus and strength. This model assumes that the visible depth of degradation does not influence the mechanical properties of the undegraded layer resulting in an effective moment of inertia, I_e.

$$I_e = \frac{1}{12} b d_e^3 \qquad (5.2)$$

Where b is the specimen width and d_e is the effective depth. Using the assumption that the stress and modulus were equal to zero in the visible depth of degradation, d_d, the effective depth can be defined as

$$d_e = d_t - d_d \qquad (5.3)$$

Where d_t is the total specimen depth. Substituting equation 5.3 into 5.2 the effective moment of inertia is equal to

$$I_e = \frac{1}{12} b (d_t - d_d)^2 \qquad (5.4)$$

Using the measured depths of degradation I_e was calculated. Figures 5.26 and 5.27 show I_e as a function of hours of exposure for Formulation 3 – wood and 4 – kenaf.

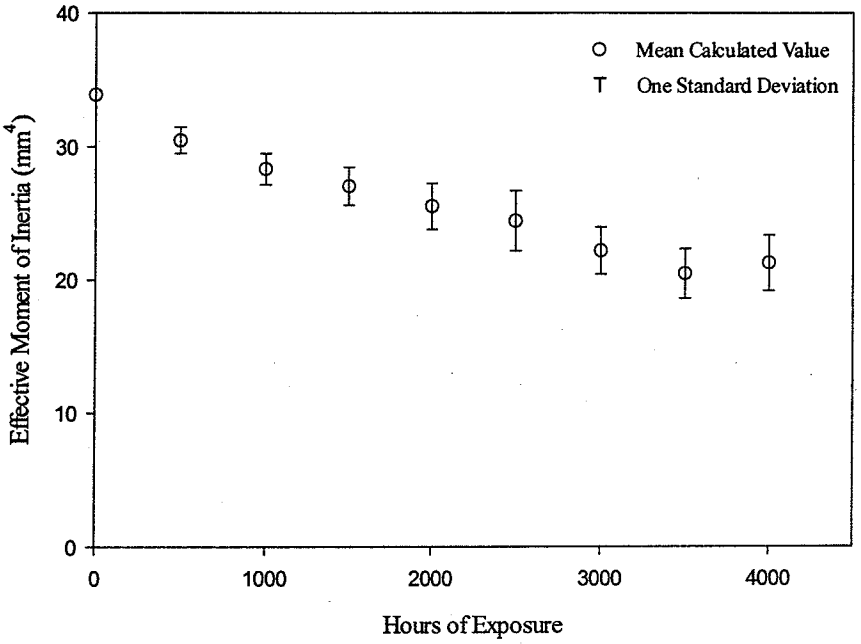

Figure 5.26 Effect of Accelerated Weathering on the Effective Moment of Inertia for Formulation 3 – Wood

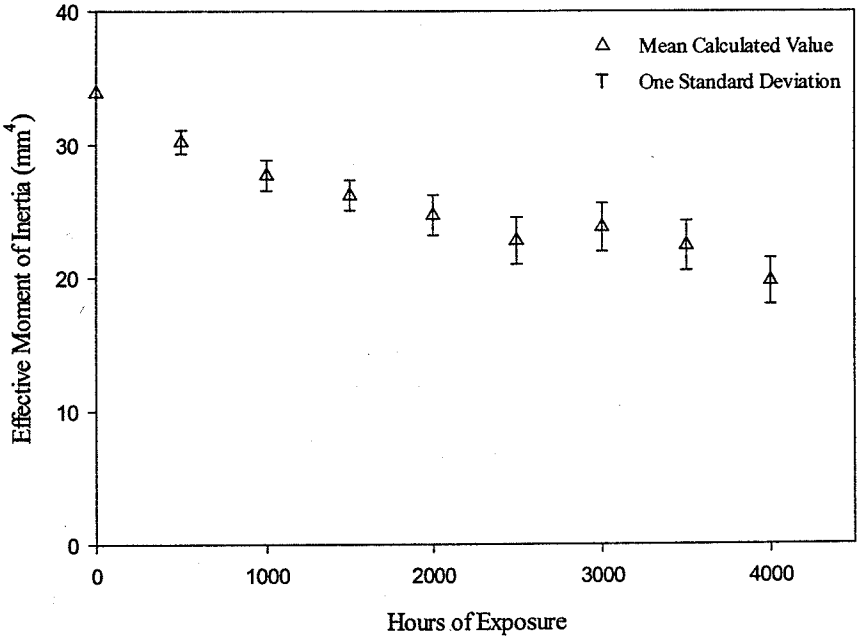

Figure 5.27 Effect of Accelerated Weathering on the Effective Moment of Inertia for Formulation 4 - Kenaf

Figure 5.26 and 5.27 show the mean calculated value using the measured depth of degradation and error bars equal to one standard deviation.

5.4.5 Flexural Modulus Calculated Using the Effective Cross Section

To predict flexural modulus the simplifying assumption was made that the composites behave according to linear elastic bending theory

$$\delta = \frac{PL^3}{48EI} \qquad (5.5)$$

Where P is the load required for deflection δ. E is the modulus of elasticity, and L is the support span. Substituting in I_e for I and solving for the modulus we are left with

$$E = \frac{PL^3}{4b(d_t - d_a)^3 \delta} \qquad (5.6)$$

Using the equation of the least square regression fit (Eq. 5.1) yields the following general equation relating the material property of modulus of elasticity to the load and deflection at length of accelerated weathering x.

$$E = \frac{PL^3}{4b(d_t - a(1 - e^{-bx}))^3 \delta} \qquad (5.7)$$

Figures 5.28 and 5.29 show the predicted flexural modulus of elasticity (Eq 5.7) calculated using the least squares regression fit for the measured depth of degradation and experimental data from Phase II. Figure 5.28 and 5.29 show the mean predicted value with error bars equal to one standard deviation and a least squares linear regression. It is shown that the coefficient of determination, R^2, is very low indicating that there is little relation between the independent and dependant variables. If the measured depth accurately predicts a reduction in cross section, the calculated modulus shown in Figures 5.28 and 5.28 would be constant with exposure assuming that the modulus is constant throughout the depth of the specimen. It is shown that the predicted flexural modulus is not constant with exposure for both Formulation 3 and 4. One possible explanation is that the visible depth of degradation is not entirely ineffective and that it influences the deflection. A second possibility is that the modulus is not constant through the depth of the specimen, which is possible because the crystallinity of the polymer is generally not constant through the depth nor is the orientation of the fibers. It should be noted that the predicted values of modulus are roughly half of those presented in Chapter 4. This is because the methods used to calculate modulus differ. In Chapter 4 the initial tangent is used. The values presented below were calculated using the secant modulus between the origin and point of maximum load.

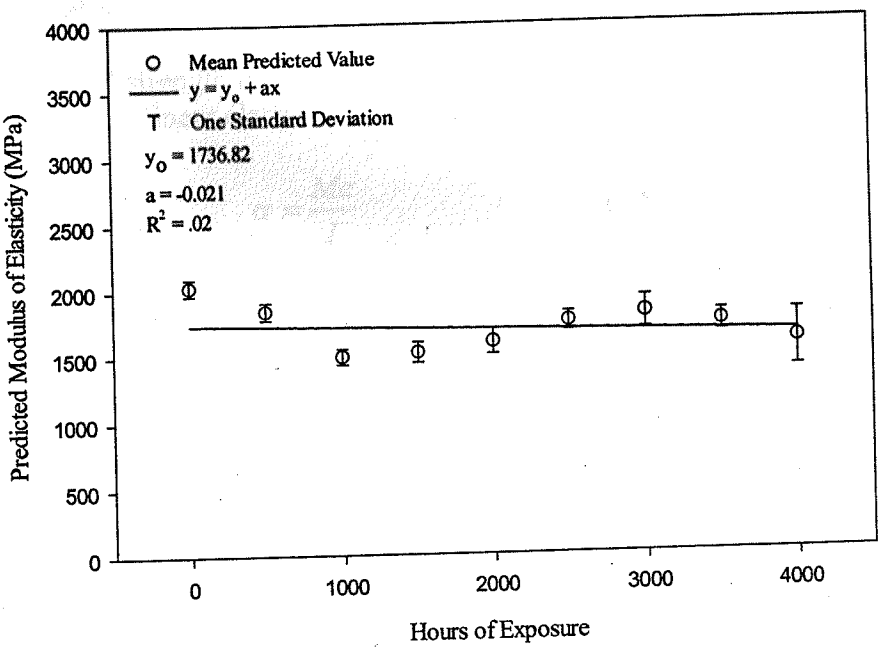

Figure 5.28 Predicted Modulus of Elasticity of Formulation 3 – Wood Calculated Using Effective Cross Section

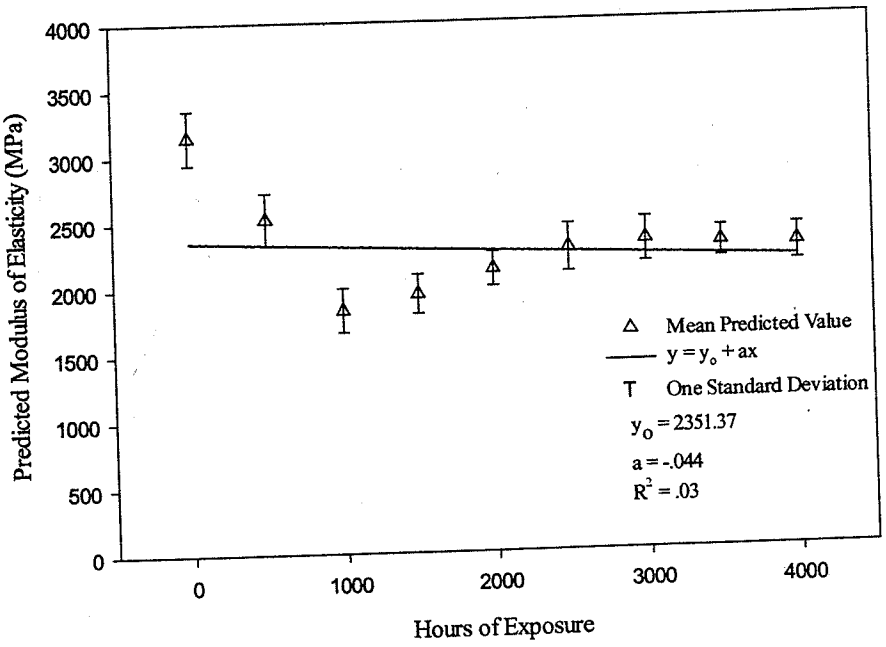

Figure 5.29 Predicted Modulus of Elasticity of Formulation 4 – Kenaf Calculated Using Effective Cross Section

5.4.6 Flexural Strength Calculated Using the Effective Cross Section

To predict flexural strength the simplifying assumption was made that the composites behave according to linear elastic bending theory.

$$\sigma = \frac{Mc}{I} \qquad (5.8)$$

Solving for the stress in the extreme tension fibers at midspan due to a concentrated midpoint force

$$\sigma = \frac{3PL}{2bd_e} \qquad (5.9)$$

Substituting equation 5.3 into 5.9 we are left with

$$\sigma = \frac{3PL}{2b(d_t - d_d)^2} \qquad (5.10)$$

Using the equation of the least squares regression fit (Eq. 5.1) we are left with the following general equation relating the material property of flexural strength to the load at failure and length of accelerated weathering x.

$$\sigma = \frac{3PL}{2b\left(d_t - \left(a\left(1 - e^{-bx}\right)\right)^2\right)} \qquad (5.11)$$

Figures 5.30 and 5.31 shows the predicted flexural strength calculated using the measured depth of degradation for formulations 3 and 4 respectively. The mean values are plotted with error bars equaling one standard deviation. If the measured depth accurately predicted a reduction in cross section, the calculated flexural stresses shown in Figure 5.30 and 5.31 would be constant with exposure assuming that the flexural yield strength is constant throughout the depth of the specimen. It is apparent from Figure 5.30 and 5.31 that for both fiber-filled composites, the visible depth of degradation under predicts the actual depth of degradation for short exposures and more accurately predicts the depth of degradation for longer exposures. Overall, equation 5.11 provides an effective mechanistic prediction of flexural strength after exposure, especially for Formulation 3 – wood.

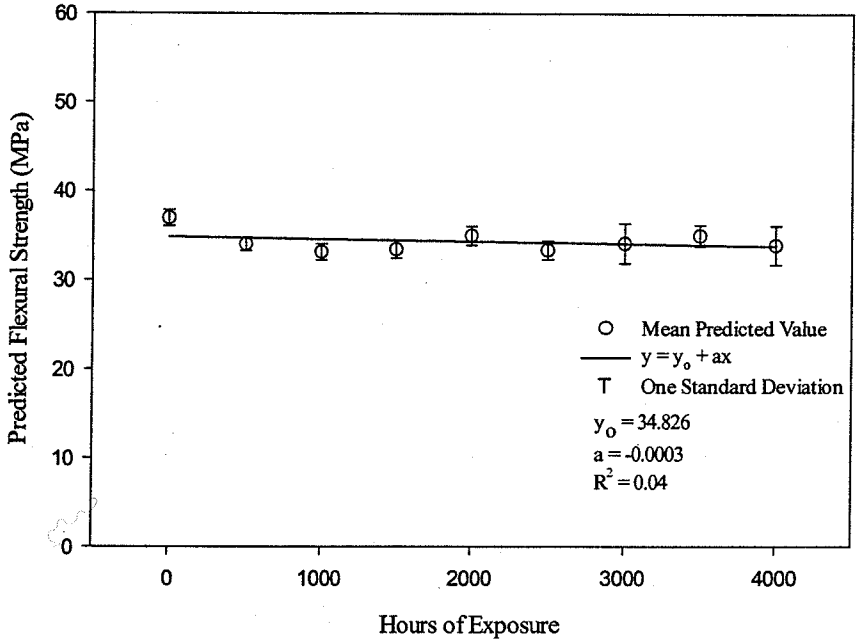

Figure 5.30 Predicted Flexural Strength of Formulation 3 – Wood Calculated Using Effective Cross Section

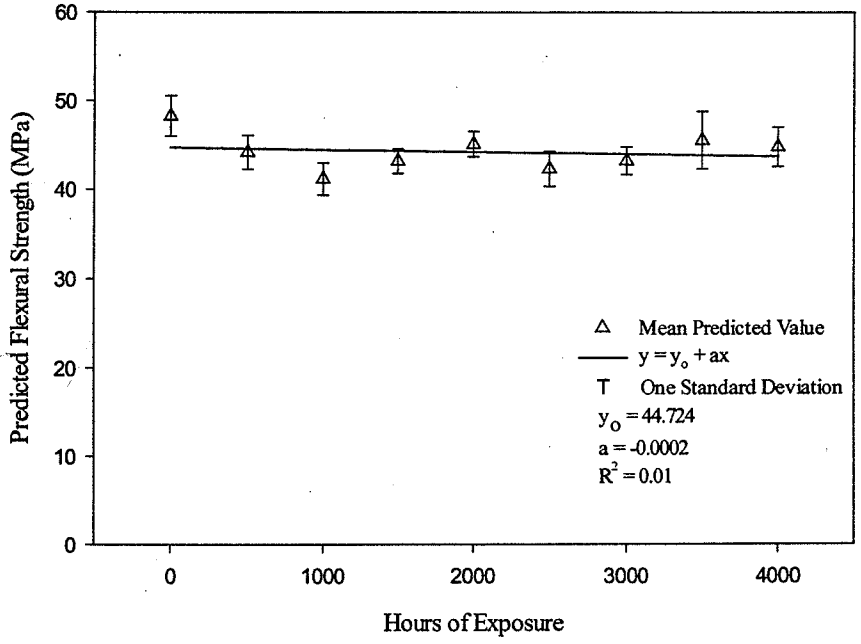

Figure 5.31 Predicted Flexural Strength of Formulation 4 – Kenaf Calculated Using Effective Cross Section

5.4.7 Flexural Modulus and Strength as a Function of Specimen Depth

A possible explanation for the variations in predicted flexural modulus and strength can be explained by the variation fiber orientation. In Chapter 2 it was discussed that there is fiber orientation in injection-molded specimens and this orientation varies with specimen depth. A set of experiments was conducted to determine the flexural strength of unexposed kenaf specimens as a function of depth. Kenaf was chosen due to the higher L/d ratios of the fibers that would presumably result in greater effects on strength and modulus due to fiber orientation. Specimens were made by milling off the surface of unexposed injection molded specimens not tested in Phase II. Specimens were milled using a fly cutter with a carbide blade on a vertical mill. The blade was oriented with a positive rake (shearing action). A total of 44 specimens were milled at various depths. These specimens were tested in flexure with the milled surface on the tension side. Figure 5.32 shows the flexural modulus as a function of specimen depth. The flexural modulus was calculated according to equation 5.5. It is seen that the flexural modulus is not consistent with specimen depth. Figure 5.33 shows the flexural strength as a function of depth. It is shown that the flexural strength is not consistent with specimen depth. Both the modulus and strength are shown to decrease with increasing specimen depth removed. A 17% decrease in modulus between specimens of full depth and those with 1.27 mm (0.05 in) removed was observed. Likewise there is a 21% decrease in strength between specimens of full depth and those with 1.27 mm (0.05 in) removed.

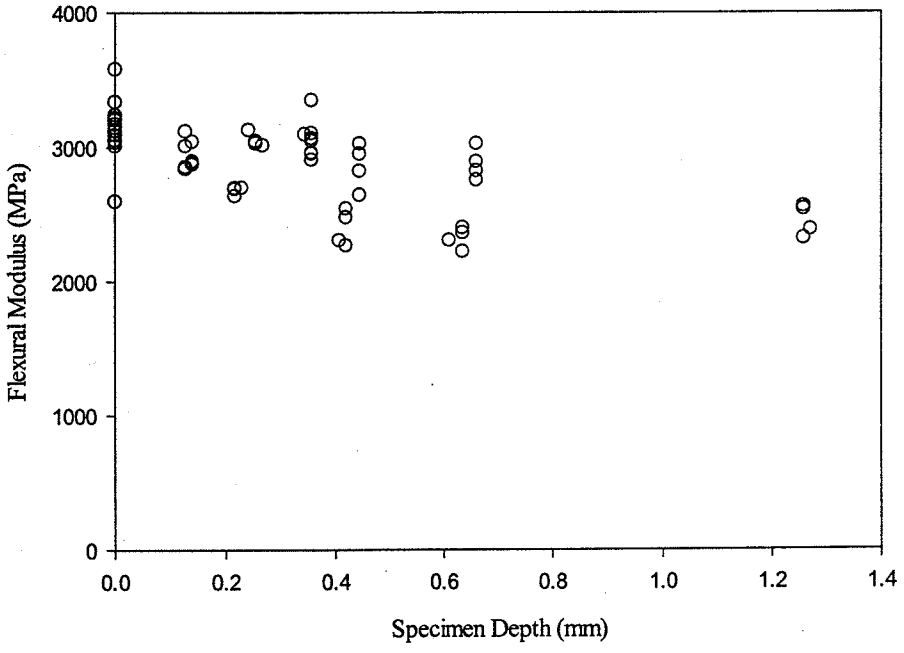

Figure 5.32 Flexural Modulus as a Function of Depth of Specimen Removed for Formulation 4 - Kenaf

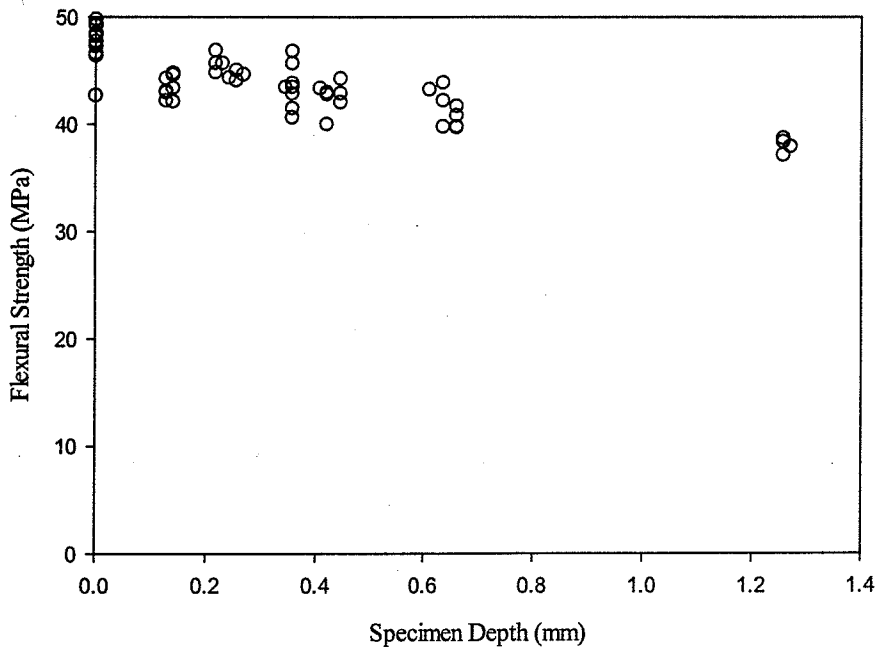

Figure 5.33 Flexural Strength as a Function of Depth of Specimen Removed for Formulation 4 - Kenaf

5.4.8 Relation between Milled and Specimens Exposed to Accelerated Weathering

Figure 5.34 and 5.35 compare the predicted flexural modulus and strength of specimens with an effective cross section to specimens that were milled. Figure 5.34 shows that the modulus of the milled specimens is consistently greater than exposed specimens with an effective cross section. This probably indicates that the effects of accelerated weathering on the flexural modulus are not confined to the visible degraded layer as assumed in the two-layer model, indicating that the modulus of the unwhitened material is also reduced due to exposure.

Figure 5.35 shows that both milled and weathered specimens have similar flexural strengths at various specimen depths. This probably indicates that the assumption that stress is not transferred in the visible degraded layer is realistic. Interestingly the two-layer model appears to reasonably account for loss in strength but appears to poorly predict the loss in modulus. This could imply that when these composites are subject to accelerated weathering, stress and strain are not directly related, or are carried differently. The assumption that modulus can be modeled using linear elastic theory is poor. Another possibility is that accelerated weathering effects the strain in the composites without inducing stress.

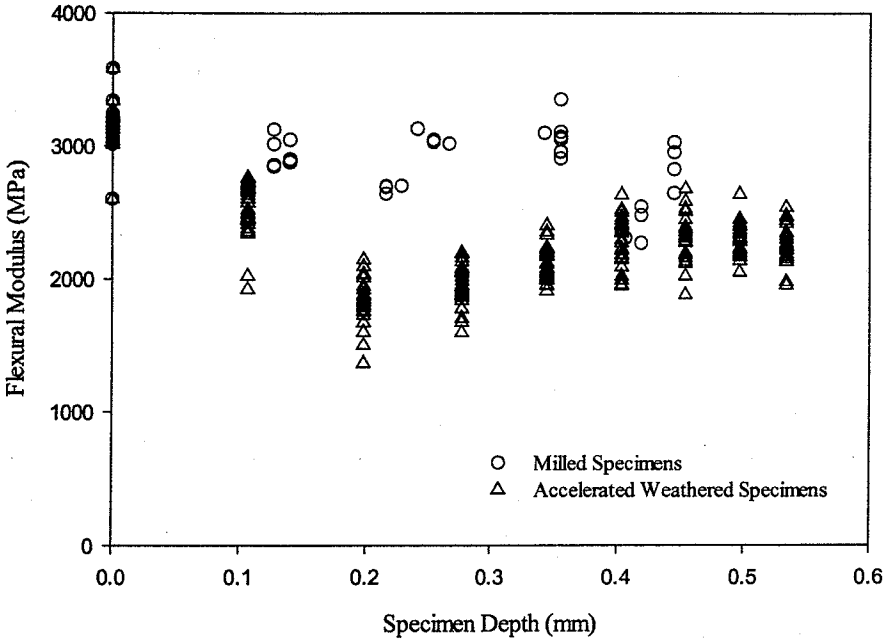

Figure 5.34 Relation Between Flexural Modulus of Milled Specimens and Weathered Specimens Using the Effective Cross Section

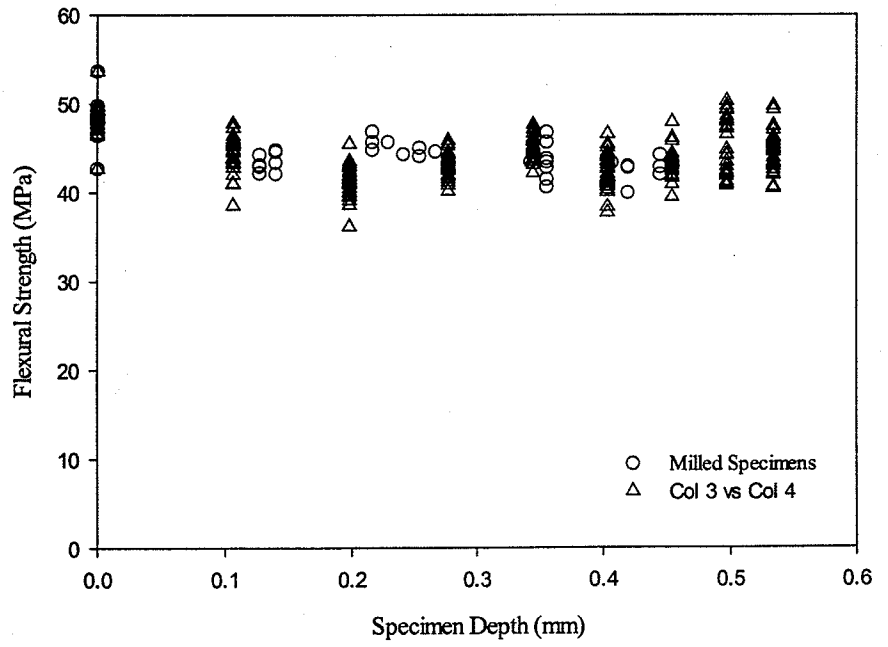

Figure 5.35 Relation between Flexural Strength of Milled Specimens and Weathered Specimens using the Effective Cross Section

5.5 Conclusions

In this chapter the correlation between changes in physical and mechanical properties due to accelerated weathering were presented. From these results the following conclusions were made:

1. Due to accelerated weathering, NFTC's developed a degraded surface layer. This surface layer was lighter than the surrounding material and was measured using an optical microscope. The visible depth of degradation increased with increasing exposure.
2. The degraded layer was characterized by loss to the interfacial bond between the fiber and matrix. The loss in bond was particularly noticeable around large pieces of fiber near the surface.
3. The visible depth of degradation was not constant in depth across the width of the specimen. The visible depth of degradation was greatest at the edges of the specimens and smallest in the middle of the specimen.
4. The changes in specimen chromaticity were less linear than changes to the visible depth of degradation for both Formulations 3 – wood and 4 - kenaf. The changes in chromaticity were relatively similar to the changes in flexural properties.
5. The two-layer model presented did not reasonably predict flexural modulus but was effective for predicting flexural strength. This could indicate that stress is carried differently than strain or during accelerated weathering there is a change in strain without changes in stress.
6. The flexural modulus and strength of injection-molded specimens containing 50% kenaf fiber was not constant through the depth of the specimen. Both the flexural modulus and strength decreased through the depth of the specimen.

Chapter 6. Phase IV. Manufactured Roofing Panels

6.1 Introduction

In the previous chapters, the effects of laboratory accelerated weathering on NFTC specimens were presented. In this chapter, the effects of both laboratory accelerated and outdoor weathering of a manufactured product are presented and discussed. The product of interest is a NFTC roofing panel. Large roofing panels dimensionally similar to three-tab asphalt shingles were subjected to exposure. Testing consisted of monitoring roof panels and laboratory testing.

The objective of this phase of research was to evaluate durability of NFTC roofing panels subjected to natural and accelerated weathering.

6.2 Experimental

6.2.1 Materials

The materials in the manufacture of roofing panels consisted of two different fiber types compounded with a mixture of virgin and recycled HDPE and a variety of additives. Table 6.1 shows the percent by weight of materials used in the production of the roof panels.

Table 6.1 Roof Panel Formulation
Values Reported are Percent by Weight

Fiber		Polymer		Colorant	Antioxidant	UV Stabilizer	Fungicide	Compatibilizer
Wood	Jute	44 - Melt HDPE	Recycled Milk Jugs	Bayer Brown	B225 IRGANOX	TINUVIAN 783 FDL	Zinc Borate	MAPE
25.0	25.0	9.7	38.7	0.40	0.20	0.40	0.60	0.02

6.2.2 Specimen Preparation

The materials were compounded by TGRT using proprietary compounding equipment. After compounding, the material was granulated and passed through a 6.35 mm (1/4 inch) screen. The material was extruded then compression molded into roof panels. These panels measured approximately 111 by 584 mm (43.5 by 23 in) and consisted of 7 shakes that varied in dimension. A typical roofing panel is shown in Figure 6.1. These panels are currently patent pending by the manufacturer.

Three different batches of panels were produced. Each batch differed due to the amount of scrap introduced into the mix. Scrap was produced during the molding process in the form of excess trim and flashing. The first batch contained no recycled scrap. The

second batch contained scrap from the first batch. The third batch contained scrap from the second batch. Successive batches appeared to be darker in color.

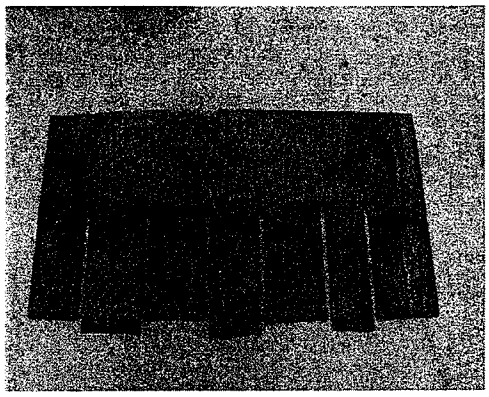

Figure 6.1 Typical Roofing Panel

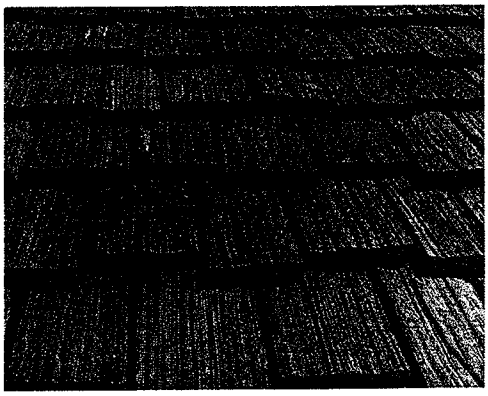

Figure 6.2 Panels after Installation

No panels were used from the fourth batch due to poor physical properties and molding problems. The first generation panels were laid on the side of the demonstration roof oriented primarily north. The demonstration structure was located in Madison Wisconsin. The second-generation panels were laid on the South side of the structure. The third-generation panels were used on the East gabled end and first-generation material was used on the West gabled end.

To allow for flexural testing and accelerated weathering, full sized roof panels were dimensionally reduced. Two sizes of specimens were cut from a randomly selected unexposed roof panels. These sizes correspond to ASTM D790 and ICBO AC07 recommended dimension. ASTM D790 recommends specimens 127 by 12.7 by 3.2 mm in dimension. ICBO AC07 recommends specimens to be 15.24 by 2.54 by 0.635 cm (6 by 1 by 0.25 in).

6.2.3 Testing

6.2.3.1 Accelerated Weathering

Accelerated weathering of the composite specimens was accomplished during the second 2000 hours of Phase II using the same weatherometer device and exposure condition described in Chapter 4.

6.2.3.2 Natural Weathering

Natural weathering began once the panels were installed on the demonstration roof. The exposure started on 7/19/2000 and was monitored every three months for one year.

6.2.3.3 Color Fade Measurement

Four locations were selected on the roof corresponding to the four corners of the building; southeast, southwest, northeast, and northwest. The specific locations in these areas were picked at random. For each tile picked a 5.1 cm (2 in) square was drawn on the lower corner closest to the exterior edge (i.e. on South West corner the square was drawn on the South West corner of the shake (Figure 6.3)). A total of four measurements were taken at each location and averaged.

6.2.3.4 Flexural Testing

Flexural tests were only performed on specimens exposed in the laboratory. For the large specimens (ICBO AC07) thirteen specimens were held as controls and fourteen specimens were exposed. All of the larger specimens were tested with the exposed surface on the tension side. For the small specimens (ASTM D790) eight specimens were held as controls and sixteen specimens were exposed, eight tested with the exposed surface on the compression side, and eight tested with the exposed surface on the tension side. Specimens were conditioned for approximately 3 months prior to testing at 73 ^{o}F and 50% R.H. All specimens were tested using the same equipment and methodology described in Chapter 4. For the larger specimens the support span was increased to maintain the same span to depth ratio (L/D). The rate of crosshead motion was maintained at 13.7 mm/mm/min (0.53 in/in/min) for both the large and small specimens, therefore the rate of strain was greater for the small specimens (0.1) than the large specimens (0.073).

6.3 Results and Discussion

6.3.1 Effects of Accelerated Weathering on Color Fade

Table 6.2 shows the average chromaticity data for all specimens. It is shown that all three chromaticity coordinates (L^* – lightness, a^* – hue, b^* – chroma) increased due to the accelerated weathering. Table 6.2 also shows that the variability in properties is low. As would be expected, there is no difference between the chromaticity response of the two sizes of specimens due to accelerated weathering. It should be noted that there is a shift from blue to yellow (increase in b^*) for all specimens. After accelerated weathering some specimens were noticeable warped. A visible depth of degradation (described in Chapter 5) was not noticeable after accelerated weathering. The lack of this visible degraded layer could be attributed to the added pigments in these specimens.

Table 6.2 Effects of Accelerated Weathering on the Total Color Difference of Specimens Cut from Manufactured Panels Values Reported: Average (% Coefficient of Variation)							
Formulation	Unexposed			Exposed			ΔE
	L^*	a^*	b^*	L^*	a^*	b^*	
ICBO AC07	44.7 (1.5)	5.6 (2.5)	7.5 (3.1)	58.6 (0.7)	10.4 (1.0)	10.2 (1.1)	14.9
ASTM D790	44.7 (1.0)	5.7 (2.7)	7.5 (2.4)	58.6 (0.8)	10.5 (1.8)	10.2 (0.5)	14.9

6.3.2 Effects of Natural Weathering on Color Fade

Table's 6.3 - 6.6 show the average chromaticity coordinates of the roof panels subjected to natural weathering. Table's 6.3 – 6.6 show that there is an increase in whiteness (L^*) at all locations measured. Hours of sunlight calculated from the Old Farmers Almanac (Thomas 2002). The Southeast corner experienced the most significant whitening (26% increase) and the southwest corner had the least significant increase in whitening (4%). It is also shown that there was a consistent shift from yellow to blue (decrease in b^*) for all four locations. The decrease in b^* differs from those specimens exposed artificially and could indicate that different degradation mechanisms are occurring. The southeast, southwest, and northeast each experienced 27%, 27%, and 30% loss in b^* respectively, while the northwest corner only had an 11% loss. No consistent trends for all four locations were observed for the a^* chromaticity coordinate. It is seen that a 16% and 14% loss in a^* (red to green) for the southeast and southwest corners, respectively. Conversely there was an increase in a^* of 4% and 11% for the Northeast and Northwest Corners respectively.

Table 6.3 Southeast Corner Color Fade Measurements				
Date of Measurement	L^*	a^*	b^*	Hours of Sunlight
7/19/00	41.61	8.62	11.35	0
11/7/00	50.33	7.60	8.89	1396
3/19/01	52.59	8.59	8.68	2708
6/14/01	52.25	7.25	8.23	3930

Table 6.4 Southwest Corner Color Fade Measurements				
Date of Measurement	L^*	a^*	b^*	Hours of Sunlight
7/19/00	46.20	8.03	10.81	0
11/7/00	44.89	7.13	8.11	1396
3/19/01	48.80	8.72	8.61	2708
6/14/01	48.26	6.89	7.89	3930

Table 6.5 Northeast Corner Color Fade Measurements				
Date of Measurement	L^*	a^*	b^*	Hours of Sunlight
7/19/00	46.56	7.64	12.76	0
11/7/00	49.09	7.35	9.57	1396
3/19/01	50.04	8.39	8.84	2708
6/14/01	51.26	7.94	8.88	3930

Table 6.6 Northwest Corner Color Fade Measurements				
Date of Measurement	L^*	a^*	b^*	Hours of Sunlight
7/19/00	42.71	6.62	9.66	0
11/7/00	48.94	6.93	9.01	1396
3/19/01	50.94	8.33	9.15	2708
6/14/01	49.95	7.32	8.57	3930

Figure 6.3 shows the color difference as a function of natural exposure for four different roof panels at various locations on the demonstration roof and for specimens exposed artificially. Figure 6.3 shows that for all roof panels the most color change occurred during the first three months (July – September). It is shown that the most dramatic change in color occurred at the southeast corner of the structure and the least amount of color change occurred at the southwest corner of the structure. The panels on the east side of the roof had a greater change in color than panels placed on the west side of the roof. One possible explanation is that frost or dew in the morning intensified the UV light or induced stress in the fibers due to swelling that would assist degradation. Another possible explanation is that in the afternoon there may be more airborne particles and debris that could reduce the intensity of the UV light. Table 6.3 also shows that specimens exposed for 2000 hours of accelerated laboratory weathering had a greater change in color than specimen exposed for 1 year in Madison Wisconsin. The total color difference for panels on the southeast corner was 75% of specimens exposed artificially. The total color difference for panels exposed on the northwest corner was only 25% of specimens exposed artificially.

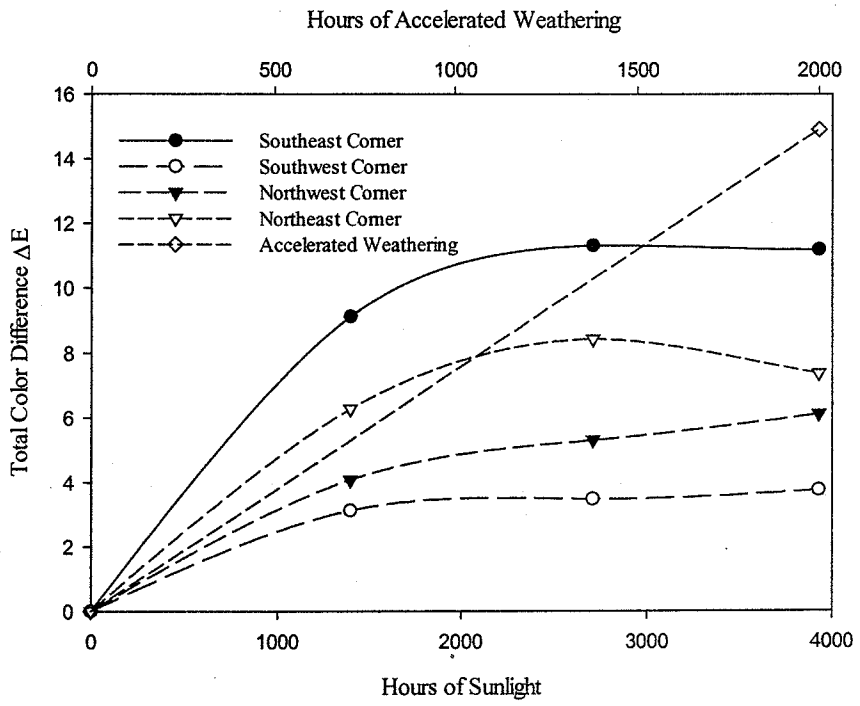

Figure 6.3 Color Change of Roof Panels Exposed Outdoors and of Specimens Exposed Artificially

6.3.3 Effects of Accelerated Weathering on Flexural Properties

A reduction in flexural properties was recorded for specimens of both sizes due to accelerated weathering. Flexural properties are computed using the gross cross for both sizes of specimens. Table 6.7 shows the effects of accelerated weathering on the average mechanical properties of the large specimens cut from manufactured roof panels. There is a 23% drop in max load after exposure and a 35% increase in deflection after exposure. The specimens also had a 42% decrease in modulus after exposure that is more than the 33% loss in modulus for Formulation 3 – wood after 2000 hours of exposure. The 24% loss in strength for the large specimens is also greater than the 20% loss in strength for Formulation 3 after 2000 hours.

Table 6.7. Effect of Accelerated Weathering on Large Specimens Cut From Manufactured Roof Panels[1]
[1]Values Reported: Average (% Coefficient of Variation)

Hours of Exposure	P_{max} (N)	Deflection (cm)	MOE (MPa)	MOR (MPa)
0	170.8 (20.7)	0.30 (16.6)	1208 (14.1)	32.0 (20.1)
2000	131.2 (21.1)	0.41 (15.8)	690.0 (16.4)	24.2 (20.8)
% Difference	23.1	34.6	42.2	24.4

Table 6.8 shows the mean values and coefficient of variation in parentheses for the small specimens. It is shown that there is a 10% drop in max load after exposure and a 44% increase in deflection after exposure. The specimens also had a 40% decrease in modulus

after exposure. The unexposed flexural modulus of the small specimens cut from the panels was 64% of the unexposed modulus for Formulation 3 – wood.

The modulus of the large specimens was 48% that of the small specimens cut from the same panel. This could be attributed to the lower rate of strain used when testing the large specimens.

The unexposed flexural strength is 85% of the unexposed strength for Formulation 3 – wood. After 2000 hours of exposure, the flexural modulus was 56% of the modulus for Formulation 3. The strength of the small specimens after 2000 hours was 91% of the strength of Formulation 3 after 2000 hours.

Table 6.8. Effect of Accelerated Weathering on the Small Specimens Cut From Manufactured Roof Panels
Values Reported: Average (% Coefficient of Variation)

Hours of Exposure	P_{max} (N)	Deflection (cm)	MOE (MPa)	MOR (MPa)
Control	60.5 (14.7)	0.30 (8.6)	2530 (9.1)	31.4 (14.5)
Exposed	54.3 (13.0)	0.43 (11.8)	1495 (12.1)	27.1 (12.5)
% Difference	10.1	44.7	40.1	13.4

Table 6.7 and 6.8 show that there is a more pronounced effect of accelerated weathering on the larger specimens than the small specimens. This may suggest that the degraded layer is greater in the larger specimens than the smaller specimens despite identical exposure conditions. It is interesting to note that 2000 hours of accelerated weathering had a greater effect on the strength and modulus of the large specimens cut from the manufactured roof panel than the unpigmented Formulation 3. For both large and small specimens the change to modulus was greater than the change in strength, which is consistent with Phase II results.

6.4 Conclusions

In this chapter the durability of NFTC roof panels subjected to natural and accelerated weathering was determined. From these results the following conclusion were made:

1. The panels did experience significant changes in color due to natural weathering. The most significant changes occurred during the first few months after installation. The panels installed on the east side of the roof had a greater change in color than panels installed on the west side of the roof and could indicate that the morning sun is more detrimental to NFTC.
2. Accelerated weathering of specimens cut from roofing panels resulted in reduced flexural properties. More significant reduction in properties was recorded for the large flexural specimens than the small flexural specimens. The modulus of the small specimens was nearly twice that of the large specimens and can probably be attributed to the difference in strain rate.

3. Unexposed specimens cut from roofing panels were both less stiff and strong than the unexposed unpigmented NFTC specimens tested in Phase II. The large specimens had a greater loss in strength and modulus than Formulation 3 – wood.
4. Specimens exposed to 2000 hours of accelerated weathering experienced greater change in chromaticity than roof panels exposed outdoors for 1 year in Madison Wisconsin. The total color difference for the panels was between 25% and 75% of the total color difference of the specimens and depended on the location of the panels on the roof.
5. The change in color for specimens exposed naturally were different from those specimens weathered artificially. The color of specimens exposed artificially shifted from blue to yellow while specimens exposed naturally shifted from yellow to blue. This could indicate that different degradation mechanisms are occurring outdoors than in the laboratory.

Chapter 7. Summary

7.1 Conclusions

The research presented in this thesis focused on the changes to physical and mechanical properties caused by accelerated weathering. It was assumed that durability under accelerated weathering provides an indication of durability under natural weathering but is acknowledged that this relationship is not direct. It was shown that NFTC degrade when exposed to both natural and accelerated weathering. Degradation consists of embrittlement of the polymer matrix and whitening of the lignocellulosic fiber. Degradation resulted in deterioration of the interfacial bond between the fiber and matrix. The loss in bond limited the transfer of stress between the fiber and matrix resulting in a reduction in the effective cross-section.

A two-layer model utilizing elementary mechanics was presented. It was shown that this model reasonably fits the flexural strength data, indicating that in the degraded layer there was limited stress transfer. This model did not reasonably fit flexural stiffness data, which may indicate that in the degraded layer strain may be carried differently than stress.

Based on the hypothesis presented in Chapter 1, the following conclusions can be drawn:

1. The general effects of natural weathering on NFTC can be reproduced using accelerated aging devices however they may not provide a direct simulation of natural exposure conditions.[1]
2. The UV stabilizer was effective in reducing surface crazing and loss in mechanical properties for unfilled HDPE and PP. The UV stabilizer was not effective in reducing color change or loss in mechanical properties for fiber filled HDPE and PP.
3. The addition of fungicide did increase surface crazing for unfilled PP and the changes in color and mechanical properties for fiber filled composites due to accelerated weathering.
4. Stiffness and strength of all composites with a greater content of lignocellulosic were more severely affected by exposure than those composites with smaller content except for PP composites filled with wood flour.
5. The addition of red and black colorants reduced the changes to physical and mechanical properties due to accelerated weathering. For all formulations tested, the addition of black colorant was more effective in reducing these changes than red colorant.
6. The orientation of the degraded surface layer in flexure affected the strength and stiffness for all formulations except the stiffness for Formulation 3 – Wood.

[1] A direct correlation between natural and accelerated aging is beyond the scope of this research

7. The mechanical behavior of weathered NFTC products can be predicted from the formation of a degraded layer.

In addition to the hypothesis presented in Chapter 1 the following observations are relevant:

1. Specimen color change was not uniform across the surface of the specimens. The end closest to the gate exhibited less color change than the non-gated end. A possible explanation for this is that as the mold cavity is filled, the polymer begins to cool as it touches the cavity wall. The longer cooling times could result in a higher degree of crystallinity and could also result in a greater volume of polymer at the surface that could protect the underlying fibers. Another possible explanation is that at the gated end there is greater molecular orientation that could result in greater scattering of UV light and less absorption.
2. The back surface of the specimens was found to degrade more than could be attributed to perfect reflection of irradiance and could indicate that other degradation mechanisms are occurring in the weatherometer chamber besides photodegradation.
3. Specimens placed in the weatherometer chamber for the final 1000 hours of the life of the lamp were less severely degraded than those specimens exposed for the first 1000 hours even though the irradiance was held constant. This could indicate a shift in the spectral distribution of energy from more damaging shorter wavelengths to less damaging longer wavelengths.
4. The most significant changes to chromaticity occurred during the first 1000 hours of the total 4000 hours for all formulations except Formulation 1 – HDPE. Formulations 2 – Additives, 3 –Wood, and 4 – Kenaf, had 76%, 65%, and 86% change in color during the first 1000 hours respectively.
5. The flexural stiffness for all formulations decreased after 4000 hours of exposure. The reduction to the flexural stiffness could be explained by the increase in strain at failure.
6. The flexural strength decreased for all formulations except Formulation 2 – Additives after 4000 hours of exposure. The reduction in strength could be attributed to the loss in effective area.
7. For the composite formulations tested in impact, it was found that a decrease in strength is a better indication of the influence of weathering than the energy to maximum load. For the NFTC formulations tested, the energy to maximum load remained relatively unchanged due to exposure and could be explained by the increase in strain at failure despite a reduction in maximum stress.
8. The total color difference of 2000 hours of accelerated weathering was 125% to 175% greater for specimens cut from manufactured roof panels than panels exposed to 1 year of natural weathering in Madison Wisconsin.
9. The orientation of the panels on the roof appears to affect the photostability of the panels. Panels layed on the southeast and northeast corner had the greatest change in color while specimens on the southwest and northwest have the

least change in color. This could indicate that morning sun is more detrimental than afternoon sunlight.

10. Differences in the changes in color were observed between accelerated and natural exposure. The color of specimens exposed artificially shifted from blue to yellow while specimens exposed naturally shifted from yellow to blue and could indicate that different degradation mechanisms are occurring.

7.2 NFTC Product Recommendations

NFTC can be used for outdoor applications, though it should be understood that these products will degrade due to weathering. Weathering of NFTC may limit the applicability of using these products to non – or semi- structural applications due to unfavorable changes to physical and mechanical properties.

To determine the usefulness of a NFTC product the following recommendations are proposed. First it would be necessary to determine all the required physical and mechanical properties required for a product in service. It is important to identify all required properties because the durability of these may be different. In this research the relative magnitude of changes to chromaticity, stiffness, and strength were all different. Appropriate product dimensions can then be estimated to provide enough material in critical areas to satisfy stiffness and stress requirements.

Second it is necessary to determine the potential exposure conditions. If multiple exposure conditions exist, different NFTC formulations may be worth investigating. A product that performs well in high temperature and UV may not perform well in a more temperate or humid climate. Critical loading conditions should then be identified.

Next, several formulations can be selected and subjected to accelerated weathering to provide an indication of weathering. The exposure conditions should be selected such that temperature and UV intensity are accelerated consistently from intended service conditions. Properties of interest should be monitored throughout the accelerated weathering because the changes may not be linear. Curves can be fit to the property data, and the length of accelerated weathering required to reach failure can be determined. From these results, the most favorable formulation can be selected.

It is recommended that in more critical environments (i.e. greater UV intensity, higher humidity), a smaller content of lignocellulosic be used. Smaller lignocellulosic content would allow for better encapsulation of the fiber in the matrix and a smaller percentage of fibers at or near the surface of the product where the intensity of UV is the greatest. The life of any NFTC could also be extended through the use of colorants.

7.3 Future Research

In chapter 2 multiple factors were shown to effect photodegradation. Of particular interest were irradiance, temperature, and moisture. In this study a standard exposure cycle was used for accelerated weathering. This cycle consisted of 102 minutes of light

followed by 18 minutes of light and water spray at one temperature. It is suggested that the variables of light and water spray be separated and tests conducted at a variety of temperatures. A matrix of exposure conditions could then be developed to determine which factors are most critical and how these factors influence each other.

It is recommended that the irradiance be monitored at several wavelengths. The wavelengths should be selected based upon those that are most critical to the materials. The exposure cycle should include a dark or lamp off period. This will allow for oxygen to diffuse into the specimen as it would at night during natural exposure.

Reasonable correlation between natural and accelerated weathering devices is necessary when predicting the outdoor service life of a product based on accelerated weathering. To accurately predict how a product would perform in service, an exhaustive study would be necessary where multiple accelerated weathering tests are performed simultaneously with natural weathering. For most non – or semi – structural applications, the need for accurately predicting the service life is not required.

It was shown that weathering of NFTC resulted in deterioration to the interfacial bond between the fiber and matrix. Interfacial bond is improved during compounding of NFTC through the use of compatiblizers. It may be worth investigating how different fiber surface treatments and compatiblizers influence the degradative reactions associated with weathering.

Finally, it may prove fruitful to evaluate the effects of different processing conditions. In Chapter 2 the effects of processing conditions on photodegradation were discussed. A variety of processing conditions and molding techniques should be investigated. Molds should be designed so that materials near the surface have greater photostability than materials in the core of a product. Depending on the application, fiber reinforcement should be oriented so that it carries the most stress and is not subject to weathering.

References

Allen, N. Degradation and Stabilization of Polyolefins, Applied Science Publishers, London, 1983.

Ashbee, K. H. G. Fundamental Principals of Fiber Reinforced Composites. Technomic Publishing Compny, Lancaster Pennsylvania 1993.

American Society for Testing and Materials, 1996 D256 Impact Resistance of Plastics and Electrical Insulating Materials.

American Society for Testing and Materials, 1996, Standard D790-96a, Test Method for the Flexural Properties of Unreinforced and Reinforced Plastics and Electrical Insulation Materials.

American Society for Testing and Materials, 1994, Standard D2244-93, Standard Test method for Calculation of Color Differences From Instrumentally Measured Color Coordinates.

American Society for Testing and Materials, 1994, Standard D2565-94, Xenon-Arc Exposure of Plastics Intended for Outdoor Applications.

American Society for Testing and Materials, 1994, Standard D2915-94, Standard Practice for Evaluating Allowable Properties for grades of Structural Lumber.

American Society for Testing and Materials, 1994, Standard D4364-94, Standard Practice for Performing Accelerated Outdoor Weathering of Plastics Under Concentrated Natural Sunlight.

American Society for Testing and Materials, 1996, Standard G 23-96, Operating Light-Exposure Apparatus (Carbon-Arc) Type with and without Water for Exposure of Non-Metallic Materials.

American Society for Testing and Materials, 1996, Standard G 26-96, Operating Light-Exposure Apparatus (Xenon-Arc) Type with and without Water for Exposure of Non-Metallic Materials.

American Society for Testing and Materials, 1996, Standard G 53-96, Operating Light-Exposure Apparatus (Fluorescent UV –Condensation) Type with and without Water for Exposure of Non-Metallic Materials.

American Society for Testing and Materials, 1996, Standard G 141-96, Addressing Variability in Exposure Testing on Nonmetallic Materials.

American Society for Testing and Materials, 1996, Standard G 147-96, Conditioning and Handling of Nonmetallic Materials for Natural and Artificial Weathering Tests.

Eckert, C. "Opportunities for Natural Fibers in Plastic Composites," Presented at Progress in Woodfibre-Plastic Composite Conference. Toronto, Canada. May 25-26, 2000.

Evans P. D., Michell A. J., Schmalzl K. J. "Studies of the Degradation and Protection of Wood Surfaces," Wood Science and Technology, Vol. 26, pp. 151-163, 1992.

Evans P. D., Thay P. D., Schmatzl K. J. "Degradation of Wood Surfaces during Natural Weathering. Effects on Lignin and Cellulose and on the Adhesion of Acrylic Latex Primers," Wood Science and Technology, Vol. 30 pp. 411-422, 1996.

Ezrin, M. Plastics Failure Guide, Cause and Prevention, Hanser Gardner Publication, Cincinnati Ohio 1996.

Falk, R., Felton, C., Lundin, T. "The Effects of Weathering on the Color Loss of Natural Fiber/Thermoplastic Composites." Proceedings of the Third International Symposium on Natural Polymers and Composites. Sao Pedro, Brazil. May 14-17, pp 382-385, 2000.

Feist, W., Mraz, E., "Comparison of Outdoor and Accelerated Weathering of Unprotected Softwoods." Forest Products Journal, Vol. 28 No. 3, pp. 38-43, 1978.

Feng D., Sanadi A. "Effect of Compatibilizer on the Structure-Property Relationships of Kenaf Fiber-Polypropylene Composites," In: Proc. Woodfiber-Plastics Composites Conference, Madison, Wi, May 1-3, 1995. Forest Products Society: pp. 157-160.

Ferry, J. Viscoelastic Properties of Polymers, John Wiley and Sons. 1980.

Furneaux G., Ledbury K., Davis A. "Photooxidation of Thick Polymer Samples – Part I: The Variation of Photooxidation with Depth in Naturally and Artificially Weathered Low Density Polyethylene," Polymer Degradation and Stability, Vol. 3, pp. 431-442, 1981.

Gillen, K. T.: Clough, R. L.: Dhooge, N. J. "Density Profiling of Polymers," Polymer, Vol. 27, 225-232, 1986.

Gijsman, P. Hennekens, J. Janssen, K. "Comparison of UV degradation of Polyethylene in Accelerated Test and Sunlight," Polymer Durability, Edited by Clough, Billingham, and Gillen. Advances in Chemistry series 249. 206th National Meeting of Polymer Chemistry Chicago Illinois 1996.

Groom, L., S. M. Shaler, and L. Mott. "The Mechanical Properties of Individual Lignocellulosic Fibers," In: Proc. Woodfiber-Plastics Composites Conference, Madison, Wisconsin, May 1-3, 1995. Forest Products Society: pp. 33-40.

Gugumus F. "Light Stabilizers," In Plastic Additives, 4th edn, ed. R. Gaechter & H. Mueller. Hanser Publishers, Munich. 1993, Pp. 129 – 170.

Gugumus F. "The Performance of Light Stabilizers in Accelerated and Natural Weathering," Polymer Degradation and Stability, Vol. 50, pp. 101-116, 1995.

Hoekstra, H. The Mechanical Behavior of UV-degraded HDPE: Consequences for Designers, PhD Thesis Delft University of Technology, 1997.

Hon, D. "Weathering and Photochemistry of Wood," Wood and Cellulosic Chemistry, pp. 513 – 546, 2001.

International Conference of Building Officials, 1997, Acceptance Criteria for Special Roofing Systems, AC07, Published by ICBO, July, Whittier, California.

Kiguchi, M., Kataoka, Y., Kaneiwa, H., Akita, K., Evans, P. "Photostabilization of Woodfiber-Plastic Composites by Chemical Modification of Woodfibre," In: Proc 5th Pacific Rim Bio-Based Composites Symposium. Canberra, Australia. December 2000.

Killough, J. "The Plastic Side of the equation," In: Proc. Woodfiber-Plastics Composites Conference, Madison, Wi, May 1-3, 1995. Forest Products Society: pp. 7-15.

Kuruvilla J., Sabu T., Pavithran C. "Dynamic Mechanical Properties of Short Sisal Fiber Reinforced Low Density Polyethylene Composites," Journal of Reinforced Plastics and Composites, Vol. 12, pp. 139-155, February 1993.

Lampo, R. "Standards Boost an Industry." ASTM Standardization News, Vol. 27, No. 7. pp. 22-26, July 1999.

Li T., NG C., Li R. "Impact Behavior of Sawdust/Recycled-PP Composites," Journal of Applied Polymer Science, Vol. 81, pp. 1420-1428, 2001.

Lu, J., Wu, Q., McNabb, H. "Chemical Coupling in Wood Fiber and Polymer Composites: A Review of Coupling Agents and Treatments," Wood and Fiber Science, Vol. 32 No. 1, pp. 88-104, 2000.

Mascia, L. Thermoplastics: Materials Engineering, Elsevier Science Publishing N.Y. N.Y. 1982.

Matuana, L., Kamdem, D., Zhang, J. "Photoaging and Stabilization of Rigid PVC/Wood-Fiber Composites," Journal of Applied Polymer Science, Vol. 80, pp. 1943-1950, 2001.

Murphy, Joseph. "Characterization of Nonlinear Materials." USDA Forest Products Laboratory Curve Fitting Technique, 1992.

Osswald, T., Menges, G. Materials Science of Polymers for engineers, Hanser/Gardner Publishing, Cincinnati Ohio 1995.

Powell, J. "The recycled plastic lumber industry: Moving Toward adulthood," Resource Recycling: North America's Recycling and Composting Journal, Vol. 15 No. 2, pp. 20-29, 1996.

Pritchard, G. Plastic Additives An A-Z reference. Chapman & Hall, London England 1998.

Rabek, J. Photodegradation of Polymers: Physical Characteristics and Applications, Springer-Verlag, Germany 1996.

Razi, P.S., Portier, R., Raman, A. "Studies on Mechanical Properties of Wood-Polymer Composites," Journal of Composite Materials, Vol. 31, No. 23, pp. 2391-2401, 1997.

Razi, P.S., Portier, R., Raman, A. "Studies on Polymer-Wood Interface Bonding: Effect on Coupling Agents and Surface Modification," Journal of Composite Materials, Vol. 33, No. 12, pp. 1999.

Rowell, R., Caulfield, D., Chen, G., Ellis, D., Jacobson, R., Lange, S., Schumann, R., Sanadi, A., Balatinecz, J., Sain, M. "Recent Advances in Agro-Fiber/Thermoplastic Composites," In: Proc. Second International Symposium on Natural Polymers and Composites ISNaPol/1998, pp. 11-20.

Rowell, R., Han, J., Rowell, J. "Characterization and Factors Effecting Fiber Properties" In: Natural Polymers and Agrofibers Based Composites. Sao Carlos – Brazil 2000.

Sanadi A., Caulfield D., Stark N., Clemons C. "Thermal and Mechanical Analysis of Lignocellulosic Polypropylene Composites," In: Proc. Woodfiber-Plastics Composites Conference, Madison, Wisconsin, May 1-3, 1995. Forest Products Society: pp. 67-78.

Schoolenberg, G. E. A Study of the Ultra-Violet Degradation Embrittlement of Polypropylene Polymer, PhD Thesis. Delft University of Technology 1988.

Schoolenberg, G. E. Vink, P. Ultra-Violet Degradation of Polypropylene: 1. Degradation profile and thickness of the embrittled surface layer, Polymer, Vol. 32, No 3, pp. 432-437, 1991.

Simonsen, J. "The Mechanical Properties of Woodfiber-Plastic Composites: Theoretical vs. Experimental." In: Proc. Woodfiber-Plastics Composites Conference, Madison, Wisconsin, May 1-3, 1995. Forest Products Society: pp. 47-55.

Simonsen John. Efficiency of Reinforcing Materials in Filled Polymer Composites. Forest Products Journal Vol. 47(1) 74-81, 1997.

Stark, N., Berger, M. "Effect of Particle Size on Properties of Wood Flour Reinforced Polypropylene Composites," In: Proc. Fourth International Conference on Woodfiber-

Plastic Composites, Madison, Wisconsin, May 1997. Forest Products Society: pp. 19 – 25.

Tarkow, H. "Wood and Moisture." In: Wood: Its Structure and Properties, Vol. 1, Edited by Wangaard, F. Pennsylvania State University 1981.

Thomas, R. The Old Farmers Almanac, Yankee Publishing 2002.

Tidjani, A., Arnauld, R., Dasilva, A. "Natural and Accelerated Photoaging of Linear Low-Density Polyethylene: Changes of the Elongation at Break." Journal of Applied Polymer Science, Vol. 47, pp. 211-216 1993a.

Tidjani A. Arnaud R. "Photooxidation of Linear Low Density Polyethylene: A Comparison of Photoproducts Formation Under Natural and Accelerated Exposure." Polymer Degradation and Stability, Vol. 39 pp. 285-292, 1993b

Torikai, A., Chigita K., Okisaki, F., Nagata, M. "Photooxidative Degradation of Polyethylene Containing Flame Retardants by Monochromatic Light," Journal of Applied Polymer Science Vol. 58, pp. 685-690, 1995.

Xu, W., Liu, P., Li, H., Xu, X. "Effect of Electron Beam Irradiation on Mechanical Properties of High Density Polyethylene and its blends with Sericite-Tridymite-Cristobalite," Journal of Applied Polymer Science Vol. 78, pp. 243-249, 2000.

Zweifel, H. Stabilization of Polymeric Materials, Springer-Verlag, Berlin 1998.

Appendices

1. Equations for Determining Chromaticity

$$L^* = 116\left(\frac{Y}{Y_o}\right)^{\frac{1}{3}} - 16 \qquad (1)$$

$$a^* = 500\left[\left(\frac{X}{X_o}\right)^{\frac{1}{3}} - \left(\frac{Y}{Y_o}\right)^{\frac{1}{3}}\right] \qquad (2)$$

$$b^* = 200\left[\left(\frac{Y}{Y_o}\right)^{\frac{1}{3}} - \left(\frac{Z}{Z_o}\right)^{\frac{1}{3}}\right] \qquad (3)$$

Where:
L^* = lightness factor (Intensity of Reflective Light)
a^* = chromaticity coordinates
b^* = chromaticity coordinates
X,Y,Z = predetermined tristimulus values based upon CIE
X_o, Yo, Z_o = tristimulus values of the illuminant used

The above equations apply only when X/X_o Y/Y_o and Z/Z_o are greater than 0.008856. When X/X_o, Y/Y_o, Z/Z_o are less than 0.008856, the following equations are used.

$$\left(\frac{X}{X_o}\right)^{\frac{1}{3}} \rightarrow 7.787\left(\frac{X}{X_o}\right) + \frac{16}{116} \qquad (4)$$

$$\left(\frac{Y}{Y_o}\right)^{\frac{1}{3}} \rightarrow 7.787\left(\frac{Y}{Y_o}\right) + \frac{16}{116} \qquad (5)$$

$$\left(\frac{Z}{Z_o}\right)^{\frac{1}{3}} \rightarrow 7.787\left(\frac{Z}{Z_o}\right) + \frac{16}{116} \qquad (6)$$

Equation for determining the total color difference using L^*, a^*, b*, chromaticity coordinates

$$\Delta E = \sqrt{\left((\Delta L^*)^2 + (\Delta a^*)^2 + (\Delta b^*)^2\right)} \qquad (7)$$

Appendices

1. Equations for Determining Chromaticity

$$L^* = 116\left(\frac{Y}{Y_o}\right)^{\frac{1}{3}} - 16 \qquad (1)$$

$$a^* = 500\left[\left(\frac{X}{X_o}\right)^{\frac{1}{3}} - \left(\frac{Y}{Y_o}\right)^{\frac{1}{3}}\right] \qquad (2)$$

$$b^* = 200\left[\left(\frac{Y}{Y_o}\right)^{\frac{1}{3}} - \left(\frac{Z}{Z_o}\right)^{\frac{1}{3}}\right] \qquad (3)$$

Where:
L^* = lightness factor (Intensity of Reflective Light)
a^* = chromaticity coordinates
b^* = chromaticity coordinates
X,Y,Z = predetermined tristimulus values based upon CIE
X_o, Yo, Z_o = tristimulus values of the illuminant used

The above equations apply only when X/X_o Y/Y_o and Z/Z_o are greater than 0.008856. When X/X_o, Y/Y_o, Z/Z_o are less than 0.008856, the following equations are used.

$$\left(\frac{X}{X_o}\right)^{\frac{1}{3}} \rightarrow 7.787\left(\frac{X}{X_o}\right) + \frac{16}{116} \qquad (4)$$

$$\left(\frac{Y}{Y_o}\right)^{\frac{1}{3}} \rightarrow 7.787\left(\frac{Y}{Y_o}\right) + \frac{16}{116} \qquad (5)$$

$$\left(\frac{Z}{Z_o}\right)^{\frac{1}{3}} \rightarrow 7.787\left(\frac{Z}{Z_o}\right) + \frac{16}{116} \qquad (6)$$

Equation for determining the total color difference using L^*, a^*, b*, chromaticity coordinates

$$\Delta E = \sqrt{\left((\Delta L^*)^2 + (\Delta a^*)^2 + (\Delta b^*)^2\right)} \qquad (7)$$

3. Equations for Non-Linear Curve Fitting

By Joseph F. Murphy, Ph.D., P.E.
Supervisory General Engineer
USDA FS Forest Products Laboratory

Woodfiber-plastic composites behave differently than woos and wood composites. This is very apparent in load-displacement plots. A linear material can be generally characterized by the maximum load, P_{max}, and maximum displacement, x_{max}, which yields the slope, P_{max}/x_{max}, as well as the area under the curve, $P_{max} * x_{max}/2$.

A nonlinear material has a constant slope as well as an area that is not a simple multiplication of maximum load and maximum displacement. The Engineering Mechanics Laboratory of the USDA Forest Service Products Laboratory ahs found that a four parameter hyperbolic and linear function can fit load-displacement data of: paper, joint slip, steel, and woodfiber-plastic composites; quite well. After the parameters are estimated, the theoretical curve can be used for determining initial slope (and therefore initial modulus of elasticity) and area under the curve to maximum load 9and therefore work or energy to maximum load).

The following function is fitted to the load-displacement data

$$P = c_1 \tanh(c_2 (x - c_4)) + c_3 (x - c_4)$$

And the slope at x is

$$\frac{dP}{dx} = c_1 c_2 \sec h^2 (c_2 (x - c_4)) + c_3$$

The initial slope at $x = c_4$ then is

$$\frac{dP}{dx} = c_1 c_2 + c_3$$

The area under the curve to x is

$$Area(x) = \frac{c_1}{c_2} \ln(\cosh(c_2 (x - c_4)) + \frac{c_3}{2} (x - c_4)^2$$

Where:
$c_1 = B_o + c_3 c_4$
$c_2 = (B_1 - c_3)/c_4$
c_3 = The slope through the ending portion of the curve
c_4 = The δ intercept through the beginning portion of the curve
B_o = The intercept of c_3 and the P-axis
B_1 = The slope through the beginning portion of the curve

4. Determine Sample Size Sufficient for Estimating the Mean by a two-stage method – ASTM D2915

$$n = \left(\frac{t}{0.05} CV\right)^2 \qquad (1)$$

Where:
n = sample size
CV = coefficient of variation s/X
0.05 = precision of estimate
t = value of t statistic from Table 1 ASTM D2915

5. Manufactures Plastic Specifications for Phase II

General Description
ExxonMobil HMA-018 (HDPE)[1] is a palletized, high flow, high density polyethylene resin designed for fast cycling injection molding applications. The resin combines good performance properties with ease of processability and is especially suitable for multicavity thin-wall tubs and deep draw housewares. Articles molded from this resin exhibit smooth, glossy surfaces and low warpage.

Table A.1 General Properties of ExxonMobil HMA-018

Property	Test Method	Unit	Typical Value
Melt Index	ASTM D 1238	g/10 min	30
Density	ASTM D1928	g/cm^3	0.954
Melting Point	ASTM D3418	°C	130

Table A.2 Mechanical Properties of ExxonMobil HMA-018

Property	Test Method	Unit	Typical Value
Elastic Modulus (0.05-0.25%)	ISO 527-2/1B/1	MPa	860
Flexural Modulus (0.05-0.25%)	ISO 178	MPa	900
Tensile at Yield	ISO 527-2/1B1	MPa	22
Elongation at Break	ISO 527-2/1B1	%	> 100
Elongation at Yield	ISO 527-2/1B1	%	10
Izod Impact	ISO 180-4A	kJ/m^2	4

[1]Properties published by ExxonMobil Chemical

6. Phase II Injection Molding Cycle Times

Table A.3 Phase II Injection Molding Cycle Times[1] [1]Times given in seconds				
	Formulation 1, HDPE	Formulation 2, Additives	Formulation 3, Wood	Formulation 4, Kenaf
Injection high	10	10	10	10
Pack	4	4	4	4
Hold	4	4	4	4
Cooling	10	10	5	5
Ext Delay	0	0	0	0
Open Dwell	1	1	1	1

7. Phase II Injection Molding Pressures and Speeds

Table A.4 Injection Molding Specifics								
Formulation	Shot Size	Injection Speed (sec.)			Fill Pressure			
		#1	#2	%	Hi Limit	Hyd Xfer	Pack	Hold
1, HDPE	1.5	0.7	0.7	20	800	1000	500/4	500/4
2, Additives	1.8	1	1.0	20	2000	1000	700/4	700/4
3, Wood	2	1	1	20	2000	1000	1000/4	1000/4
4, Kenaf	2	1	1	20	2000	1000	1000/4	1000/4

8, Tension and 3 – Point Bending Stress-Strain Curves for Phase II Formulations 1 – 4. (Rate of Strain 0.1 mm/mm/min)

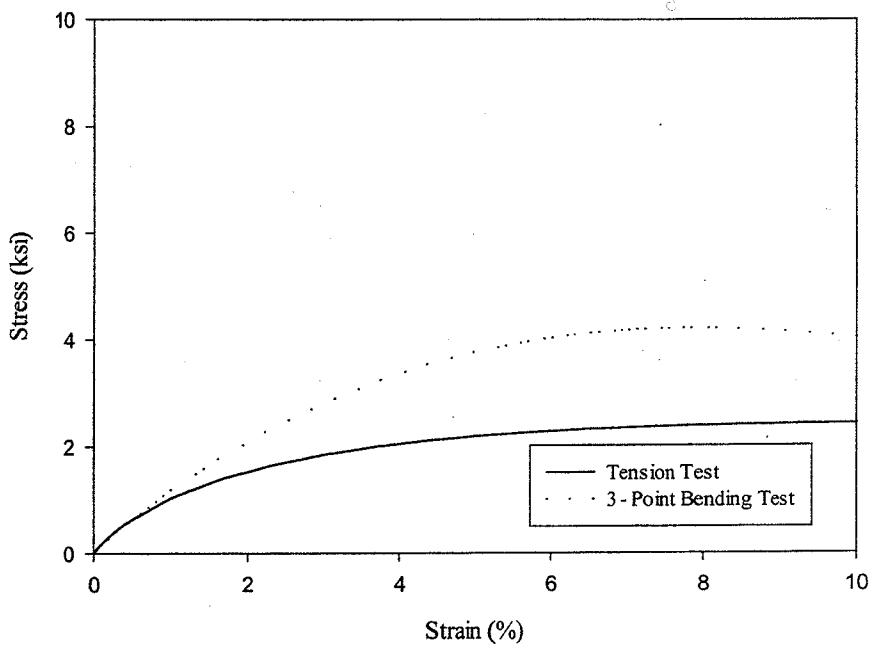

Stress Strain Curves for Unexposed Tension and 3-Point Bending Tests for Formulation 1, HDPE

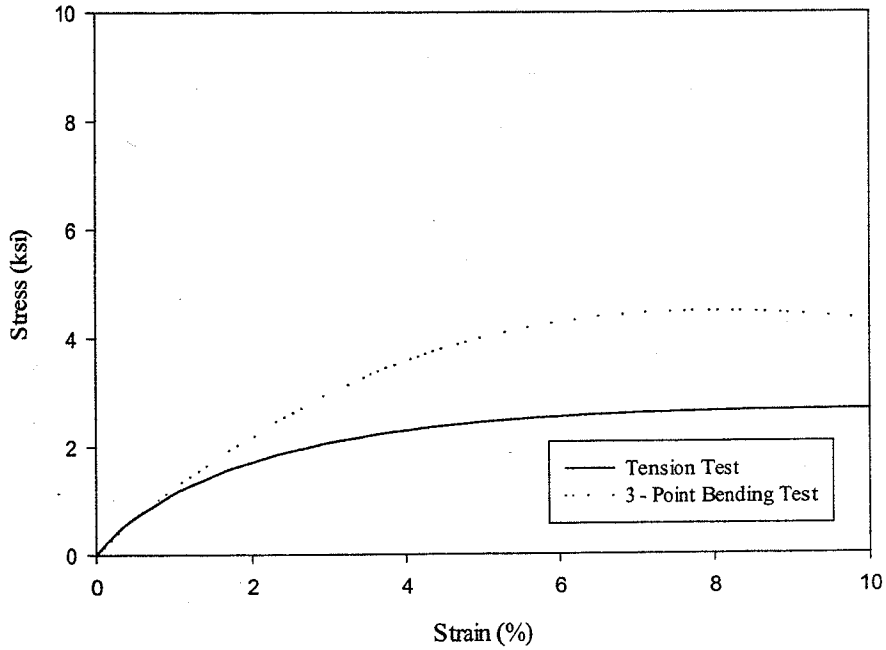

Stress Strain Curves for Unexposed Tension and 3-Point Bending Tests for Formulation 2, Additives

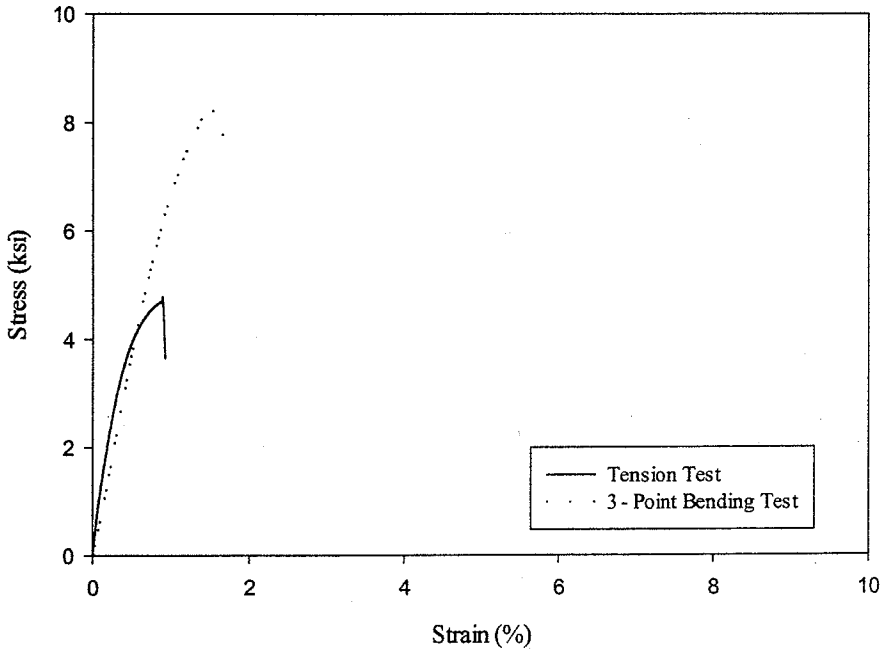

Stress Strain Curves for Unexposed Tension and 3-Point Bending Tests for Formulation 3, Wood

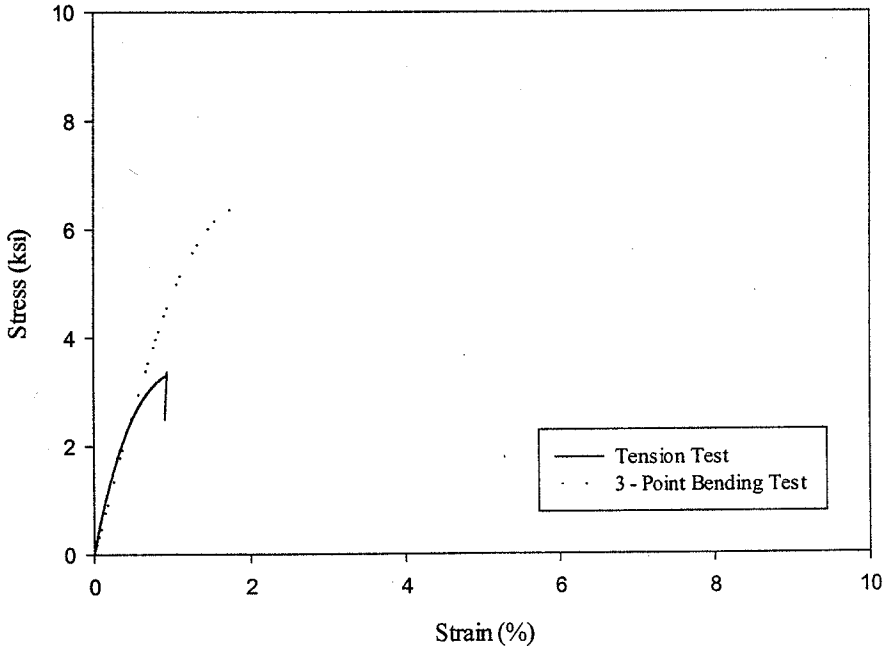

Stress Strain Curves for Unexposed Tension and 3-Point Bending for Formulation 4, Kenaf

9. Three Point Bending and Impact Testing Specimen Rotation for Phase II Accelerated Weathering

Table A.5 Specimen Rotation for Phase II Accelerated Weathering								
Total Hours of Exposure								
0	500	1000	1500	2000	2500	3000	3500	4000
120 Specimens – Controls	120 Specimens – 4000 hours of exposure							
120 Specimens – 500 hours exposure	120 Specimens – 3500 hours of exposure							
120 Specimens – 1000 hours exposure	120 Specimen – 3000 hours of exposure							
120 Specimens – 1500 hours of exposure	120 Specimens – 2500 hours of exposure							
120 Specimens – 2000 hours of exposure	200 Impact Specimens							

10. Non – Linear Least Squares Regression Fits

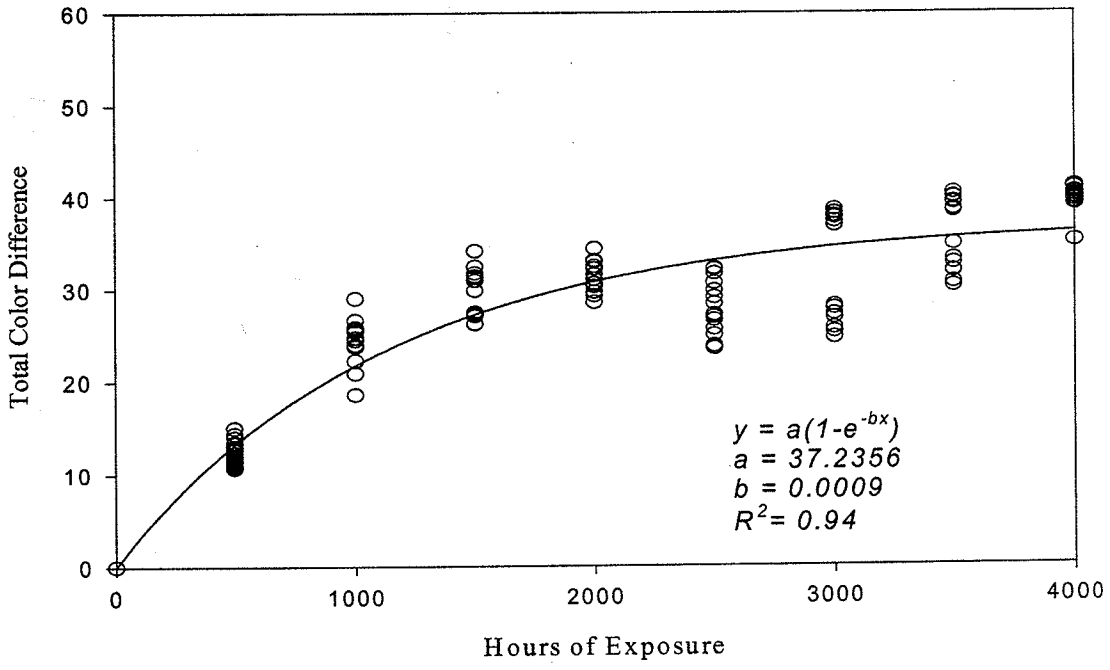

Effect of Accelerated Weathering on the Total Color Difference
Formulation 3: 50% Wood Flour

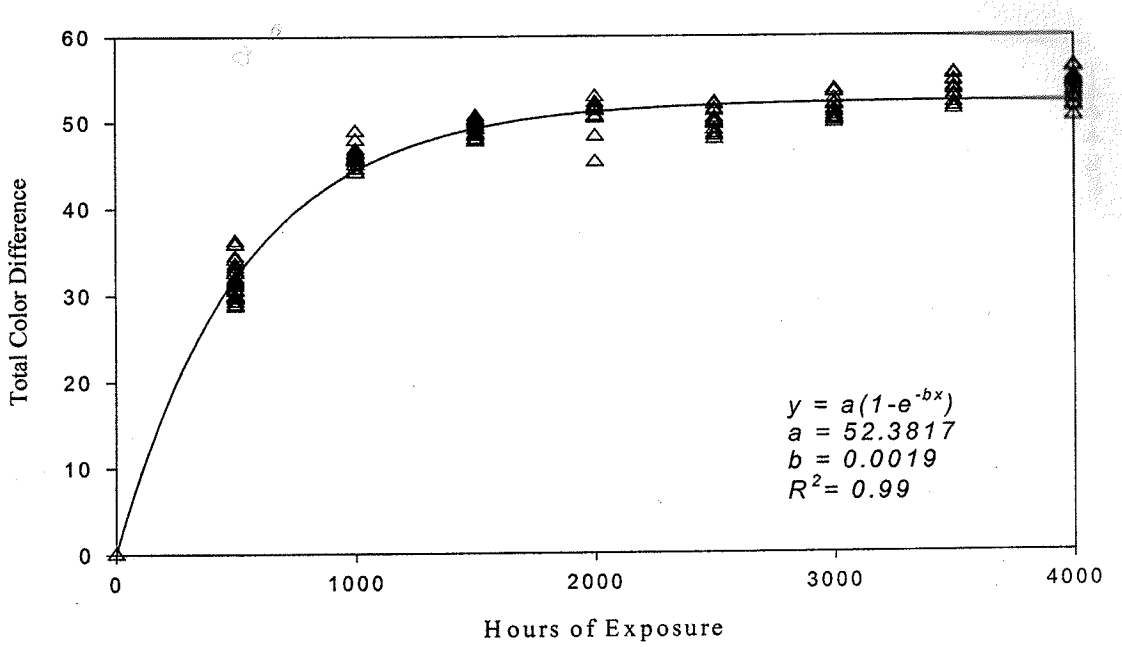

Effect of Accelerated Weathering on the Total Color Difference
Formulation 4: 50% Kenaf

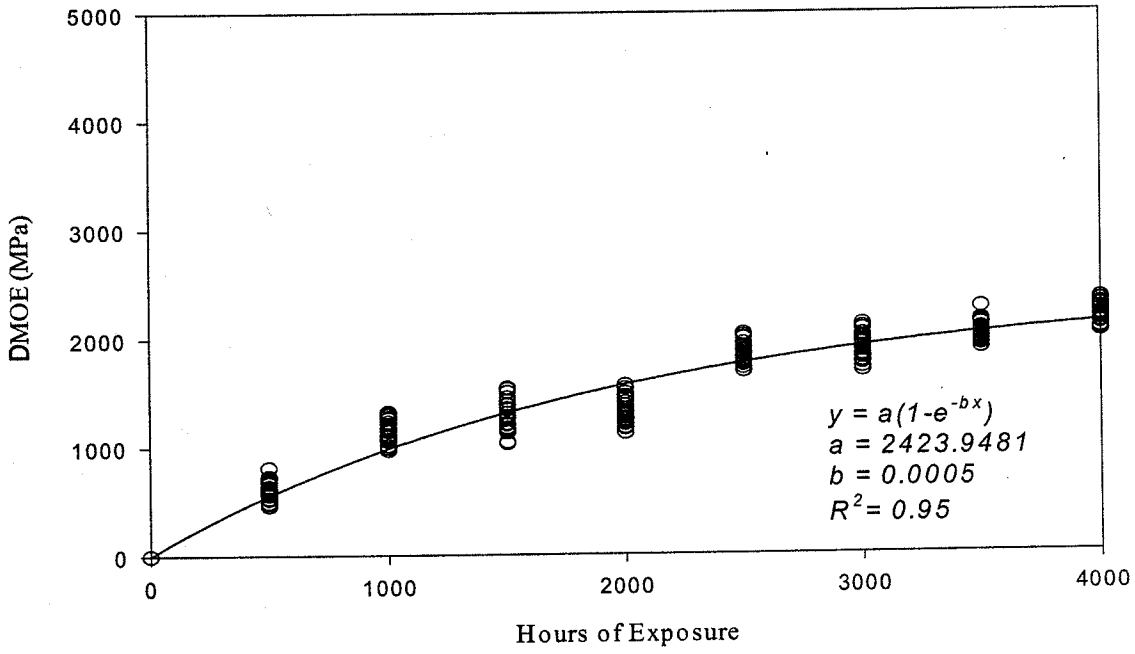

Effect of Accelerated Weathering on the Change in MOE
Formulation 3: 50% Wood Flour

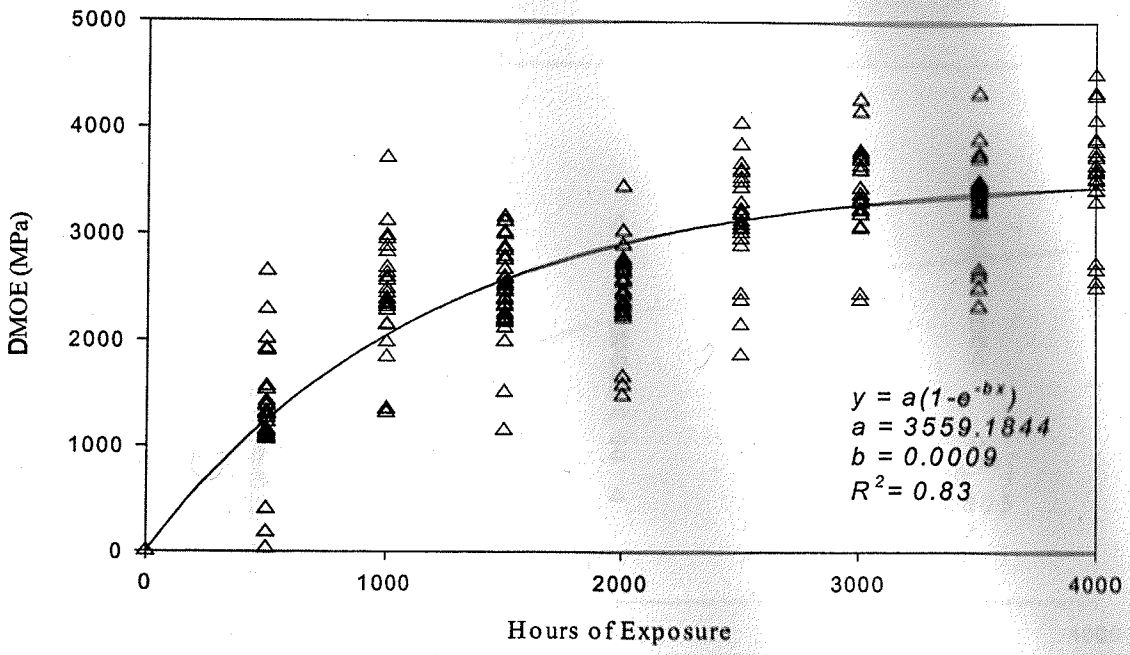

Effect of Accelerated Weathering on the Change in MOE
Formulation 4: 50% Kenaf

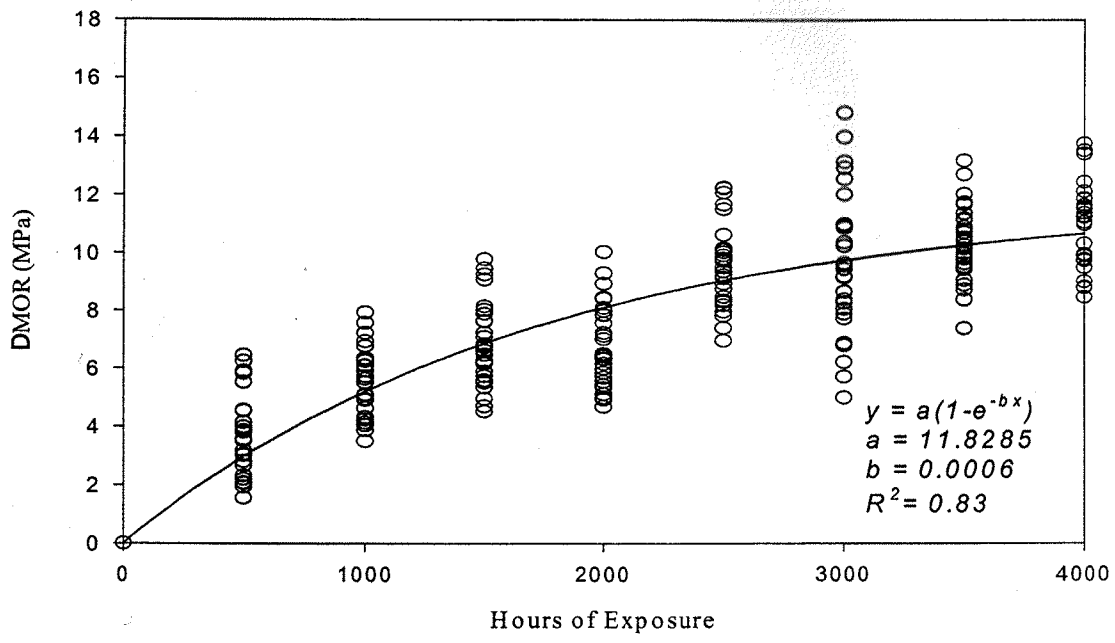

Effect of Accelerated Weathering on the Change in MOR
Formulation 3: 50% Wood Flour

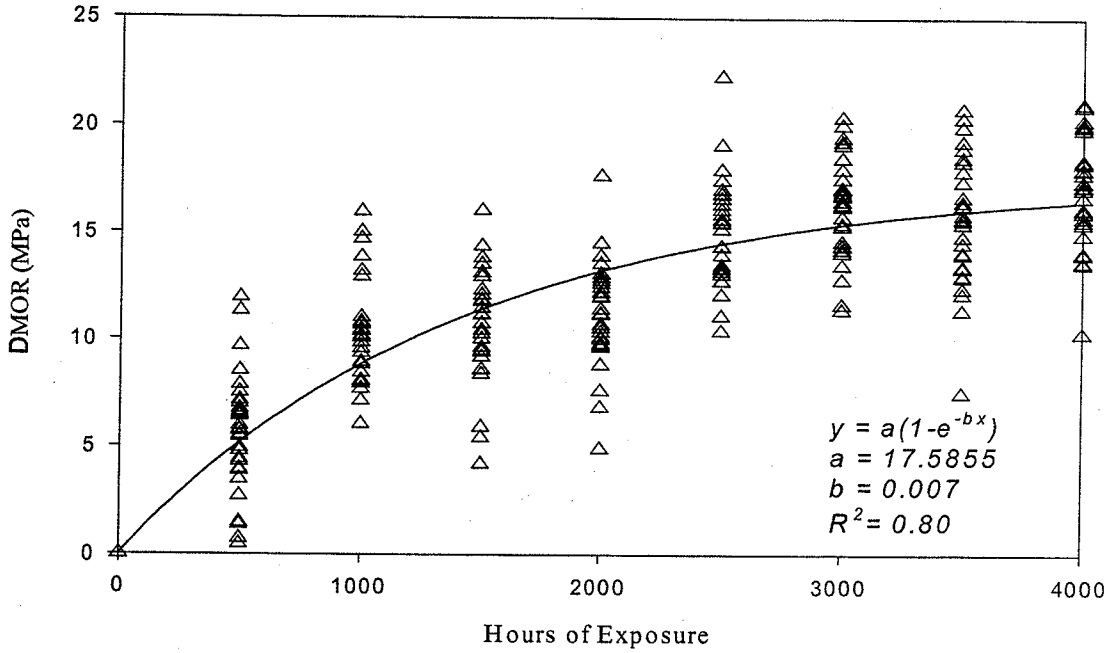

Effect of Accelerated Weathering on the Change in MOR
Formulation 4: 50% Kenaf